

Genetic and neuroinflammatory components of familial and sporadic cerebral Small Vessel Disease

Citation for published version (APA):

Koizumi, T. (2019). *Genetic and neuroinflammatory components of familial and sporadic cerebral Small Vessel Disease*. [Doctoral Thesis, Maastricht University]. Maastricht University. <https://doi.org/10.26481/dis.20190828tk>

Document status and date:

Published: 01/01/2019

DOI:

[10.26481/dis.20190828tk](https://doi.org/10.26481/dis.20190828tk)

Document Version:

Publisher's PDF, also known as Version of record

Please check the document version of this publication:

- A submitted manuscript is the version of the article upon submission and before peer-review. There can be important differences between the submitted version and the official published version of record. People interested in the research are advised to contact the author for the final version of the publication, or visit the DOI to the publisher's website.
- The final author version and the galley proof are versions of the publication after peer review.
- The final published version features the final layout of the paper including the volume, issue and page numbers.

[Link to publication](#)

General rights

Copyright and moral rights for the publications made accessible in the public portal are retained by the authors and/or other copyright owners and it is a condition of accessing publications that users recognise and abide by the legal requirements associated with these rights.

- Users may download and print one copy of any publication from the public portal for the purpose of private study or research.
- You may not further distribute the material or use it for any profit-making activity or commercial gain
- You may freely distribute the URL identifying the publication in the public portal.

If the publication is distributed under the terms of Article 25fa of the Dutch Copyright Act, indicated by the "Taverne" license above, please follow below link for the End User Agreement:

www.umlib.nl/taverne-license

Take down policy

If you believe that this document breaches copyright please contact us at:

repository@maastrichtuniversity.nl

providing details and we will investigate your claim.

Download date: 16 Apr. 2024

Genetic and neuroinflammatory components of familial and sporadic cerebral Small Vessel Disease

Citation for published version (APA):

Koizumi, T. (2019). *Genetic and neuroinflammatory components of familial and sporadic cerebral Small Vessel Disease*. Maastricht University. <https://doi.org/10.26481/dis.20190828tk>

Document status and date:

Published: 01/01/2019

DOI:

[10.26481/dis.20190828tk](https://doi.org/10.26481/dis.20190828tk)

Document Version:

Publisher's PDF, also known as Version of record

Please check the document version of this publication:

- A submitted manuscript is the version of the article upon submission and before peer-review. There can be important differences between the submitted version and the official published version of record. People interested in the research are advised to contact the author for the final version of the publication, or visit the DOI to the publisher's website.
- The final author version and the galley proof are versions of the publication after peer review.
- The final published version features the final layout of the paper including the volume, issue and page numbers.

[Link to publication](#)

General rights

Copyright and moral rights for the publications made accessible in the public portal are retained by the authors and/or other copyright owners and it is a condition of accessing publications that users recognise and abide by the legal requirements associated with these rights.

- Users may download and print one copy of any publication from the public portal for the purpose of private study or research.
- You may not further distribute the material or use it for any profit-making activity or commercial gain
- You may freely distribute the URL identifying the publication in the public portal.

If the publication is distributed under the terms of Article 25fa of the Dutch Copyright Act, indicated by the "Taverne" license above, please follow below link for the End User Agreement:

www.umlib.nl/taverne-license

Take down policy

If you believe that this document breaches copyright please contact us at:

repository@maastrichtuniversity.nl

providing details and we will investigate your claim.

Download date: 24 Jul. 2020

**Genetic and neuroinflammatory
components of
familial and sporadic
cerebral Small Vessel Disease**

Takashi Koizumi

© Takashi Koizumi, Maastricht 2019

Layout: Takashi Koizumi

Cover design: Takashi Koizumi

Production: Ipskamp Printing BV

ISBN: 978-94-028-1635-8

Genetic and neuroinflammatory
components of
familial and sporadic
cerebral Small Vessel Disease

Dissertation

To obtain the degree of Doctor at Maastricht University
on the authority of the Rector Magnificus,
Prof. Dr. Rianne M. Letschert,
in accordance with the decision of the Board of Deans,
to be defended in public
on Wednesday 28th of August 2019 at 10.00 hours

By
Takashi Koizumi

Promoters:

Prof. Dr. H.W.M. Steinbusch

Prof. Dr. T. Mizuno (Kyoto Prefectural University of Medicine, Japan)

Co-promoter:

Dr. S. Foulquier

Assessing Committee:

Prof. Dr. R.J. van Oostenbrugge (Chair)

Prof. Dr. E.A.L. Biessen

Prof. Dr. C.G. Schalkwijk

Prof. Dr. M. Tanaka (Kyoto Prefectural University of Medicine, Japan)

Dr. Ir. T. Vanmierlo (Hasselt University, Belgium)

CONTENTS

CHAPTER 1 **9**

General Introduction

CHAPTER 2 **27**

The CADASIL scale-J, a modified scale to prioritize access to genetic testing for Japanese CADASIL-suspected patients

Journal of Stroke and Cerebrovascular Disease: 2019; 28: 1431-1439.

CHAPTER 3 **51**

Perivascular immune cells in cerebrovascular diseases: From perivascular macrophages to perivascular microglia

Frontiers in Neuroscience, in revision

CHAPTER 4 **71**

Transiently proliferating perivascular microglia harbor M1-type and precede cerebrovascular changes in a chronic hypertension model

Journal of Neuroinflammation. 2019; 16(1): 79.

CHAPTER 5 **95**

Type 2 Diabetes accelerates the activation of perivascular microglia in hypertensive rats

In preparation

CHAPTER 6 **117**

General discussion

ADDENDUM

Summary / Samenvatting **127**

Valorization / Valorisatie **133**

Acknowledgements **139**

Biography **143**

Publications **144**

List of abbreviations

AD	Alzheimer's disease
AGEs	Advanced Glycation End-products
AngII	Angiotensin II
AUC	Area under the curve
BBB	Blood brain-barrier
BM	Basement membrane
CAA	Cerebral amyloid angiopathy
CADASIL	Cerebral Autosomal Dominant Arteriopathy with Subcortical Infarcts and Leukoencephalopathy
CARASAL	Cathepsin A-related arteriopathy with strokes and leukoencephalopathy
CARASIL	Cerebral Autosomal Recessive Arteriopathy with Subcortical Infarcts and Leukoencephalopathy
CBF	Cerebral blood flow
CCLs	Clodronate-containing liposomes
CNS	Central nervous systems
CPMs	Choroid plexus macrophages
CSF	Cerebrospinal fluid
cSVD	Cerebral small vessel disease
CV	Cardiovascular disease
DAMPs	Damaged-associated molecular patterns
DAPI	4', 6-diamino-2-phenylindole
DCE	Dynamic contrast-enhanced
DM	Diabetes mellitus
DOCA	Deoxycorticosterone acetate
ECs	Endothelial cells
EGF	Epidermal growth factor
ERK	Extracellular signal-regulated kinase
FLAIR	Fluid-attenuated inversion recovery
FOVs	Field of views
GFAP	Glial fibrillary acidic protein
HE	Hematoxylin and eosin
HFpEF	Heart failure with preserved ejection fraction
HMGB1	High-mobility group box 1
HTRA1	High temperature requirement protein A1

Iba-1	Ionized calcium-binding adapter molecule 1
IL	Interleukin
ISF	Interstitial fluid
KB	Klüver Barrera
MCI	Mild cognitive impairment
MetS	Metabolic syndrome
MMP	Matrix metalloproteinases
MMs	Meningeal macrophages
MRI	Magnetic resonance imaging
MS	Multiple sclerosis
NFκB	Nuclear factor kappa-light-chain-enhancer of activated B cells
NOTCH3	Notch homolog 3
NVU	Neurovascular unit
P2RY12	P2Y purinoceptor 12
PADMAL	Pontine Autosomal Dominant Microangiopathy and Leukoencephalopathy
PD	Parkinson's disease
PMG	Perivascular microglia
PVMs	Perivascular macrophages
RAGE	Receptor for AGEs
RCVL	Retinal vasculopathy with cerebral leukodystrophy
ROC	Receiver operating characteristic
ROS	Reactive oxygen species
SALL1	Sal-like protein 1
SHR	Spontaneously Hypertensive Rats
Siglec-H	Sialic acid-binding immunoglobulin-type lectins
SMCs	Smooth muscle cells
T2D	Type 2 diabetes
TBST	Tris-buffered saline with 0.1% Tween20
tMCAO	Transient middle cerebral artery occlusion
TMEM119	Transmembrane protein 119
TNF-α	Tumor necrosis factor- α
TREX1	Three prime exonuclease-1
VaD	Vascular dementia

VCI	Vascular cognitive impairment
WMH	White matter hyperintensity
WML	White Matter Lesions
ZSF-1	Zucker fatty/Spontaneously hypertensive heart failure F1 hybrid

Chapter 1

General Introduction

Takashi Koizumi

Worldwide, around 50 million people have dementia, and there are nearly 10 million new cases every year. The total number of people with dementia is projected to reach 82 million in 2030 and 152 in 2050¹. Alzheimer's Disease (AD) is the most common form of dementia and may contribute to 60–70% of cases. Other major forms include vascular dementia (VaD), dementia with Lewy bodies, and a group of diseases that contribute to frontotemporal dementia. The boundaries between different forms of dementia are indistinct and mixed forms often coexist.

Vascular cognitive impairment (VCI) refers to all forms of cognitive disorders affecting at least one cognitive domain, from mild cognitive impairment (MCI) to full-blown dementia, associated with a vascular origin². VaD is the second most prevalent form of dementia after AD and VaD accounts for at least 20% of dementia cases³. The prevalence of VCI, which includes milder forms of cognitive impairment, is strongly age related. In subjects aged 65 to 84 years, the prevalence of VCI patients with MCI is higher than that of VaD. Rates of conversion to dementia, institutionalization, and mortality are significantly increased in these patients, making the identification of VCI patients an important target population for prevention⁴. VCI/VaD can result from large-artery atherosclerosis or cardioembolic stroke, cerebral amyloid angiopathy (CAA), brain hemorrhages, brain hypoperfusion, and cerebral small vessel disease (cSVD)⁵, the latter being the most prevalent cause of VCI.

cSVD refers to a heterogeneous group of vascular disorders resulting from the pathological impairment of the small vessels in the brain⁶, including penetrating arterioles, parenchymal branching arterioles, capillaries, and venules of the brain. In a hospital-based cohort of individuals with cSVD, the 5.5-year cumulative risk of dementia was 11%, which indicates that cSVD might go unnoticed or result in only mild functional deficits in the majority of people⁷. The vascular changes in cSVD lead to lacunar infarcts, leukoaraiosis (White Matter Lesions: WMLs), dilated perivascular spaces (also known as the enlargement of the Virchow-Robin space), and cerebral microbleeds^{8,9}. They are clinically recognized as important contributors to dementia^{10,11}, lacunar stroke¹², gait disturbances¹³, depression¹⁴, and functional loss in the elderly¹⁵. Several hereditary forms of cSVD have been identified, such as CADASIL^{16,17}, CARASIL¹⁸, PADMAL^{19,20}, RCVL²¹, and CARASAL²², featuring specific small vessel impairments. The most prevalent form is sporadic cSVD which results from the exposure of intertwined environmental and cardiovascular risk factors. Ageing, hypertension, and diabetes have been shown to be strongly associated with cSVD^{8,23,24}.

Magnetic resonance imaging (MRI) is the sole imaging modality for the diagnosis of cSVD. Morphological brain abnormalities referring to pathologies, such as white matter hyperintensity (WMH), enlarged perivascular spaces, and

lacunar infarcts can be observed by fluid-attenuated inversion recovery (FLAIR) imaging on MRI²⁵. Microbleeds can be well detected by T2*WI or Susceptibility-weighted image²⁶. White matter integrity and damage can be estimated by diffusion tensor imaging^{27,28}. Recently, several studies indicated blood brain-barrier (BBB) permeability could be measured by arterial spin labeling MRI²⁹ or dynamic contrast-enhanced (DCE)-MRI³⁰. Although MRI protocols have been progressing allowing the detection of subtle BBB leakage or microinfarcts^{30,31} and have highlighted the detrimental effect of white matter abnormalities³², the problem remains that those abnormalities only reflect the pathological consequences of cSVD that can silently progress until the emergence of clinical symptoms including impairment of the cognitive function.

Although MRI and histological findings have improved our understanding of cSVD pathology, therapeutic approaches are missing because of our lack of mechanistic understanding of cSVD pathobiology. It becomes therefore urgent to elucidate the cellular and molecular mechanisms involved in the initiation and progression of cSVD to prevent or delay its occurrence. Several pathophysiological mechanisms are being studied, including the impact of small vessel arteriopathy and the development of BBB dysfunction, which can initiate the vessel wall vulnerability, the impairment of vascular clearance, the reduction of cerebral blood flow, as well as neuroinflammation³³ (Figure 1).

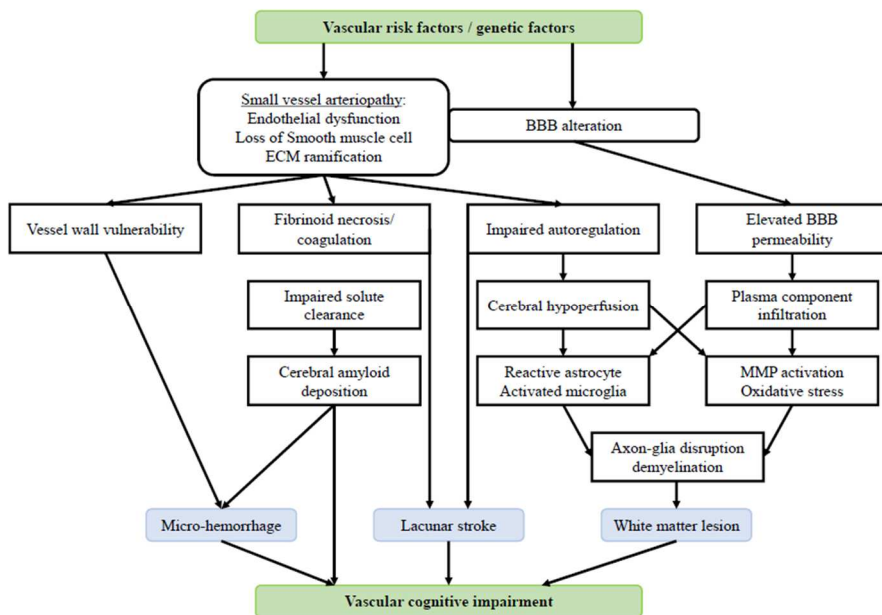


Figure 1. Mechanisms relevant to cerebral small vessel disease. Schematic representation of mechanisms relevant to cerebral small vessel disease (cSVD) and vascular cognitive impairment (VCI). A cascade of risk

factor leading events may cause VCI. BBB: blood brain barrier; ECM: extracellular matrix; MMP matrix metalloproteinase.

The anatomy of cerebral small vessels

The study of cSVD requires a good understanding of the structural organization of the cerebral small vessels and their surroundings. Pial arteries run on the brain surface in the subarachnoid space and give rise to smaller arterioles that penetrate into the brain. As penetrating deeper into the brain, cortical penetrating arterioles are branching, thinning, and convoluting before becoming capillaries (Figure2).

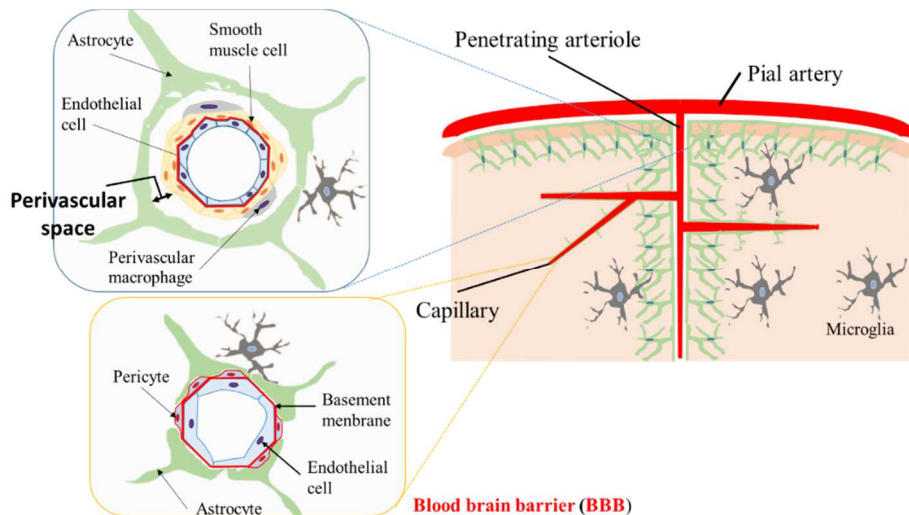


Figure 2. The illustration of cerebral small vessels. Cortical penetrating arterioles enter the brain and get thinner while branching deeper into the cortex. Penetrating arterioles are surrounded by endothelial cells, smooth muscle cells, basement membrane, perivascular spaces, and astrocyte endfeet. At the capillary level, smooth muscle cells and perivascular spaces are absent. Endothelial cells, basement membranes, and astrocyte endfeet form the so-called blood brain barrier.

Arterioles consist of endothelial cells (ECs) and smooth muscle cells (SMCs) and are surrounded by a basement membrane (BM), the perivascular space (known as Virchow Robin space), and astrocyte endfeet. As arterioles penetrate deeper into the brain, the SMCs layers and perivascular spaces disappear. In capillaries, astrocyte endfeet directly cover the basal side of ECs and pericytes appear sparsely between astrocyte endfeet and ECs³⁴. Cerebral veins have no muscular tissue in their thin walls and possess no valves contrary to systemic veins³⁵.

Brain ECs are key regulators of the vascular functions. Tight junctions and adherens junctions are fusing adjacent ECs and thus restrict paracellular

diffusion of ions, molecules and other solutes³⁶. In addition to this physical barrier, ECs regulate several functions; the vascular tone and the blood flow controlling via the production of numerous endothelial cell-derived vasoactive agents; fibrinolysis; coagulation; inflammations; and fibrosis³⁷. ECs dysfunction occurs before the onset of VaD³⁸ and can eventually lead to dysregulation of cerebral blood flow due to a decrease in the release of nitric oxide³⁹ and increase BBB permeability^{40,41}, followed by the activation of glia and inflammatory environment in the brain. It is therefore considered as one of the detrimental step leading to cSVD⁴².

At the level of Pial arteries and penetrating arterioles, SMCs are key players for the autoregulation of the cerebral blood flow⁴³. Layers of SMCs surround the penetrating arterioles and get progressively thinner while branching in the parenchyma, where only a monolayer of SMCs persists or even becomes discontinuous. At the capillary level, SMCs are completely absent.

BMs are located at the interface between ECs and astrocytes. The inner vascular BM is an extracellular matrix secreted by ECs, whereas the parenchymal BM is primarily secreted by astrocyte endfeet. BMs are comprised of different secreted molecules including type IV collagens, laminin, heparin sulfate proteoglycans and other glycoproteins. These BMs provide an anchor for many signaling processes as well as an additional physical barrier for molecules and cells before reaching the brain parenchyma³⁶. Disruption of these BMs by matrix metalloproteinases (MMP) is an important component of BBB dysfunction that allows the infiltration of leukocytes in many different neurological disorders^{44,45}.

Astrocyte endfeet almost completely sheath the vascular tube to form the glia limitans, a barrier that further limits movement of molecules across the BBB. Furthermore, astrocytes provide a cellular link between the neurons and ECs, the so-called neurovascular coupling that enables astrocytes to relay signals to regulate blood flow in response to neuronal activity⁴⁶. This includes the regulation of the contraction/dilation of vascular smooth muscle cells surrounding arterioles as well as pericytes surrounding capillaries⁴⁷. In addition, the most abundant water channel protein, aquaporin 4, is predominantly expressed in astrocytic end-feet surrounding central nervous systems (CNS) vessels and forms orthogonal arrays of particles in plasma membranes that are critical for regulating water homeostasis in the CNS⁴⁸.

Perivascular macrophages (PVMs) are derived from a monocyte lineage and sit on the abluminal side of the vascular tube commonly found in the Virchow–Robin space, a small fluid filled canal that lines the abluminal surface of the veins and arteries that enter/ leave the CNS⁴⁹. PVMs migrate from the yolk sac into the brain early in development and, like microglia, are likely to be a self-

renewing cell population that, in the normal state, is not replenished by circulating monocytes⁵⁰. Increasing evidence indicates that PVMs are involved in a wide variety of pathological cerebrovascular states in the brain, such as AD⁵¹, multiple sclerosis⁵², and cognitive dysfunction associated with hypertension⁵³.

Microglia are located in brain parenchyma and involved in regulating neuronal development, innate immune response, and wound healing, and can act as antigen-presenting cells in adaptive immunity⁵⁴. Microglia become activated under brain injury and immunological stimuli and undergo several alterations from a “resting state” to an “active state”. Recent studies suggest that microglial activation may be related to BBB disruption. For example, *in vivo* experiments using intra-hippocampal injections of A β in rat brains, microglial responses to A β could promote vascular changes that induced BBB breakdown plasma protein infiltration⁵⁵. In animal models of transient middle cerebral artery occlusion (tMCAO), numbers of anti-inflammatory M2-state microglia rapidly increase around vessels in the penumbra after infarction, and, in a few days, pro-inflammatory M1-state microglia dominantly increase. This process is called “M2-to-M1 phenotype-switching” or “shift in the M2-to-M1 phenotypes”^{56,57}.

Although the evidence of the involvement of microglia or PVMs in neurological diseases have been increasing, their role in cSVD remain unclear. In this thesis, we therefore aim to study perivascular immune cells during cSVD formation (Chapter 4 and 5)

Hereditary small vessel disease

Hereditary cSVD affects 5% of cSVD patients and is characterized by lacunar infarcts and white matter hyperintensities on MRI⁸. Several monogenic hereditary diseases causing cSVD and stroke have been identified. There are increasing numbers of reports on new monogenic syndromes causing cSVD; such as CADASIL, CARASIL, PADMAL, RCVL, hereditary cerebral hemorrhage with amyloidosis, and *forkhead box C1* mutation. The genetic cause of these syndromes, their pathology, clinical manifestation, imaging, and diagnosis criteria have been described in the last two decades. While some specific imaging features have been identified for some hereditary forms, their diagnosis cannot be solely based on imaging. Although their prevalence is low, the study of hereditary monogenic cSVD may help our understanding of sporadic cSVD and the mechanisms of cerebrovascular components.

CADASIL (Cerebral Autosomal Dominant Arteriopathy with Subcortical Infarcts and Leukoencephalopathy) has been mapped to *Notch homolog 3* (*NOTCH3*) gene located on chromosome 19p13.1 and all CADASIL mutations have been identified in exons 2–24 encoding the epidermal growth factor (EGF)-

like repeat domain^{16,58}. *NOTCH3* is only expressed in arterial smooth muscle cells albeit throughout the body, only cerebral arteriopathy causes symptoms⁵⁹. *NOTCH3* encodes a transmembrane receptor with an extracellular component with six cysteine residues. Mutations occur within EGF-like repeats and cause odd number cysteine repeats in the extracellular component⁶⁰. The odd numbered cysteine repeats leads to impaired signaling of the receptor⁶¹. Recent work with *NOTCH3* transgenic mouse models suggests that deposition of NOTCH3 protein and others, including TIMP3 (tissue inhibitor of metalloproteinase 3) as an extracellular matrix regulator, in cerebral blood vessels reduces maximal vasodilation capacity and attenuated myogenic tone of cerebral arteries, and thereby reduces cerebral blood flow⁶². Diagnosis criteria for CADASIL have been proposed by Davous et al.⁶³ and Mizuta et al.⁶⁴ Clinical signs include migraine, progressive WMLs at temporal lobes and external capsule, brain ischemic events, neurological symptoms, and mood disturbance, and it frequently leads to subcortical dementia⁶⁵.

CARASIL (Cerebral Autosomal Recessive Arteriopathy with Subcortical Infarcts and Leukoencephalopathy) is caused by mutation in the *high temperature requirement protein A1 (HTRA1)* on chromosome 10q, resulting in loss of function of HtrA1 serine protease activity that down-regulates TGF- β signaling^{18,66}. Histopathological findings have revealed that CARASIL is characterized by the loss of arterial smooth muscle cells and thinning of the arterial adventitial extra cellular matrix leading to both centrifugally enlargement and collapse of cerebral arteries, thereby compromising local blood flow⁶⁷. Clinical features are characterized by early-onset of gait and balance disturbance, lacunar stroke, WMLs, mood changes, dementia, and, typically, alopecia and spondylosis⁶⁸.

PADMAL (Pontine Autosomal Dominant Microangiopathy and Leukoencephalopathy) is an autosomal dominant disease caused by a mutation in an untranslated region of *COL4A1*, leading to upregulated expression of COL4A1²⁰. *COL4A1* is located on chromosome 13q34 coding for type IV collagen, a component of vascular basement membranes. *COL4A1* mutations are associated with systemic small vessel disease and various symptoms affecting especially the eyes, the muscles, the kidneys, and the brain; all very vascularized organs. The pathophysiology may be initiated by both an intracellular accumulation of collagen and by an extracellular deposition of defective collagen, causing the fragility of cerebral small vessels⁶⁹. These mutations are dominantly inherited and lead to structural instability of all basement membranes⁷⁰ and can cause hemorrhagic stroke¹⁹. The distinct MRI characteristics with pontine lesions and rare occurrence of temporal lesions differ from CADASIL⁷¹.

An increasing number of genes involved in hereditary cSVD are being reported. A variant *CTSA* gene, which encodes cathepsin A which is involved in the degradation of endothelin-1, was found in CARASAL (Cathepsin A-related arteriopathy with strokes and leukoencephalopathy) patients²². Frameshift mutations in the gene encoding truncated *three prime exonuclease-1 (TREX1)* are found in Patient with RVCL (Retinal vasculopathy with cerebral leukodystrophy)²¹. Gene mutations have been identified in the *A β Precursor Protein (APP)* gene and lead to the deposition of misfolded A β protein in vessel walls and brain parenchyma in HCHWA (Hereditary cerebral hemorrhage with amyloidosis)⁷². *Forkhead Box transcription factor C1 (FOXC1)* gene mutations lead to alteration of endothelial and pericyte proliferations and has been found to be associated with an impairment of the BBB integrity⁷³. A more extensive description of these genes and their contribution to cSVD has been reviewed elsewhere⁷⁴.

Beyond their important diagnostic value, the identification and study of genes involved in hereditary cSVD also contributes to our cellular and molecular understanding of the cerebrovascular dysfunction observed in sporadic cSVD. In this thesis, we perused crucial contributors for cSVD by comparing clinical information of CADASIL patients and CADASIL-suspected patients (Chapter 2).

Blood-brain barrier (BBB) dysfunction, the cradle of cSVD

Experimental and clinical investigations have suggested BBB dysfunction as one of the main pathological causes of cSVD initiation^{6,75,76}. BBB dysfunction leads to an enhanced barrier permeability that may allow blood components to infiltrate into the brain parenchyma thus altering brain homeostasis. Leaked components and damaged cells from the BBB may initiate over time an exaggerated neuroinflammatory reaction producing inflammatory cytokines and free radicals, thus creating a vicious circle by worsening BBB dysfunction⁷⁷. Several clinical studies have demonstrated that a compromised BBB integrity was associated with the characteristic abnormalities of cSVD on MRI. By applying DCE-MRI, a higher BBB permeability was identified in cSVD patients³⁰. The volume of WMH on FLAIR image was associated with the volume of BBB leakage image by DCE-MRI⁷⁸. Total MRI cSVD burden score with the presence of lacunes, WMH, cerebral microbleeds, and enlarged perivascular spaces were associated with compromised BBB integrity⁷⁹. Those results indicate that BBB dysfunction could be a crucial contributor to cSVD pathology. BBB dysfunction is associated with a pro-oxidative and pro-inflammatory environment generated by a complex set of interactions including the presence of vascular risk factors, inflammatory diseases, brain hypoperfusion, and hereditary factors^{8,36,80}. While many different triggers are able to initiate

BBB dysfunction experimentally, the exact risks and outcomes due to the exposure of different triggers remain difficult to assess in humans.

The link between vascular risk factors and cSVD pathology

Epidemiological investigations indicate that vascular risk factors, such as aging, diabetes, and hypertension in particular, are strongly associated with cSVD^{8,81}. To a broader extent, similar evidences have confirmed hypertension and diabetes as risk factors for VCI^{2,3}. In a population-based study, an average follow-up of 21 years in subjects aged 65 to 79 years showed that the effect of systolic blood pressure in midlife was a significant risk factor in the development of MCI in the late life⁸². In the Rotterdam scan study, aged 60 to 90 years people underwent repeated MRI scanning and neuropsychological testing within 3-year follow-up. Older age and high blood pressure were independently associated with progression of WMLs²³.

Hypertension is the most leading cause of sporadic cSVD. The impact of hypertension on cSVD has been studied in a range of experimental models. Studies using Spontaneously Hypertensive Rats (SHR), a chronic model of hypertension, have revealed the presence of BBB leakages in the absence of ischemic and hemorrhagic injuries⁸³. At 12-week, intraluminal accumulations of erythrocytes were evidenced within capillaries⁶, while Evans blue extravasation was first observed in 20-week, with cognitive decline onset in 30-week old SHR rats⁸⁴. In a prolonged Angiotensin II-mediated hypertension mice, the number of BBB leakages was increased and were associated with microglial activation and an impairment of short-term memory⁸⁵. Other studies with hypertensive animals have also reported that decreased occludin and zonula occludens-1 expressions with the ultrastructural changes of tight junctions, as determined by electron microscopy might induce WMLs⁸⁶. Those results suggest that hypertension-induced BBB impairment occurs prior to the emergence of cognitive dysfunction. Hypertension could induce neuroinflammation. Circulating inflammatory molecules; tumor necrosis factor- α (TNF- α), C-reactive protein, interleukin (IL)-6, monocyte chemoattractant protein-1, and IL-1 β , have all been found to be upregulated in both hypertensive patients and hypertensive animal models⁸⁷. In angiotensin II-induced hypertensive rat, microglia are activated with correlation to BBB leakage and clinical cognitive impairments⁸⁵. In renal hypertension rats by partial occlusion of the left renal artery, hypertension increased the expression of adhesion molecules like JAM-1, ICAM-1, and VCAM-1 on brain endothelium and resulted in the deposition of platelets in the brain. Platelet deposition in hypertensive rats was associated with augmented CD40 and CD40L and activation of astrocytes and microglia in the brain⁸⁸. In SHR, the expression of the pro-inflammatory interleukins (IL-1b, IL-6) and TNF- α increased in SHR brain, and activation of astrocytes and microglia in the brain were observed⁸⁹.

While activated microglia in parenchyma were observed in the animal models of hypertension⁸⁴ and lacunar stroke patients increased monocyte/macrophage activation relate to cSVD manifestation⁹⁰, it remains unclear that inflammation is cause or result of BBB dysfunction in sporadic cSVD.

Diabetes mellitus (DM) is the second most frequent risk factor associated with cerebrovascular dysfunction^{2,91-93}. Magnetic resonance imaging of type 2 diabetic (T2D) patients showed an increased BBB permeability to gadolinium diethylenetriamine pentaacetic acid (DTPA; 570 Da)⁹⁴. In another MRI study involving T2D patients, a more global brain atrophy was observed that increased gradually over time compared with normal aging²⁴. T2D has been related to a reduction of cerebral blood flow and a reduced cerebrovascular reactivity, particularly in advanced diabetic stages²⁴. In streptozotocin-injected rats, a type 1 diabetes animal model, a progressive increase in BBB permeability was observed after 28 days. In addition, this study showed that insulin treatment was able to attenuate BBB disruption, especially during the first few weeks of the disease. However, while the disease progressed, microvascular damages were observed even when hyperglycemia was controlled⁹⁵. Hyperglycemia in DM results in increased inflammation and a number of complications including retinopathy, nephropathy, neuropathy, and dysfunction of the BBB⁹³. Microglia activation was also observed in diabetic retinopathy.

Over the years, the prevalence of the metabolic syndrome (MetS) has drastically increased not only in the elderly but also in the young population. According to the new International Diabetes Federation definition, for a person to be defined as having the metabolic syndrome they have: central obesity plus any two of the following four factors: raised triglycerides, reduced HDL cholesterol, raised blood pressure, and raised fasting plasma glucose⁹⁶. The cardiovascular risk associated with the MetS varies on the basis of the combination of risk factors present⁹⁷. MetS was associated with an increased risk of white matter lesion in MetS patients. Amongst MetS components, elevated blood pressure, elevated fasting blood glucose and low high density lipoprotein cholesterol were associated with periventricular WMLs, while elevated blood pressure and low high density lipoprotein cholesterol were related to deep WMLs⁹⁸. The use of experimental models mimicking the human MetS is detrimental to understand if and how the combination of cardiovascular risk factors can further accelerate the initiation and progression of cSVD. While most animal studies on MetS are dedicated to atherosclerosis research, we aimed to study the contribution of MetS to cSVD in a rat model of MetS in chapter 5.

Perivascular immune cells: important players in the Neuro-glial-vascular interaction

The concept of neurovascular unit (NVU) emerged from the first Stroke Progress Review Group meeting of the National Institute of Neurological Disorders and Stroke of the NIH (July 2001) to emphasize the unique relationship between brain cells and the cerebral vasculature. At this time, less attention was paid on the presence and function of perivascular immune cells, including perivascular macrophages (PVMs) and microglia. As cerebrovascular dysfunction is being recognized of importance for the initiation and progression of neurodegenerative diseases, more attention is being paid to these perivascular immune cells due to their close location with cerebral vessels.

Microglia are resident brain immune cells present throughout the whole brain parenchyma and they play crucial roles to maintain brain homeostasis. Under physiological conditions, microglia are constantly monitoring their surroundings in the CNS with their fine ramified motile processes⁹⁹. Once these cells encounter harmful substances, such as infiltrating components from blood, burden abnormal proteins, or cell debris, they become activated to phagocytose these harmful substances or to ameliorate the damaged cells⁵⁷. Our knowledge on parenchymal microglia and their activation dynamics is increasing in several neurological diseases¹⁰⁰, from acute ischemic stroke⁵⁶ to chronic neurodegenerative diseases^{101,102}. The activated parenchymal microglia show a biphasic influence, promoting beneficial repair and causing harmful damage. Those responsible for the former are sometimes referred to as anti-inflammatory M2 microglia, and the latter as pro-inflammatory M1 microglia¹⁰³. These different phenotypes have been attempted to be distinguished based on the expression of specific markers¹⁰³. A widely consensus examples as cell surface markers are CD68 for M1-state¹⁰⁴ and CD206 for M2-state^{56,104}, and as cytokines are inducible nitric oxide synthase (iNOS) for M1-state^{56,105} and Arginase-1 for M2-state⁵⁶. Microglia activation in the acute phase of ischemic stroke has been well studied in animal models of tMCAO^{104,106}. In the tMCAO model, numbers of M2-state microglia rapidly increase around vessels in the penumbra after infarction, and, in a few days, M1-state microglia dominantly increase. This process is called "M2-to-M1 phenotype-switching"⁵⁶.

Although the interaction of microglia with cerebral vessels has gained importance in the context of acute ischemia and angiogenesis¹⁰⁷⁻¹⁰⁹, the exact fate of perivascular immune cells during chronic injuries remained unclear. In that respect, we should differentiate parenchymal microglia from vascular-related microglia. We named the latter perivascular microglia (PMG) located outside of glia limitans in opposition to perivascular macrophages (PVMs) located in the

perivascular spaces. Although PMG are juxtaposed to the vessel walls, their interplay with the cerebral vessels has not been explored in the context of cSVD.

Macrophages in the CNS are involved in the maintenance of brain border's homeostasis. They reside in the non-parenchymal perivascular space, subdural meningeal spaces, and choroid plexus spaces — namely PVMs, meningeal macrophages, and choroid plexus macrophages respectively. Due to an emerging hypothesis suggesting the presence of a lymphatic drainage in perivascular spaces¹¹⁰, called “glymphatic” pathway¹¹¹, PVMs could possibly be of importance to screen early changes both in the systemic and the parenchymal environments. The role of PVMs in cSVD has also been largely underexplored.

Finally, as microglia and macrophages share many functions and markers, most studies did not differentiate PVMs from microglia including PMG. However, current state-of-the-art techniques provide now new opportunities to differentiate PVMs and PMG and to understand their respective roles in the initiation and progression of BBB dysfunction (Chapter 3).

Thesis aim and outline

The general aim of this thesis was to investigate the genetic and neuroinflammatory mechanisms that contribute to the development of familial and sporadic cerebral small vessel disease (cSVD). To address this aim, a hereditary form (CADASIL) and sporadic forms of cSVD were studied using respectively cohorts of patients and animal models.

This general aim is addressed by several objectives:

1) To distinguish hereditary and sporadic cSVD accurately. This is of importance for patients to prevent the worsening of their symptoms and to adjust their life styles. We established a score to prioritize the genetic testing of CADASIL-suspected patients (Chapter 2).

2) To summarize the knowledge on brain perivascular immune cells and discuss their involvement in cerebrovascular diseases and more specifically in cSVD. To clarify and distinguish between microglia and brain macrophages. Till recently a clear distinction has not been made between both perivascular immune cells. Hence, we have summarized the current knowledge and highlighted some knowledge gaps on the interaction between perivascular immune cells and cerebrovascular dysfunction and cSVD (Chapter 3).

3) To study the dynamics of perivascular microglia in hypertensive cSVD using a chronic hypertension model, the deoxycorticosterone acetate (DOCA)-salt rat. Activated microglia show a biphasic influence, promoting beneficial repair and causing harmful damage via M2 and M1 microglia, respectively. In acute ischemic models, microglia are known to be initially activated to the M2-state and subsequently switch to the M1-state, namely M2-to-M1 class-switching. However, the microglia dynamics in cSVD is poorly understood (Chapter 4).

4) To study the impact of co-morbidities on the behavior of perivascular immune cells in an animal model of the metabolic syndrome. While in Chapter 4 we studied the sole impact of hypertension on microglial dynamics, its effect in combination with diabetes and obesity on the phenotype of perivascular immune cells is unknown. In this study, we characterized the phenotype of perivascular microglia and perivascular macrophages in the Zucker fatty/Spontaneously hypertensive heart failure F1 hybrid (ZSF-1) rat (Chapter 5).

In Chapter 6, the main findings of this thesis are discussed, concluded and presented with an emphasis on societal issues.

References

1. WHO. Home/ News/ Fact sheets/ Detail/ Dementia. 2019 [cited 2019 30 May]; Available from: <https://www.who.int/en/news-room/fact-sheets/detail/dementia>.
2. Dichgans M, Leys D. Vascular Cognitive Impairment. *Circ Res*. 2017 Feb 3;120(3):573-91.
3. Gorelick PB, Scuteri A, Black SE, et al. Vascular contributions to cognitive impairment and dementia: a statement for healthcare professionals from the american heart association/american stroke association. *Stroke*. 2011 Sep;42(9):2672-713.
4. Dichgans M, Zietemann V. Prevention of vascular cognitive impairment. *Stroke*. 2012 Nov;43(11):3137-46.
5. Iadecola C. The pathobiology of vascular dementia. *Neuron*. 2013 Nov 20;80(4):844-66.
6. Schreiber S, Bueche CZ, Garz C, Braun H. Blood brain barrier breakdown as the starting point of cerebral small vessel disease? - New insights from a rat model. *Exp Transl Stroke Med*. 2013;5(1):4.
7. van Uden IW, van der Holst HM, Tuladhar AM, et al. White Matter and Hippocampal Volume Predict the Risk of Dementia in Patients with Cerebral Small Vessel Disease: The RUN DMC Study. *J Alzheimers Dis*. 2016;49(3):863-73.
8. Pantoni L. Cerebral small vessel disease: from pathogenesis and clinical characteristics to therapeutic challenges. *The Lancet Neurology*. 2010 Jul;9(7):689-701.
9. Rouhl RP, van Oostenbrugge RJ, Knottnerus IL, Staals JE, Lodder J. Virchow-Robin spaces relate to cerebral small vessel disease severity. *Journal of neurology*. 2008 May;255(5):692-6.
10. Ter Telgte A, van Leijsen EMC, Wiegertjes K, Klijn CJM, Tuladhar AM, de Leeuw FE. Cerebral small vessel disease: from a focal to a global perspective. *Nat Rev Neurol*. 2018 Jul;14(7):387-98.
11. Inzitari D, Pracucci G, Poggesi A, et al. Changes in white matter as determinant of global functional decline in older independent outpatients: three year follow-up of LADIS (leukoaraiosis and disability) study cohort. *BMJ (Clinical research ed)*. 2009 Jul 6;339:b2477.
12. Greenberg SM. Small vessels, big problems. *N Engl J Med*. 2006 Apr 6;354(14):1451-3.
13. Baezner H, Blahak C, Poggesi A, et al. Association of gait and balance disorders with age-related white matter changes: the LADIS study. *Neurology*. 2008 Mar 18;70(12):935-42.
14. Grool AM, Gerritsen L, Zuithoff NP, Mali WP, van der Graaf Y, Geerlings MI. Lacunar infarcts in deep white matter are associated with higher and more fluctuating depressive symptoms during three years follow-up. *Biological psychiatry*. 2013 Jan 15;73(2):169-76.
15. Ueno M, Chiba Y, Matsumoto K, et al. Blood-brain barrier damage in vascular dementia. *Neuropathology*. 2016 Apr;36(2):115-24.
16. Joutel A, Corpechot C, Ducros A, et al. Notch3 mutations in CADASIL, a hereditary adult-onset condition causing stroke and dementia. *Nature*. 1996 Oct 24;383(6602):707-10.
17. Mizuno T. [Diagnosis, pathomechanism and treatment of CADASIL]. *Rinsho Shinkeigaku*. 2012;52(5):303-13.
18. Hara K, Shiga A, Fukutake T, et al. Association of HTRA1 mutations and familial ischemic cerebral small-vessel disease. *N Engl J Med*. 2009 Apr 23;360(17):1729-39.
19. Gould DB, Phalan FC, van Mil SE, et al. Role of COL4A1 in small-vessel disease and hemorrhagic stroke. *N Engl J Med*. 2006 Apr 6;354(14):1489-96.
20. Verdura E, Herve D, Bergametti F, et al. Disruption of a miR-29 binding site leading to COL4A1 upregulation causes pontine autosomal dominant microangiopathy with leukoencephalopathy. *Ann Neurol*. 2016 Nov;80(5):741-53.
21. Richards A, van den Maagdenberg AM, Jen JC, et al. C-terminal truncations in human 3'-5' DNA exonuclease TREX1 cause autosomal dominant retinal vasculopathy with cerebral leukodystrophy. *Nat Genet*. 2007 Sep;39(9):1068-70.
22. Bugiani M, Kevelam SH, Bakels HS, et al. Cathepsin A-related arteriopathy with strokes and leukoencephalopathy (CARASAL). *Neurology*. 2016 Oct 25;87(17):1777-86.
23. van Dijk EJ, Prins ND, Vrooman HA, Hofman A, Koudstaal PJ, Breteler MM. Progression of cerebral small vessel disease in relation to risk factors and cognitive consequences: Rotterdam Scan study. *Stroke*. 2008 Oct;39(10):2712-9.
24. Brundel M, Kappelle LJ, Biessels GJ. Brain imaging in type 2 diabetes. *European Neuropsychopharmacology*. 2014 2014/12/01;24(12):1967-81.
25. Wardlaw JM, Smith EE, Biessels GJ, et al. Neuroimaging standards for research into small vessel disease and its contribution to ageing and neurodegeneration. *The Lancet Neurology*. 2013 Aug;12(8):822-38.
26. Shams S, Martola J, Cavallin L, et al. SWI or T2*: Which MRI Sequence to Use in the Detection of Cerebral Microbleeds? The Karolinska Imaging Dementia Study. *American Journal of Neuroradiology*. 2015;36(6):1089-95.

27. Salat DH. Imaging small vessel-associated white matter changes in aging. *Neuroscience*. 2014 Sep 12;276:174-86.
28. Zeestraten EA, Benjamin P, Lambert C, et al. Application of Diffusion Tensor Imaging Parameters to Detect Change in Longitudinal Studies in Cerebral Small Vessel Disease. *PLoS One*. 2016;11(1):e0147836.
29. Tiwari YV, Lu J, Shen Q, Cerqueira B, Duong TQ. Magnetic resonance imaging of blood-brain barrier permeability in ischemic stroke using diffusion-weighted arterial spin labeling in rats. *J Cereb Blood Flow Metab*. 2017 Aug;37(8):2706-15.
30. Wong SM, Jansen JFA, Zhang CE, et al. Measuring subtle leakage of the blood-brain barrier in cerebrovascular disease with DCE-MRI: Test-retest reproducibility and its influencing factors. *Journal of Magnetic Resonance Imaging*. 2017;46(1):159-66.
31. De Cocker LJ, Lindenholz A, Zwaneburg JJ, et al. Clinical vascular imaging in the brain at 7T. *NeuroImage*. 2018 Mar;168:452-8.
32. Schmidt R, Seiler S, Loitfelder M. Longitudinal change of small-vessel disease-related brain abnormalities. *Journal of Cerebral Blood Flow & Metabolism*. 2016;36(1):26-39.
33. Horsburgh K, Wardlaw JM, van Agtmael T, et al. Small vessels, dementia and chronic diseases - molecular mechanisms and pathophysiology. *Clin Sci (Lond)*. 2018 Apr 30;132(8):851-68.
34. Iadecola C. The Neurovascular Unit Coming of Age: A Journey through Neurovascular Coupling in Health and Disease. *Neuron*. 2017 Sep 27;96(1):17-42.
35. Kilic T, Akakin A. Anatomy of cerebral veins and sinuses. *Frontiers of neurology and neuroscience*. 2008;23:4-15.
36. Daneman R, Prat A. The blood-brain barrier. *Cold Spring Harbor perspectives in biology*. 2015 Jan;7(1):a020412.
37. Michiels C. Endothelial cell functions. *J Cell Physiol*. 2003 Sep;196(3):430-43.
38. Wang F, Cao Y, Ma L, Pei H, Rausch WD, Li H. Dysfunction of Cerebrovascular Endothelial Cells: Prelude to Vascular Dementia. *Front Aging Neurosci*. 2018;10:376.
39. Attwell D, Buchan AM, Chappak S, Lauritzen M, Macvicar BA, Newman EA. Glial and neuronal control of brain blood flow. *Nature*. 2010 Nov 11;468(7321):232-43.
40. Argaw AT, Zhang Y, Snyder BJ, et al. IL-1beta regulates blood-brain barrier permeability via reactivation of the hypoxia-angiogenesis program. *J Immunol*. 2006 Oct 15;177(8):5574-84.
41. Fleegal-DeMotta MA, Doghu S, Banks WA. Angiotensin II modulates BBB permeability via activation of the AT(1) receptor in brain endothelial cells. *J Cereb Blood Flow Metab*. 2009 Mar;29(3):640-7.
42. Hainsworth AH, Oommen AT, Bridges LR. Endothelial Cells and Human Cerebral Small Vessel Disease. *Brain Pathology*. 2015;25(1):44-50.
43. Pointhevin M, Lozeron P, Hilal R, Levy BI, Merkulova-Rainon T, Kubis N. Smooth muscle cell phenotypic switching in stroke. *Translational stroke research*. 2014 Jun;5(3):377-84.
44. Chaturvedi M, Kaczmarek L. Mmp-9 inhibition: a therapeutic strategy in ischemic stroke. *Mol Neurobiol*. 2014 Feb;49(1):563-73.
45. Kook SY, Seok Hong H, Moon M, Mook-Jung I. Disruption of blood-brain barrier in Alzheimer disease pathogenesis. *Tissue barriers*. 2013 Apr 1;1(2):e23993.
46. Abbott NJ, Rönnbäck L, Hansson E. Astrocyte-endothelial interactions at the blood-brain barrier. *Nature Reviews Neuroscience*. 2006 01/01/online;7:41.
47. MacVicar BA, Newman EA. Astrocyte regulation of blood flow in the brain. *Cold Spring Harbor perspectives in biology*. 2015 Mar 27;7(5).
48. Keane J, Campbell M. The dynamic blood-brain barrier. *The FEBS Journal*. 2015;282(21):4067-79.
49. Lapenna A, De Palma M, Lewis CE. Perivascular macrophages in health and disease. *Nature reviews Immunology*. 2018 Nov;18(11):689-702.
50. Goldmann T, Wieghofer P, Jordao MJ, et al. Origin, fate and dynamics of macrophages at central nervous system interfaces. *Nat Immunol*. 2016 Jul;17(7):797-805.
51. Park L, Uekawa K, Garcia-Bonilla L, et al. Brain Perivascular Macrophages Initiate the Neurovascular Dysfunction of Alzheimer Abeta Peptides. *Circ Res*. 2017 Jul 21;121(3):258-69.
52. Poffliet MM, van de Veerdonk F, Dopp EA, et al. The role of perivascular and meningeal macrophages in experimental allergic encephalomyelitis. *J Neuroimmunol*. 2002 Jan;122(1-2):1-8.
53. Faraco G, Sugiyama Y, Lane D, et al. Perivascular macrophages mediate the neurovascular and cognitive dysfunction associated with hypertension. *J Clin Invest*. 2016 Dec 1;126(12):4674-89.
54. Ajami B, Bennett JL, Krieger C, Tetzlaff W, Rossi FM. Local self-renewal can sustain CNS microglia maintenance and function throughout adult life. *Nat Neurosci*. 2007 Dec;10(12):1538-43.
55. Ryu JK, McLarnon JG. A leaky blood-brain barrier, fibrinogen infiltration and microglial reactivity in inflamed Alzheimer's disease brain. *J Cell Mol Med*. 2009 Sep;13(9a):2911-25.

56. Hu X, Li P, Guo Y, et al. Microglia/macrophage polarization dynamics reveal novel mechanism of injury expansion after focal cerebral ischemia. *Stroke*. 2012 Nov;43(11):3063-70.
57. Hu X, Leak RK, Shi Y, et al. Microglial and macrophage polarization[mdash]new prospects for brain repair. *Nat Rev Neurol*. 2015 01//print;11(1):56-64.
58. Federico A, Bianchi S, Dotti MT. The spectrum of mutations for CADASIL diagnosis. *Neurol Sci*. 2005 Jun;26(2):117-24.
59. Joutel A, Corpechot C, Ducros A, et al. Notch3 mutations in cerebral autosomal dominant arteriopathy with subcortical infarcts and leukoencephalopathy (CADASIL), a mendelian condition causing stroke and vascular dementia. *Ann N Y Acad Sci*. 1997 Sep 26;826:213-7.
60. Dichgans M, Ludwig H, Müller-Höcker J, Messerschmidt A, Gasser T. Small in-frame deletions and missense mutations in CADASIL: 3D models predict misfolding of Notch3v EGF-like repeat domains. *European Journal of Human Genetics*. 2000 2000/04/01;8(4):280-5.
61. Joutel A, Monet M, Domenga V, Riant F, Tournier-Lasserre E. Pathogenic Mutations Associated with Cerebral Autosomal Dominant Arteriopathy with Subcortical Infarcts and Leukoencephalopathy Differently Affect Jagged1 Binding and Notch3 Activity via the RBP/JK Signaling Pathway. *The American Journal of Human Genetics*. 2004 2004/02/01;74(2):338-47.
62. Baron-Menguy C, Domenga-Denier V, Ghezali L, Faraci FM, Joutel A. Increased Notch3 Activity Mediates Pathological Changes in Structure of Cerebral Arteries. *Hypertension*. 2017;69(1):60-70.
63. Davous P. CADASIL: a review with proposed diagnostic criteria. *Eur J Neurol*. 1998 May;5(3):219-33.
64. Mizuta I, Watanabe-Hosomi A, Koizumi T, et al. New diagnostic criteria for cerebral autosomal dominant arteriopathy with subcortical infarcts and leukoencephalopathy in Japan. *J Neurol Sci*. 2017 Oct 15;381:62-7.
65. Chabriat H, Joutel A, Dichgans M, Tournier-Lasserre E, Bousser MG. Cadasil. *The Lancet Neurology*. 2009 Jul;8(7):643-53.
66. Beaufort N, Scharer E, Kremmer E, et al. Cerebral small vessel disease-related protease HtrA1 processes latent TGF- β binding protein 1 and facilitates TGF- β signaling. *Proceedings of the National Academy of Sciences*. 2014;111(46):16496-501.
67. Oide T, Nakayama H, Yanagawa S, Ito N, Ikeda S-i, Arima K. Extensive loss of arterial medial smooth muscle cells and mural extracellular matrix in cerebral autosomal recessive arteriopathy with subcortical infarcts and leukoencephalopathy (CARASIL). *Neuropathology*. 2008;28(2):132-42.
68. Fukutake T, Hirayama K. Familial young-adult-onset arteriosclerotic leukoencephalopathy with alopecia and lumbago without arterial hypertension. *Eur Neurol*. 1995;35(2):69-79.
69. Kuo DS, Labelle-Dumais C, Gould DB. COL4A1 and COL4A2 mutations and disease: insights into pathogenic mechanisms and potential therapeutic targets. *Human Molecular Genetics*. 2012;21(R1):R97-R110.
70. Van Agtmael T, Schlötzer-Schrehardt U, McKie L, et al. Dominant mutations of Col4a1 result in basement membrane defects which lead to anterior segment dysgenesis and glomerulopathy. *Human Molecular Genetics*. 2005;14(21):3161-8.
71. Ding XQ, Hagel C, Ringelstein EB, et al. MRI features of pontine autosomal dominant microangiopathy and leukoencephalopathy (PADMAL). *Journal of neuroimaging : official journal of the American Society of Neuroimaging*. 2010 Apr;20(2):134-40.
72. Mehndiratta P, Manjila S, Ostergard T, et al. Cerebral amyloid angiopathy-associated intracerebral hemorrhage: pathology and management. 2012;32(4):E7.
73. French CR, Seshadri S, Destefano AL, et al. Mutation of FOXC1 and PITX2 induces cerebral small-vessel disease. *The Journal of Clinical Investigation*. 2014 11/03;124(11):4877-81.
74. Rutten-Jacobs LCA, Rost NS. Emerging insights from the genetics of cerebral small-vessel disease. *Ann N Y Acad Sci*. 2019 Jan 8.
75. Hainsworth AH, Markus HS. Do in vivo experimental models reflect human cerebral small vessel disease? A systematic review. *J Cereb Blood Flow Metab*. 2008 Dec;28(12):1877-91.
76. Huang J, Li J, Feng C, et al. Blood-Brain Barrier Damage as the Starting Point of Leukoaraiosis Caused by Cerebral Chronic Hypoperfusion and Its Involved Mechanisms: Effect of Agrin and Aquaporin-4. *Biomed Res Int*. 2018;2018:2321797.
77. da Fonseca AC, Matias D, Garcia C, et al. The impact of microglial activation on blood-brain barrier in brain diseases. *Front Cell Neurosci*. 2014;8:362.
78. Zhang CE, Wong SM, van de Haar HJ, et al. Blood-brain barrier leakage is more widespread in patients with cerebral small vessel disease. *Neurology*. 2017 Jan 31;88(5):426-32.
79. Li Y, Li M, Zuo L, et al. Compromised Blood-Brain Barrier Integrity Is Associated With Total Magnetic Resonance Imaging Burden of Cerebral Small Vessel Disease. *Frontiers in neurology*. 2018;9:221.
80. Li Q, Yang Y, Reis C, et al. Cerebral Small Vessel Disease. *Cell Transplant*. 2018 Dec;27(12):1711-22.

81. Longstreth WT, Jr., Manolio TA, Arnold A, et al. Clinical correlates of white matter findings on cranial magnetic resonance imaging of 3301 elderly people. The Cardiovascular Health Study. *Stroke*. 1996 Aug;27(8):1274-82.
82. Kivipelto M, Helkala EL, Hanninen T, et al. Midlife vascular risk factors and late-life mild cognitive impairment: A population-based study. *Neurology*. 2001 Jun 26;56(12):1683-9.
83. Ueno M, Sakamoto H, Tomimoto H, et al. Blood-brain barrier is impaired in the hippocampus of young adult spontaneously hypertensive rats. *Acta Neuropathologica*. 2004;107(6):532-8.
84. Kaiser D, Weise G, Moller K, et al. Spontaneous white matter damage, cognitive decline and neuroinflammation in middle-aged hypertensive rats: an animal model of early-stage cerebral small vessel disease. *Acta Neuropathol Commun*. 2014 Dec 18;2(1):169.
85. Foulquier S, Namsolleck P, Van Hagen BT, et al. Hypertension-induced cognitive impairment: insights from prolonged angiotensin II infusion in mice. *Hypertension research : official journal of the Japanese Society of Hypertension*. 2018 Oct;41(10):817-27.
86. Fan Y, Yang X, Tao Y, Lan L, Zheng L, Sun J. Tight junction disruption of blood-brain barrier in white matter lesions in chronic hypertensive rats. *Neuroreport*. 2015 Dec 2;26(17):1039-43.
87. Coffman TM. Under pressure: the search for the essential mechanisms of hypertension. *Nat Med*. 2011 Nov 7;17(11):1402-9.
88. Bhat SA, Goel R, Shukla R, Hanif K. Platelet CD40L induces activation of astrocytes and microglia in hypertension. *Brain Behav Immun*. 2017 Jan;59:173-89.
89. Tayebati SK, Tomassoni D, Amenta F. Neuroinflammatory Markers in Spontaneously Hypertensive Rat Brain: An Immunohistochemical Study. *CNS Neurol Disord Drug Targets*. 2016;15(8):995-1000.
90. Rouhl RP, Damoiseaux JG, Lodder J, et al. Vascular inflammation in cerebral small vessel disease. *Neurobiol Aging*. 2012 Aug;33(8):1800-6.
91. Feit-Leichman RA, Kinouchi R, Takeda M, et al. Vascular damage in a mouse model of diabetic retinopathy: relation to neuronal and glial changes. *Invest Ophthalmol Vis Sci*. 2005 Nov;46(11):4281-7.
92. Kayano R, Morofuji Y, Nakagawa S, et al. In vitro analysis of drugs that improve hyperglycemia-induced blood-brain barrier dysfunction. *Biochem Biophys Res Commun*. 2018 Sep 10;503(3):1885-90.
93. Van Dyken P, Lacoste B. Impact of Metabolic Syndrome on Neuroinflammation and the Blood-Brain Barrier. *Front Neurosci*. 2018;12:930.
94. Starr JM, Wardlaw J, Ferguson K, MacLulich A, Deary IJ, Marshall I. Increased blood-brain barrier permeability in type II diabetes demonstrated by gadolinium magnetic resonance imaging. *J Neurol Neurosurg Psychiatry*. 2003 Jan;74(1):70-6.
95. Huber JD, VanGilder RL, Houser KA. Streptozotocin-induced diabetes progressively increases blood-brain barrier permeability in specific brain regions in rats. *Am J Physiol Heart Circ Physiol*. 2006 Dec;291(6):H2660-8.
96. IDF. IDF Consensus Worldwide Definition of the Metabolic Syndrome. [cited 2019 31 May]; Available from: <https://www.idf.org/e-library/consensus-statements/60-idfconsensus-worldwide-definition-of-the-metabolic-syndrome>.
97. Franco OH, Massaro JM, Civil J, Cobain MR, O'Malley B, D'Agostino RB, Sr. Trajectories of entering the metabolic syndrome: the framingham heart study. *Circulation*. 2009 Nov 17;120(20):1943-50.
98. Yin Z-G, Cui M, Zhou S-M, Yu M-M, Li R, Zhou H-D. Association between metabolic syndrome and white matter lesions in middle-aged and elderly patients. *European Journal of Neurology*. 2014;21(7):1032-9.
99. Nimmerjahn A, Kirchhoff F, Helmchen F. Resting microglial cells are highly dynamic surveillants of brain parenchyma in vivo. *Science*. 2005 May 27;308(5726):1314-8.
100. Salter MW, Stevens B. Microglia emerge as central players in brain disease. *Nat Med*. 2017 09/print;23(9):1018-27.
101. Keren-Shaul H, Spinrad A, Weiner A, et al. A Unique Microglia Type Associated with Restricting Development of Alzheimer's Disease. *Cell*. 2017 Jun 15;169(7):1276-90.e17.
102. Deczkowska A, Keren-Shaul H, Weiner A, Colonna M, Schwartz M, Amit I. Disease-Associated Microglia: A Universal Immune Sensor of Neurodegeneration. *Cell*. 2018 May 17;173(5):1073-81.
103. Franco R, Fernandez-Suarez D. Alternatively activated microglia and macrophages in the central nervous system. *Prog Neurobiol*. 2015 Jun 8.
104. Perego C, Fumagalli S, De Simoni MG. Temporal pattern of expression and colocalization of microglia/macrophage phenotype markers following brain ischemic injury in mice. *J Neuroinflammation*. 2011 Dec 10;8:174.
105. David S, Kroner A. Repertoire of microglial and macrophage responses after spinal cord injury. *Nat Rev Neurosci*. 2011 Jul;12(7):388-99.

106. Erdo F, Trapp T, Mies G, Hossmann KA. Immunohistochemical analysis of protein expression after middle cerebral artery occlusion in mice. *Acta Neuropathol.* 2004 Feb;107(2):127-36.
107. Zhao X, Eyo UB, Murugan M, Wu LJ. Microglial interactions with the neurovascular system in physiology and pathology. *Developmental neurobiology.* 2018 Jun;78(6):604-17.
108. Dudvarski Stankovic N, Teodorczyk M, Ploen R, Zipp F, Schmidt MH. Microglia-blood vessel interactions: a double-edged sword in brain pathologies. *Acta Neuropathol.* 2016 Mar;131(3):347-63.
109. Rymo SF, Gerhardt H, Wolfhagen Sand F, Lang R, Uv A, Betsholtz C. A two-way communication between microglial cells and angiogenic sprouts regulates angiogenesis in aortic ring cultures. *PLoS One.* 2011 Jan 10;6(1):e15846.
110. Ramirez J, Berezuk C, McNeely AA, Gao F, McLaurin J, Black SE. Imaging the Perivascular Space as a Potential Biomarker of Neurovascular and Neurodegenerative Diseases. *Cell Mol Neurobiol.* 2016 Mar;36(2):289-99.
111. Nedergaard M. Neuroscience. Garbage truck of the brain. *Science.* 2013 Jun 28;340(6140):1529-30.

Chapter 2

The CADASIL scale-J, a modified scale to prioritize access to genetic testing for Japanese CADASIL-suspected patients

Takashi Koizumi, Ikuko Mizuta, Akiko Watanabe-Hosomi, Mao Mukai,
Ai Hamano, Jun Matsuura, Tomoyuki Ohara, and Toshiki Mizuno

Journal of Stroke and Cerebrovascular Disease: 2019; 28: 1431-1439

Abstract

Background: Cerebral autosomal dominant arteriopathy with subcortical infarcts and leukoencephalopathy (CADASIL) is definitely diagnosed by genetic testing. Such testing involves the analysis of exons 2–24 of *NOTCH3*, which encode the epidermal growth factor-like repeat domain where CADASIL mutations are localized. We previously reported clinical diagnostic criteria for screening CADASIL-suspected Japanese patients prior to genetic testing. Because of its high sensitivity but low specificity, most patients need to undergo genetic testing. In this study, we aimed to develop the CADASIL scale-J, a modified scale to prioritize access to genetic testing for CADASIL-suspected Japanese patients.

Methods: We modified the CADASIL scale reported by Pescini et al. based on clinical features of 126 CADASIL patients and 53 *NOTCH3*-negative CADASIL-like patients diagnosed up until March 2016 (Phase 1). For validation, we recruited 69 consecutive patients for genetic testing of *NOTCH3* from April 2016 to March 2017 (Phase 2).

Results: We developed the CADASIL scale-J with a score ranging from 0 to 25 and the cut-off value of 16, using eight items: hypertension, diabetes, young onset (≤ 50 years old), pseudobulbar palsy, stroke/TIA, family history, subcortical infarction, and temporal pole lesion. The sensitivity and specificity of the CADASIL scale-J were 78.9 and 85.7%, respectively. In Phase 2, we obtained a positive predictive value of 70.0% and a negative predictive value of 89.2%. In this study, we identified 54 mutations, 7 of which were novel.

Conclusions: The CADASIL scale-J is helpful to prioritize access to genetic testing for CADASIL-suspected Japanese patients.

Introduction

Cerebral autosomal dominant arteriopathy with subcortical infarcts and leukoencephalopathy (CADASIL, OMIM #125310) is one of the most frequent hereditary cerebral small vessel diseases, manifested by recurrent strokes, migraine, and white matter lesions^{1,2}. Typical CADASIL patients are young individuals, despite the absence of traditional cardiovascular risk factors; however, several atypical CADASIL cases, including those involving an elderly onset and asymptomatic disease, solely with magnetic resonance imaging (MRI) findings of white matter lesions have been reported³⁻⁵. Therefore, for a definite diagnosis of CADASIL, genetic testing of the causative gene *Notch homolog 3* (*NOTCH3*) on chromosome 19² or pathological detection of granular osmiophilic material in a skin biopsy sample^{6,7} is essential.

NOTCH3 encodes a transmembranous receptor, and all CADASIL mutations have been identified in exons 2–24 encoding the epidermal growth factor (EGF)-like repeat domain^{1,8}. When no mutation is identified at mutational hotspots, exons 3-6, the remaining 19 exons should be analyzed. To perform genetic analysis efficiently, prioritizing access to genetic testing for CADASIL-suspected patients is necessary.

Recently, we reported new diagnostic criteria with high sensitivity, helpful to screen CADASIL-suspected patients to determine who should undergo genetic testing⁴. However, because of their extremely low specificity, the new criteria are not useful to prioritize access for such patients. Previously, Pescini et al. proposed the CADASIL scale as a screening tool to determine patients who should receive genetic testing of *NOTCH3*⁹. Patients with a high CADASIL scale score are preferentially tested. The CADASIL scale showed high sensitivity in European studies; however, low sensitivity was reported in Chinese patients¹⁰, possibly due to ethnic differences in the clinical characteristics of CADASIL.

In the present study, we aimed to develop the CADASIL scale-J, a scale optimized for CADASIL-suspected Japanese patients, by modifying the CADASIL scale by Pescini et al⁹.

Materials and Methods

Participants

All participants were Japanese adults who underwent genetic testing of *NOTCH3* at Kyoto Prefectural University of Medicine (KPUM). To propose the CADASIL scale-J, we recruited 126 CADASIL patients and 53 *NOTCH3*-negative patients genetically diagnosed up until March 2016 (Phase 1). 102 of the 126 CADASIL patients and all the 53 *NOTCH3*-negative patients were included in our previous

study⁴. *NOTCH-3*-negative patients were suspected for CADASIL because of white matter lesions extending to anterior temporal tip and/or their family history of stroke, but had no mutations in *NOTCH3* exons 2–24. To validate the CADASIL scale-J, we recruited 69 consecutive patients underwent genetic testing of *NOTCH3* by us from April 2016 to March 2017 (Phase 2). The negative genetic testing result in Phase 2 means no mutations in *NOTCH3* exons 2–24. Blood samples and clinical information on patients were transferred to KPUM by their physicians. Informed consent was obtained from all participants, and approval for the study was obtained from the ethical committee of KPUM.

Collection of clinical information

We collected clinical information including data on the clinical backgrounds (age at onset, sex, family history, and vascular risk factors), neurological symptoms, and MRI findings. The onset of the symptoms and family history included stroke/TIA, cognitive impairment, seizure, and mood disturbance. Neurological symptoms included stroke/TIA, migraine, motor palsy, sensory disturbance, dizziness, Parkinsonism, pseudobulbar palsy, seizure, mood disturbance, and cognitive impairment. MRI studies included T2-weighted imaging, fluid-attenuated inversion recovery imaging (FLAIR), susceptibility-weighted or T2-star-weighted imaging, and MR angiography. MRI acquisitions and imaging parameters were based on each institute standard.

Genetic testing

Genetic testing of *NOTCH3* was performed as described previously⁴. In brief, *NOTCH3* exons 2–24, which encode the EGF-like repeat domain of the *NOTCH3* receptor, were analyzed by direct sequencing of genomic DNA extracted from the peripheral blood. The sequence data were analyzed with SEQUENCHER (Gene Codes, HITACHI) to screen for mutations. Nucleotide substitutions were confirmed by restriction fragment length polymorphism analysis. We concluded that the variation was pathogenic when it was previously reported as pathogenic and/or when it resulted in cysteine-related missense mutation in one of the EGF-like repeats.

Application of the CADASIL scale

The CADASIL scale of Pescini et al⁹ was developed as a simple scale to be applied in a clinical setting as a screening tool able to predict the genetic diagnosis of CADASIL. The scale involves the additive score of twelve items (ranging from 0 to 25), whose cut-off score is 15 (Supplemental Fig. 1C). Result categories of the CADASIL scale were determined as positive (≥ 15) or negative (< 15). When calculating the CADASIL scale score, patients with insufficient clinical information were excluded.

Development of the CADASIL scale-J in Phase 1

The CADASIL scale-J, a scale suitable for Japanese patients, was developed by modifying the CADASIL scale by Pescini et al⁹ based on the difference in clinical features between CADASIL patients and *NOTCH3*-negative patients in Phase 1. We assigned weighted scores as follows: five points for items showing both a significant difference on multivariate analysis and $\geq 70\%$ frequency in CADASIL patients; three points for items showing a significant difference on multivariate analysis but $< 70\%$ frequency in CADASIL patients; two points for items showing a significant difference with a P-value < 0.01 on univariate analysis; and one point for items showing a significant difference with $0.01 < P$ -value < 0.05 on univariate analysis (Table 1).

The CADASIL scale-J was applied to the patients with sufficient information (114 CADASIL patients and 49 *NOTCH3*-negative patients). The accuracy of the CADASIL scale-J versus genetic diagnosis was evaluated based on the area under the curve (AUC) value of the receiver operating characteristic (ROC) curve using JMP12 (SAS Institute). Simultaneously, the cut-off value was determined to maximize the Youden index (Sensitivity – (1- Specificity)) by ROC analysis.

Validation of the CADASIL scale-J in Phase 2

We validated the CADASIL scale-J by applying it to patients in Phase 2. Result categories of the CADASIL scale-J were determined as positive (score equal to or more than the cut-off value) or negative (score lower than the cut-off value). The positive predictive value was calculated as the proportion of patients with *NOTCH3* mutation among those positive using the CADASIL scale-J. The negative predictive value was calculated as the proportion of patients without *NOTCH3* mutation among those negative using the CADASIL scale-J.

Statistics

The frequencies of clinical features variables in CADASIL patients were compared with those of *NOTCH3*-negative patients by logistic regression analysis. The covariate was dichotomized into with or without each clinical item. The outcome variable was dichotomized into CADASIL or *NOTCH3*-negative non-CADASIL diagnosed by genetic testing. After the univariate logistic regression analysis, only the significant variables were included in the multivariate logistic regression analysis. We used JMP12 (SAS Institute) for statistical calculations. Values of $P < 0.05$ were considered significant.

Results

The CADASIL scale-J based on clinical features of Japanese CADASIL patients

The flow of participants is shown in Figure 1A. Mean ages at the assessment of CADASIL patients (n=126, 111 families) and *NOTCH3*-negative patients (n=53) were 49.6 ± 9.4 and 60.2 ± 11.9 , respectively. Fifty-one out of the 53 *NOTCH3*-negative patients (96%) were tentatively diagnosed as cerebral small vessel disease (cSVD)¹¹, indicating that they were appropriate for the control in this study (Supplemental Table 1). According to the classification by Pantoni¹¹, they were classified into cSVD type 1 (age-related and vascular risk factor-related, n=35), cSVD type 2 (cerebral amyloid angiopathy, n=1), cSVD type 3 (inherited or genetic, n=8), cSVD type 4 (inflammatory and immunologically mediated, n=2), and cSVD type 6 (other, n=6). The remaining two were diagnosed as suspected leukodystrophy. Eight patients with cSVD type 3 included 7 patients with family history and without vascular risk factors and one diagnosed as mitochondrial encephalopathy.

To develop the CADASIL scale-J, we compared the clinical features of CADASIL and *NOTCH3*-negative patients in Phase 1 (Table 1). In univariate analysis, significant differences were noted in eight items: ages at first onset of symptom, family history, hypertension, diabetes, stroke/TIA, pseudobulbar palsy, white matter hyperintensity (WMH) on MRI in the temporal pole, and subcortical infarcts (Table 1). After multivariate logistic regression analysis of these eight items, significant differences remained in the family history, hypertension, pseudobulbar palsy, and subcortical infarcts. Considering the frequencies of these significant items (see Materials and Method section), we assigned a weighted score of 5 for hypertension, subcortical infarcts, and family history, 3 for pseudobulbar palsy, 2 for leukoencephalopathy at temporal lobe, age at first onset ≤ 50 , stroke/TIA, and 1 for diabetes to the CADASIL scale-J (Fig. 2A). The total score ranged from 0 to 25. Modified points are shown by comparing the previously reported CADASIL scale and the CADASIL scale-J (Supplemental Fig. 1C). Then, we extracted 114 CADASIL patients and 49 *NOTCH3*-negative patients with sufficient clinical information and calculated the score for each patient. Scores ranged from 8 to 25 with a maximum of 20 in CADASIL patients, whereas they ranged from 0 to 20 with a maximum of 13 in *NOTCH3*-negative patients (Fig. 2B).

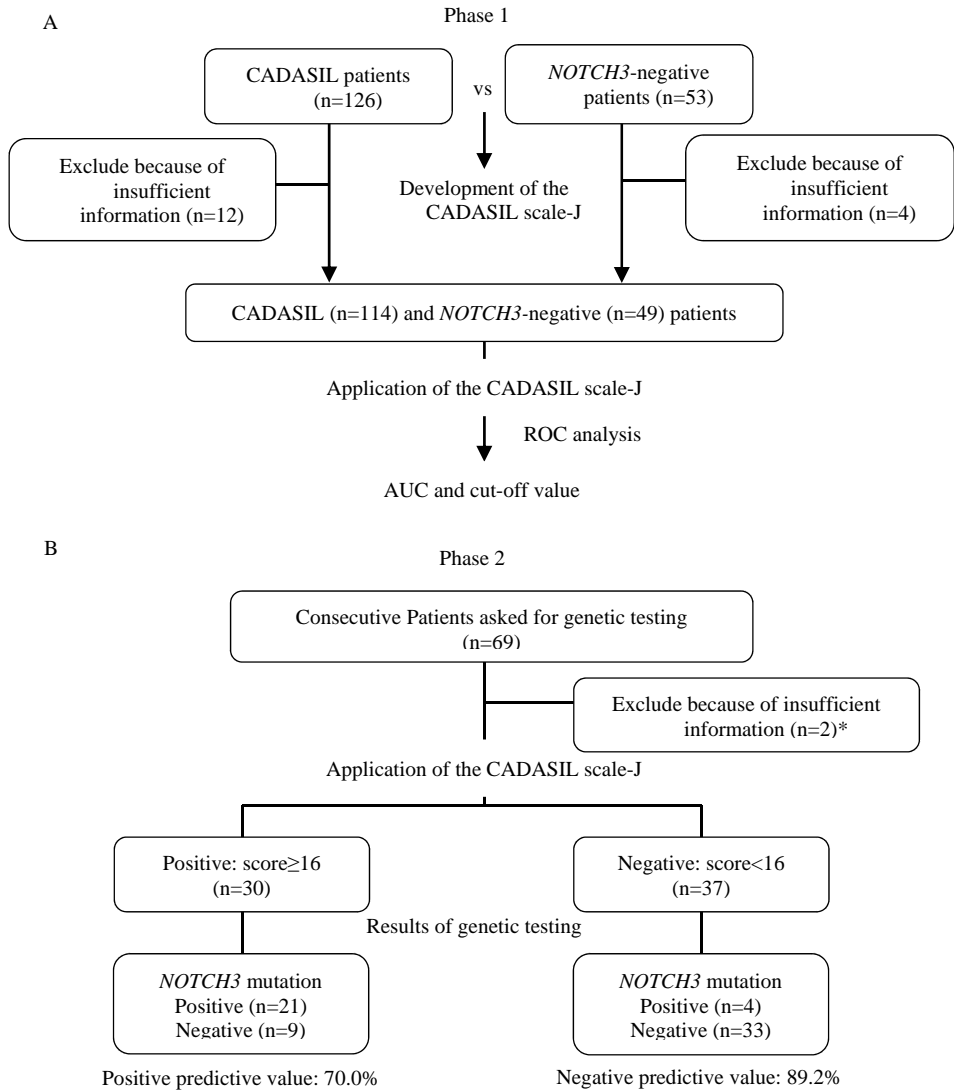


Figure 1. Flowchart of participants. A. Development of the CADASIL scale-J in Phase 1. B. Validation of the CADASIL scale-J in Phase 2. *Two patients excluded because of insufficient information were CADASIL patients.

Table 1. Clinical features of CADASIL patients and *NOTCH3*-negative patients in Phase 1

	CADASIL patients (n=126)	<i>NOTCH3</i> -negative patients (n=53)	P-value ^{#2}	Corrected P-value ^{#3}
Background, n (%)				
Age at onset ^{#1} ≤50 y	50/126 (39.7)	9/53 (17.0)	0.00030	0.097
Sex (male)	60/126 (47.6)	24/53 (45.3)	0.96	
Family history ^{#1}	104/117 (88.9)	34/50 (68.0)	0.0017	0.008
Vascular risk factors				
Smoking	38/123 (30.9)	24/53 (45.3)	0.44	
Hypertension	20/124 (16.1)	31/52 (59.6)	<0.001	<0.0001
Diabetes	6/123 (4.9)	8/52 (15.4)	0.026	0.31
Hyperlipidemia	32/122 (26.2)	16/53 (30.2)	0.59	
Neurological symptoms, n (%)				
Stroke/TIA	89/126 (70.6)	20/53 (37.7)	<0.001	0.19
Migraine	54/122 (44.3)	18/52 (34.6)	0.23	
Motor palsy	63/125 (50.4)	21/53 (39.6)	0.19	
Sensory disturbance	20/121 (16.5)	8/53 (15.1)	0.81	
Dizziness	24/123 (19.5)	5/53 (9.4)	0.084	
Parkinsonism	16/123 (13.0)	5/53 (9.4)	0.49	
Pseudobulbar palsy	32/124 (25.8)	4/53 (7.5)	0.0030	0.017
Seizure	7/122 (5.7)	4/53 (7.5)	0.66	
Mood disturbance	26/122 (21.3)	12/52 (23.1)	0.80	
Cognitive impairment	58/124 (46.8)	31/52 (59.6)	0.12	
MRI findings, n (%)				
White matter hyperintensity				
Temporal pole	99/125 (79.2)	31/53 (58.5)	0.0053	0.083
External capsule	70/106 (66.0)	35/53 (66.0)	1.00	
Brain stem	29/ 52 (55.8)	25/53 (47.2)	0.38	
Corpus callosum	2/ 18 (11.1)	14/52 (26.9)	0.24	
Cerebral microbleeds	19/ 35 (54.3)	21/40 (52.5)	0.82	
Subcortical infarcts	109/125 (87.2)	30/53 (56.6)	<0.001	0.0004
MR angiography: stenosis	16/102 (15.7)	13/47 (27.7)	0.093	

^{#1}Onset of the symptoms and family history included stroke/TIA, cognitive impairment, seizure, and mood disorders. ^{#2}Univariate logistic regression analysis was employed. ^{#3}Corrected P-values were calculated by multiple logistic regression analysis.

A

CADASIL scale-J

- Without hypertension 5
- Subcortical infarcts 5
- Family history* 5
- Pseudobulbar palsy 3
- Leukoencephalopathy at temporal pole 2
- Age at first onset* ≤ 50 y 2
- Stroke / TIA 2
- Without diabetes 1

B

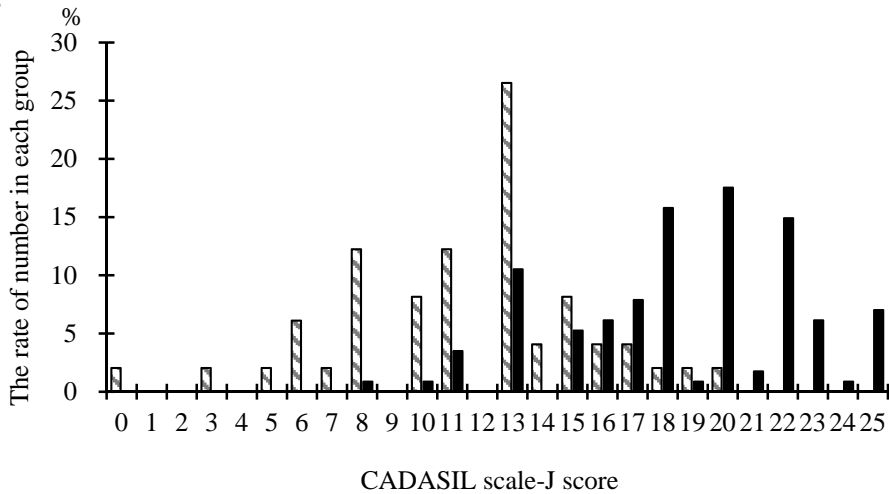


Figure 2. The CADASIL scale-J. A. The score for each item. The total score ranges from 0 to 25. The cut-off value is 16 points. *Family history and onset of the symptoms included stroke/TIA, cognitive impairment, seizure, and mood disturbance, but excluded migraine. B. Distribution of the CADASIL scale-J score of CADASIL patients (black) and NOTCH3 negative patients (striped).

To evaluate the accuracy of this scale, we performed ROC analysis and obtained an AUC of 0.89 and a cut-off value of 16 (Supplemental Fig. 1A). Using this cut-off value, the sensitivity and specificity of the CADASIL scale-J in Phase 1 were 78.9 and 85.7%, respectively (Table 2).

Table 2. Sensitivity and specificity of the CADASIL scale-J in Phases 1 and 2

	Phase 1		Phase 2	
	CADASIL patients	<i>NOTCH3</i> -negative patients	CADASIL patients	<i>NOTCH3</i> -negative patients
Positive (score ≥ 16) (n)	90	7	21	9
Negative (score < 16) (n)	24	42	4	33
Sensitivity (%)	78.9		84.0	
Specificity (%)	85.7		78.6	

Sensitivity was calculated as the positive (score ≥ 16) rate in CADASIL patients. Specificity was calculated as the negative (score < 16) rate in *NOTCH3*-negative patients.

Validation of the CADASIL scale-J in Phase 2

The flow of participants is shown in Figure 1B. Two patients, both of whom were positive for genetic testing, were excluded because of insufficient information. The CADASIL scale-J scores were ≥ 16 in 30 patients, 21 of whom had *NOTCH3* mutations. This yielded a positive predictive value of 70.0% (21/30). On the other hand, the CADASIL scale-J scores were < 16 in 37 patients, 33 of whom did not have *NOTCH3* mutations. This yielded a negative predictive value of 89.2% (33/37). The overall sensitivity and specificity in Phase 2 were 84.0 and 78.6%, respectively (Table 2).

The clinical characteristics of the CADASIL patients and *NOTCH3*-negative patients in Phase 2 are shown in Supplemental Table 2. Significantly different items between CADASIL patients and *NOTCH3*-negative patients in Phase 2 were similar to those in Phase 1, except for the absence of significant differences in family history and diabetes in Phase 2 (Supplemental Table 2).

Comparison between the CADASIL scale and the CADASIL scale-J

In our patients, the diagnostic accuracy of the CADASIL scale-J was higher compared with that of the CADASIL scale of Pescini et al⁹ ROC analysis of the CADASIL scale in Phase 1 showed an AUC of 0.61, which was lower than that

of the CADASIL scale-J at 0.89, and an optimal cut-off value of 16 (Supplemental Fig. 1A and 1B). Both scales showed high specificity (78.6-85.7%) in Phase 1 and Phase 2. However, sensitivities of the CADASIL scale-J (78.9% in Phase 1 and 84.0% in Phase 2) were apparently higher than those of the CADASIL scale (40.6% in Phase 1 and 48.0% in Phase 2) (Table 2 and Supplemental Table 3).

NOTCH3 mutations

In the total of 153 CADASIL patients in Phases 1 and 2, including those with insufficient information to calculate the scores, we identified one 54 pathogenic mutations of *NOTCH3* located in exons 2-8, 11, 14, and 18-21 (Table 3). Seven mutations: p.C55R, p.C419R, p.C435Y, p.C606S, p.C1015W, p.C1022G, and p.S1067C, were novel ones. The patients with p.C323W were reported elsewhere¹². One of the patients with p.R544C was homozygous and recently reported elsewhere by us¹³. Most of the mutations existed in exons 3–6 (107 of the 153 patients, 69.9%), particularly exons 3–4 (96 of the 153 patients, 62.7%).

Table 3. Summary of *NOTCH3* mutations identified in 153 Japanese CADASIL patients

Amino acid change	Nucleotide change	Exon	EGF-like repeat	Number of individuals
p.C43F	c.128G>T	2	1	1
p.R54C	c.160C>T	2	1	2
p.C55G	c.163T>G	2	1	2
p.C55R*	c.163T>C	2	1	1
p.C65S	c.194G>C	2	1	3
p.C65Y	c.194G>A	2	1	1
p.W71C	c.213G>T	3	1	1
p.R75P	c.224G>C	3	1	14
p.C76Y	c.227G>A	3	1	2
p.C87F	c.260G>T	3	2	1
p.R90C	c.268C>T	3	2	2
p.C93G	c.277T>G	3	2	2
p.C93Y	c.278G>A	3	2	2
p.C106R	c.316T>C	3	2	2
p.C108F	c.323G>T	3	2	2
p.R110C	c.328C>T	3	2	2
p.R133C	c.397C>T	4	3	8
p.R141C	c.421C>T	4	3	17
p.C146W	c.438C>G	4	3	1

p.R153C	c.457C>T	4	3	8
p.R169C	c.505C>T	4	4	6
p.C174L	c.521_522delinsT G	4	4	2
p.S180C	c.539C>G	4	4	6
p.R182C	c.544C>T	4	4	13
p.C185Y	c.554G>A	4	4	2
p.C194Y	c.581G>A	4	4	1
p.C212R	c.634T>C	4	5	2
p.C233S	c.697T>A	5	5	1
p.C245Y	c.734G>A	5	6	1
p.C260F	c.779G>T	5	6	2
p.C323W	c.969C>G	6	8	2
p.C329Y	c.986G>A	6	8	1
p.R332C	c.994C>T	6	8	4
p.G382C	c.1144G>T	7	9	1
p.C388Y	c.1163G>A	7	9	3
p.S396C	c.1187C>G	7	10	1
p.C419R*	c.1255T>C	8	10	3
p.C435Y*	c.1304G>A	8	11	1
p.C455R	c.1363T>C	8	11	1
p.C457S	c.1370G>C	8	11	1
p.C542R	c.1624T>C	11	13	3
p.C542Y	c.1625G>A	11	13	1
p.R544C	c.1630C>T	11	13-14	2
p.C606S*	c.1817G>C	11	15	1
p.R607C	c.1819C>T	11	15	7
p.C729G	c.2185T>G	14	18	1
p.R985C	c.2953C>T	18	25	1
p.C988F	c.2963G>T	18	25	1
p.C1004G	c.3010T>G	19	26	3
p.C1015W*	c.3045C>G	19	26	1
p.Y1021C	c.3062A>G	19	26	1
p.C1022G*	c.3064T>G	19	26	1
p.S1067C*	c.3200C>G	20	27	1
p.R1143C	c.3427C>T	21	29	1
Total				153

*Novel mutations not reported by Rutten et al. (2014), Mizuta et al. (2017), Yeung et al. (2018), the Leiden Open Variation Database, or references therein.

Discussion

We developed the CADASIL scale-J, which can effectively discriminate between CADASIL patients and *NOTCH3*-negative CADASIL-like patients among Japanese patients (Table 2, Fig. 1B, and Supplemental Fig. 1A). The ROC analysis of our scale in Phase 1 yielded an AUC of 0.89 showing marked accuracy¹⁴. Sensitivity and specificity were high in both Phase 1 (78.9 and 85.7%, respectively) and Phase 2 (84.0 and 78.6%, respectively). Also, the positive predictive value was high at 70.0% and the negative predictive value was high at 89.2% in Phase 2.

The CADASIL scale-J exhibited a higher diagnostic accuracy compared with the CADASIL scale (Supplemental Fig. 1B). This may be at least partially due to ethnic differences in the clinical characteristics of CADASIL. The CADASIL scale of Pescini et al. is based on data reported on 536 CADASIL patients, most of whom were Caucasians. Although the items of migraine and leukoencephalopathy extending to the external capsule were highly weighted in the CADASIL scale of Pescini et al., they were not specific to Japanese CADASIL patients in our study (Table 1, Supplemental Fig. 1C). Because the frequency of migraine, mood disturbance, cognitive impairment, or external capsule lesions was not significantly different between CADASIL and *NOTCH3*-negative patients, we omitted these items in the CADASIL scale-J (Table 1, Supplemental Fig. 1C). Leukoencephalopathy extending to the temporal pole was more specific to CADASIL rather than the external capsule in Japanese patients. In addition, items of the CADASIL scale did not include hypertension or pseudobulbar palsy, both of which showed a clearly significant difference between CADASIL patients and *NOTCH3* negative patients in this study. Our findings suggest that it is necessary to develop a new scale suitable for Japanese patients, in agreement with a previous study in a Chinese population. Similar to our findings, Liu et al. reported a higher rate of temporal pole involvement, but not external capsule involvement in CADASIL compared with non-CADASIL Chinese patients¹⁰. They also noted a significant difference in the rate of hypertension but no significant difference in that of migraine between CADASIL and non-CADASIL patients¹⁰.

By applying the CADASIL scale-J to consecutive patients (Phase 2), we obtained a positive predictive value of 70.0%, being higher than the positive rate of genetic testing of 39.1% (27/69). We also obtained a negative predictive value of 89.1%, being higher than the negative rate of genetic testing of 59.4% (42/69), among CADASIL-suspected patients (Fig. 1B). Four CADASIL patients who failed to exceed the cut-off score of 16 were asymptomatic or older-onset with multiple vascular risk factors.

We calculated a positive rate and an average score using the CADASIL scale-J for seven genotypes, each of which included more than five patients (Supplemental Table 4). The low positive rate was 63.6% for p.R75P and 61.5% for p.R182C. The p.R75P subgroup showed the lowest average score of the CADASIL scale-J at 15.5 ± 3.8 , which was lower than the cut-off value at 16. The p.R75P mutation is an atypical cysteine-sparing but already pathologically confirmed one mainly reported from Japan and Korea^{15,16}. The low positive rate and the low average score in p.R75P subgroup are thought to be due to a lower frequency of temporal pole lesions and older age at onset compared with other genotypes, as reported previously¹⁷. The average score of the CADASIL scale-J in p.R182C subgroup at 17.2 ± 4.3 was the second lowest among the genotypes studied, but exceeded cut-off score of 16, suggesting another reason for the lowest sensitivity at 61.5% in p.R182C. We next compared the distribution of individual scores among p.R75P, p.R182C, and p.R141C, and found the widest distribution in p.R182C (Supplemental Fig. 2). We, therefore, think that especially low sensitivity in p.R182C subgroup was mainly due to a wide variety of scores among the individuals.

Because Rutten et al. recently reported that *NOTCH3* EGF-like repeat (EGFr) 1-6 pathogenic variants are associated with a more severe phenotype compared with EGFr 7-34 pathogenic variants¹⁸, we also compared the CADASIL scale-J positive rate between EGFr 1-6 and 7-34 subgroups. The positive rates for EGFr 1-6 group and 7-34 groups were similar, 79.8% and 80.0%, respectively (supplemental Table 4). The average score of the CADASIL scale-J for EGFr 1-6 group and 7-34 groups also were similar, 18.3 ± 3.3 and 18.9 ± 4.1 , respectively (supplemental Table 4).

One limitation of this study was that it was performed in a single center. To confirm and improve the accuracy of the CADASIL scale-J, replication analysis in multiple centers is necessary. Another limitation was that patients with insufficient information were not included in this study. Finally, the possibility of hereditary small vessel diseases other than CADASIL in *NOTCH3*-negative patients was not excluded from this study. When we compared clinical features of 16 *NOTCH3*-negative patients with the high score (≥ 16) to those of 139 CADASIL patients, no item of clinical features showed a significant difference between them (Supplemental Table 5). This suggested that patients with CADASIL-like disease caused by other than *NOTCH3* may be included in *NOTCH3*-negative patients with high score. To clarify how many patients with other known hereditary cerebral small vessel diseases were included in *NOTCH3*-negative controls, further genetic testing of the causative genes including *HTRA1*¹⁹⁻²¹, *COL4A1*²²⁻²⁴, *TREX1*^{25,26}, and *CTSA*²⁷ for cerebral autosomal recessive arteriopathy with subcortical infarcts and leukoencephalopathy (CARASIL), pontine autosomal dominant

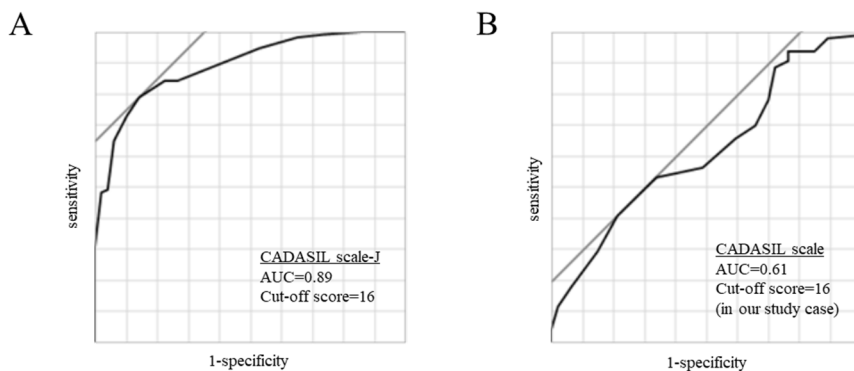
microangiopathy with leukoencephalopathy (PADMAL), retinal vasculopathy and cerebral leukodystrophy (RVCL), and cathepsin A–related arteriopathy with strokes and leukoencephalopathy (CARASAL), respectively, is necessary.

In conclusion, we established the CADASIL scale-J for Japanese patients. It is useful to prioritize access to genetic testing among CADASIL-suspected Japanese patients and helpful for researchers to perform genetic testing efficiently.

References

1. Chabriat H, Joutel A, Dichgans M, Tournier-Lasserre E, Bousser MG. Cadasil. *The Lancet Neurology*. 2009 Jul;8(7):643-53.
2. Joutel A, Corpechot C, Ducros A, et al. Notch3 mutations in CADASIL, a hereditary adult-onset condition causing stroke and dementia. *Nature*. 1996 Oct 24;383(6602):707-10.
3. Watanabe M, Adachi Y, Jackson M, et al. An unusual case of elderly-onset cerebral autosomal dominant arteriopathy with subcortical infarcts and leukoencephalopathy (CADASIL) with multiple cerebrovascular risk factors. *J Stroke Cerebrovasc Dis*. 2012 Feb;21(2):143-5.
4. Mizuta I, Watanabe-Hosomi A, Koizumi T, et al. New diagnostic criteria for cerebral autosomal dominant arteriopathy with subcortical infarcts and leukoencephalopathy in Japan. *J Neurol Sci*. 2017 Oct 15;381:62-7.
5. Pescini F, Bianchi S, Salvadori E, et al. A pathogenic mutation on exon 21 of the NOTCH3 gene causing CADASIL in an octogenarian paucisymptomatic patient. *J Neurol Sci*. 2008 Apr 15;267(1-2):170-3.
6. Baudrimont M, Dubas F, Joutel A, Tournier-Lasserre E, Bousser MG. Autosomal dominant leukoencephalopathy and subcortical ischemic stroke. A clinicopathological study. *Stroke*. 1993 Jan;24(1):122-5.
7. Joutel A, Corpechot C, Ducros A, et al. Notch3 mutations in cerebral autosomal dominant arteriopathy with subcortical infarcts and leukoencephalopathy (CADASIL), a mendelian condition causing stroke and vascular dementia. *Ann N Y Acad Sci*. 1997 Sep 26;826:213-7.
8. Federico A, Bianchi S, Dotti MT. The spectrum of mutations for CADASIL diagnosis. *Neurol Sci*. 2005 Jun;26(2):117-24.
9. Pescini F, Nannucci S, Bertaccini B, et al. The Cerebral Autosomal-Dominant Arteriopathy With Subcortical Infarcts and Leukoencephalopathy (CADASIL) Scale: a screening tool to select patients for NOTCH3 gene analysis. *Stroke*. 2012 Nov;43(11):2871-6.
10. Liu X, Zuo Y, Sun W, et al. The genetic spectrum and the evaluation of CADASIL screening scale in Chinese patients with NOTCH3 mutations. *Journal of the Neurological Sciences*.354(1):63-9.
11. Pantoni L. Cerebral small vessel disease: from pathogenesis and clinical characteristics to therapeutic challenges. *The Lancet Neurology*. 2010 Jul;9(7):689-701.
12. Tojima M, Saito S, Yamamoto Y, Mizuno T, Ihara M, Fukuda H. Cerebral Autosomal Dominant Arteriopathy with Subcortical Infarcts and Leukoencephalopathy with a Novel NOTCH3 Cys323Trp Mutation Presenting Border-Zone Infarcts: A Case Report and Literature Review. *J Stroke Cerebrovasc Dis*. 2016 Aug;25(8):e128-30.
13. Mukai M, Mizuta I, Ueda A, et al. A Japanese CADASIL patient with homozygous NOTCH3 p.Arg544Cys mutation confirmed pathologically. *J Neurol Sci*. 2018 Nov 15;394:38-40.
14. Simundic AM. Measures of Diagnostic Accuracy: Basic Definitions. *Ejifcc*. 2009 Jan;19(4):203-11.
15. Mizuno T, Muranishi M, Torugun T, et al. Two Japanese CADASIL families exhibiting Notch3 mutation R75P not involving cysteine residue. *Intern Med*. 2008;47(23):2067-72.
16. Kim Y, Choi EJ, Choi CG, et al. Characteristics of CADASIL in Korea: a novel cysteine-sparing Notch3 mutation. *Neurology*. 2006 May 23;66(10):1511-6.
17. Ueda A, Ueda M, Nagatoshi A, et al. Genotypic and phenotypic spectrum of CADASIL in Japan: the experience at a referral center in Kumamoto University from 1997 to 2014. *Journal of neurology*. 2015 Aug;262(8):1828-36.
18. Rutten JW, Van Eijdsen BJ, Duering M, et al. Correction: The effect of NOTCH3 pathogenic variant position on CADASIL disease severity: NOTCH3 EGFr 1-6 pathogenic variant are associated with a more severe phenotype and lower survival compared with EGFr 7-34 pathogenic variant. *Genetics in medicine : official journal of the American College of Medical Genetics*. 2018 Sep 20.
19. Hara K, Shiga A, Fukutake T, et al. Association of HTRA1 mutations and familial ischemic cerebral small-vessel disease. *N Engl J Med*. 2009 Apr 23;360(17):1729-39.
20. Verdura E, Herve D, Scharrer E, et al. Heterozygous HTRA1 mutations are associated with autosomal dominant cerebral small vessel disease. *Brain*. 2015 Aug;138(Pt 8):2347-58.
21. Nozaki H, Kato T, Nihonmatsu M, et al. Distinct molecular mechanisms of HTRA1 mutants in manifesting heterozygotes with CARASIL. *Neurology*. 2016 May 24;86(21):1964-74.
22. Gould DB, Phalan FC, van Mil SE, et al. Role of COL4A1 in small-vessel disease and hemorrhagic stroke. *N Engl J Med*. 2006 Apr 6;354(14):1489-96.
23. Vahedi K, Boukobza M, Massin P, Gould DB, Tournier-Lasserre E, Bousser MG. Clinical and brain MRI follow-up study of a family with COL4A1 mutation. *Neurology*. 2007 Oct 16;69(16):1564-8.

24. Verdura E, Herve D, Bergametti F, et al. Disruption of a miR-29 binding site leading to COL4A1 upregulation causes pontine autosomal dominant microangiopathy with leukoencephalopathy. *Ann Neurol*. 2016 Nov;80(5):741-53.
25. Richards A, van den Maagdenberg AM, Jen JC, et al. C-terminal truncations in human 3'-5' DNA exonuclease TREX1 cause autosomal dominant retinal vasculopathy with cerebral leukodystrophy. *Nat Genet*. 2007 Sep;39(9):1068-70.
26. Jen J, Cohen AH, Yue Q, et al. Hereditary endotheliopathy with retinopathy, nephropathy, and stroke (HERNS). *Neurology*. 1997 Nov;49(5):1322-30.
27. Bugiani M, Kevelam SH, Bakels HS, et al. Cathepsin A-related arteriopathy with strokes and leukoencephalopathy (CARASAL). *Neurology*. 2016 Oct 25;87(17):1777-86.



C

CADASIL scale (Pescini et al. 2012)

- Migraine
- Migraine with aura
- TIA or stroke
- TIA or stroke onset ≤ 50 y
- Psychiatric disturbances
- Cognitive decline / cognitive impairment
- Leukoencephalopathy
 - extended to temporal pole
 - extended to external capsule
- Subcortical infarcts
- Family history in at least 1 generation
 - at least 2 generations

- 1
- 3
- 1
- 2
- 1
- 3
- 3
- 1
- 5
- 2
- 1
- 2

CADASIL scale-J

- omitted
- omitted
- 2
- 2*
- omitted
- omitted
- omitted
- 2
- omitted
- 5
- 5*
- omitted
- 5 Without hypertension
- 1 Without diabetes
- 3 Pseudobulbar palsy

Total score range

0-25

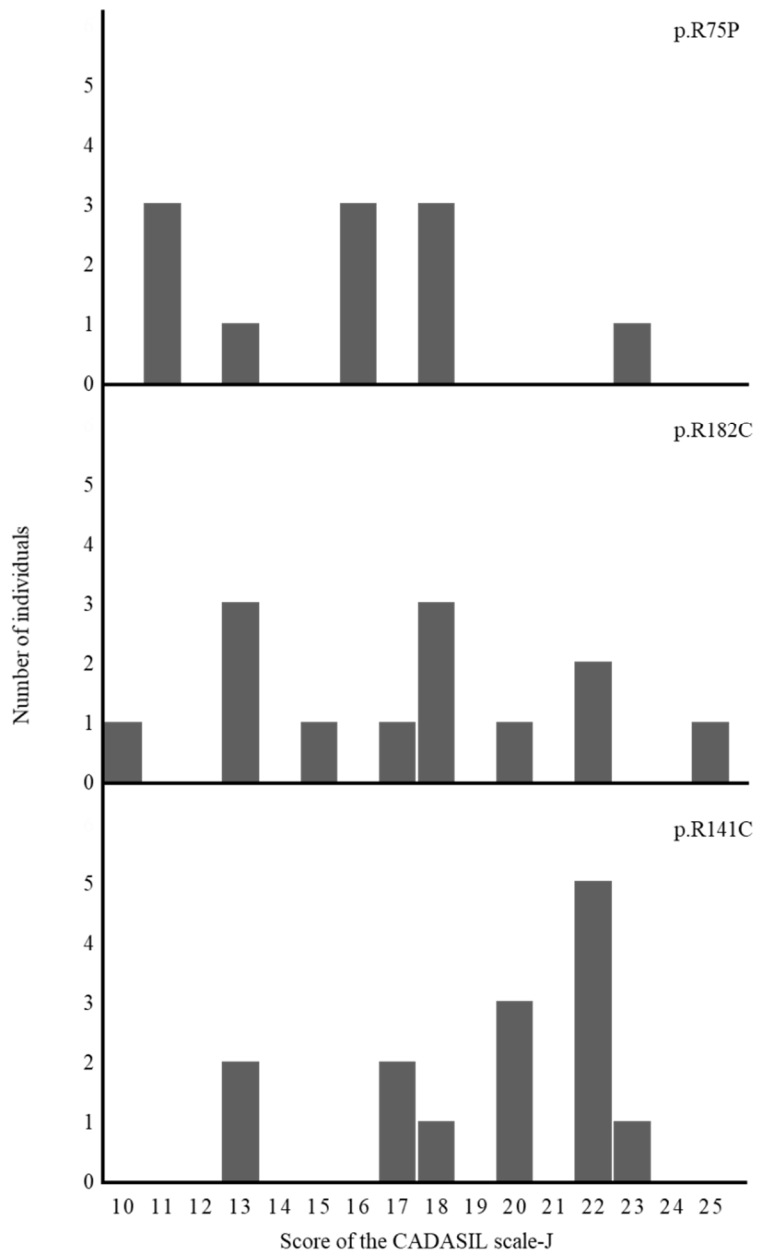
0-25

Positive cut-off score

≥ 15

≥ 16

Supplemental Figure 1. A and B. ROC curve using the CADASIL scale-J (A) and the CADASIL scale (B) in Phase 1. C. Comparison of items and each score in the CADASIL scale by Pescini et al. and the CADASIL scale-J in this study. *In the CADASIL scale-J, family history and onset of the symptoms included stroke/TIA, cognitive impairment, seizure, and mood disturbance, but excluded migraine



Supplemental Figure 2. Distributions of scores of the CADASIL scale-J in patients with p.R75P (top), p.R182C (middle), and p.R141C (bottom).

Supplemental Table 1. List of tentative diagnosis of 53 *NOTCH3*-negative patients enrolled as controls to develop the CADASIL scale-J

Tentative diagnosis	Number of individuals
Cerebral small vessel disease (CSVD)*	
Type 1 (age-related and vascular risk factor-related)	35
Type 2 (cerebral amyloid angiopathy)	1
Type 3 (inherited or genetic)	8
Type 4 (inflammatory and immunologically mediated)	2
Type 6 (other)	6
Leukodystrophy suspected	2
Total	53

*Classification of cerebral vascular disease was according to Pantoni. (Lancet Neurol. 2010;9:689-701.)

Supplemental Table 2. Clinical features of CADASIL patients and *NOTCH3*-negative patients in Phase 2

	CADASIL patients (n=25)	<i>NOTCH3</i> -negative patients (n=42)	P-value ^{#2}	Corrected P-value ^{#3}
Background, n (%)				
Age at first onset ^{#1} ≤50 y	15/23 (65.2)	15/41 (36.6)	0.04	0.094
Sex (male)	15/25 (60.0)	22/42 (52.4)	0.62	
Family history ^{#1}	23/25 (92.0)	30/42 (71.4)	0.06	
Vascular risk factors				
Smoking	9/25 (36.0)	16/40 (40.0)	0.80	
Hypertension	6/25 (24.0)	25/42 (59.5)	0.006	0.049
Diabetes	1/25 (4.0)	9/42 (21.4)	0.08	
Hyperlipidemia	7/24 (29.0)	11/42 (26.2)	0.78	
Neurological symptoms, n (%)				
Stroke/TIA	20/25 (80.0)	18/42 (42.9)	0.005	0.027
Migraine	5/25 (20.0)	15/42 (35.7)	0.27	
Motor palsy	11/24 (45.8)	17/42 (40.5)	0.80	
Sensory disturbance	4/25 (16.0)	9/41 (22.0)	0.75	
Dizziness	2/24 (8.3)	5/41 (12.2)	1.00	
Parkinsonism	4/25 (16.0)	9/41 (22.0)	0.75	
Pseudobulbar palsy	9/25 (36.0)	5/42 (11.9)	0.03	0.49
Seizure	3/25 (12.0)	2/41 (4.9)	0.36	
Mood disturbance	2/25 (8.0)	9/42 (21.4)	0.19	
Cognitive impairment	13/23 (56.5)	18/40 (45.0)	0.44	
MRI findings, n (%)				
White matter hyperintensity				
Temporal pole	23/25 (92.0)	23/40 (57.5)	0.004	0.009
External capsule	20/25 (80.0)	26/42 (61.9)	0.17	
Brain stem	10/23 (43.5)	14/37 (37.8)	0.79	
Corpus callosum	4/25 (16.0)	6/39 (15.3)	1.00	
Cerebral microbleeds	15/19 (78.9)	13/28 (46.4)	0.04	0.001
Subcortical infarcts	22/25 (88.0)	25/42 (59.5)	0.02	0.29
MR angiography: stenosis	2/23 (8.7)	2/37 (5.4)	0.63	

^{#1}Onset of the symptoms and family history included stroke/TIA, cognitive impairment, seizure, and mood disturbance. ^{#2}Univariate logistic regression analysis was employed. ^{#3}Corrected P-values were calculated by multiple logistic regression analysis.

Supplemental Table 3. Evaluation of the CADASIL scale in Phase 1 and 2

	Phase 1			Phase 2		
	CADASIL patients (n=126)	<i>NOTCH3</i> -negative patients (n=53)	p-value	CADASIL patients (n=25)	<i>NOTCH3</i> -negative patients (n=42)	p-value
CADASIL scale score ≥ 16^{#1}, n (%)	39/96 (40.6)	10/47 (21.3)	0.025	12/25 (48.0)	8/42 (19.0)	0.026
	Sensitivity	Specificity		Sensitivity	Specificity	
	40.6%	78.7%		48.0%	81.0%	
CADASIL scale (score), n (%)						
Migraine (1)	54/122 (44.3)	18/52 (34.6)	0.31	5/25 (20.0)	15/42 (35.7)	0.27
Migraine with aura (3)	1/122 (0.8)	1/52 (1.9)	1.00	2/25 (8.0)	5/42 (11.9)	0.70
TIA or stroke (1)	89/126 (70.6)	20/53 (37.7)	<0.001	20/25 (80.0)	18/42 (42.9)	0.005
TIA / stroke onset ≤ 50 y (2)	49/126 (38.9)	7/53 (13.2)	0.0007	14/25 (56.0)	8/42 (19.0)	0.003
Psychiatric disturbances (1)	26/122 (21.3)	12/52 (23.1)	0.84	2/25 (8.0)	9/42 (21.4)	0.19
Cognitive decline / cognitive impairment (3)	58/124 (46.8)	31/52 (59.6)	0.14	13/23 (56.5)	18/40 (45.0)	0.44
Leukoencephalopathy (3)	125/126 (99.2)	53/53 (100.0)	1.00	25/25 (100.0)	40/42 (95.2)	0.53
extended to temporal pole (1)	99/125 (79.2)	31/53 (58.5)	0.0058	23/25 (92.0)	23/40 (57.5)	0.003
extended to external capsule (5)	70/106 (66.0)	35/53 (66.0)	1.00	20/25 (80.0)	26/42 (61.9)	0.17
Subcortical infarcts (2)	109/125 (87.2)	30/53 (56.6)	<0.001	22/25 (88.0)	25/42 (59.5)	0.015
Family history in at least 1 generation (1)	104/117 (88.9)	34/50 (68.0)	0.003	22/25 (88.0)	30/42 (71.4)	0.07
Family history in at least 2 generations (2)	43/117 (36.7)	14/50 (28.0)	0.29	13/25 (52.0)	12/42 (28.6)	0.07

The CADASIL scale of Pescini et al. was applied to Phase 1 and 2. ^{#1}Optimal cut-off value calculated from ROC analysis in Phase 1 (Supplemental Fig.1). Sensitivity is the positive rate (total score ≥ 16 in CADASIL patients). Specificity is the negative rate (total score < 16) in *NOTCH3*-negative patients. Clinical features focused on items of the CADASIL scale are also shown. For P-value calculation, univariate logistic regression analysis was employed.

Supplemental Table 4. Sensitivity of the CADASIL scale-J in *NOTCH3* genotype subgroups

<i>NOTCH3</i> mutation	Number of individuals assessed	Sensitivity of the CADASIL scale-J (%)	mean \pm SD of score of the CADASIL scale-J
p.R75P	11	63.6	15.5 \pm 3.8
p.R133C	8	75.0	19.0 \pm 3.6
p.R141C	14	82.4	19.4 \pm 3.3
p.R153C	7	85.7	18.3 \pm 3.7
p.S180C	6	83.3	20.3 \pm 4.4
p.R182C	13	61.5	17.2 \pm 4.3
p.R607C	7	85.7	18.7 \pm 2.1
EGFr 1-6	99	79.8	18.3 \pm 3.3
EGFr 7-34	40	80.0	18.9 \pm 4.1

Sensitivity, the positive rate using the CADASIL scale-J (score \geq 16), and mean \pm SD of the score were calculated for the common genotypes (n \geq 6).

Supplemental Table 5. Clinical features of *NOTCH3*-negative patients with high CADASIL scale-J score (≥ 16) and CADASIL patients in this study

	<i>NOTCH3</i> -negative patients with high CADASIL scale-J score (≥ 16) (n=16)	CADASIL patients (n=139)	p-value ^{#2}
Background			
Age at onset ^{#1} ≤ 50 y	6/16 (37.5)	63/137 (41.2)	0.60
Sex (male)	5/11 (31.3)	67/72 (48.2)	0.29
Family history ^{#1}	14/16 (87.5)	123/139 (88.5)	1.0
Vascular risk factors			
Smoking	6/15 (40.0)	54/139 (38.9)	1.0
Hypertension	4/16 (24.0)	23/139 (16.6)	0.48
Diabetes	1/16 (6.3)	7/139 (5.0)	0.59
Hyperlipidemia	5/16 (31.3)	35/136 (25.7)	0.76
Neurological symptoms			
Stroke/TIA	9/16 (56.3)	99/139 (71.2)	0.25
Migraine	5/16 (31.3)	54/137 (39.4)	0.60
Motor palsy	9/16 (56.3)	68/138 (49.3)	0.79
Sensory disturbance	5/15 (33.3)	23/135 (17.0)	0.16
Dizziness	1/15 (6.7)	25/137 (18.3)	0.47
Parkinsonism	3/15 (20.0)	19/138 (13.8)	0.45
Pseudobulbar palsy	6/16 (37.5)	39/139 (28.1)	0.56
Seizure	2/15 (13.3)	9/137 (6.6)	0.30
Mood disturbance	2/16 (12.5)	25/137 (18.3)	0.74
Cognitive impairment	10/16 (62.5)	64/136 (47.1)	0.30
MRI findings			
White matter hyperintensity	16/16 (100.0)	138/139 (99.3)	1.0
Temporal pole	12/16 (75.0)	113/139 (81.3)	0.52
External capsule	12/16 (75.0)	80/120 (66.7)	0.58
Brain stem	8/16 (50.0)	34/69 (49.3)	1.0
Corpus callosum	6/16 (37.5)	6/41 (14.6)	0.076
Cerebral microbleeds	6/13 (46.2)	33/52 (63.5)	0.35
Subcortical infarcts	15/16 (93.8)	121/139 (87.1)	0.69
MR angiography: stenosis	4/16 (25.0)	19/115 (16.5)	0.48

The number of observed/studied (%), and number of males/females (% of males) are shown. ^{#1}Onset of the symptoms and family history included stroke/TIA, cognitive impairment, seizure, and mood disturbance.

^{#2}Univariate logistic regression analysis was employed.

Chapter 3

Perivascular immune cells in cerebrovascular diseases:

From perivascular macrophages to perivascular microglia

Takashi Koizumi, Danielle Kerkhofs, Toshiki Mizuno,
Harry W.M. Steinbusch, Sébastien Foulquier

Frontiers in Neuroscience, in revision

Abstract

Cerebral small vessels feed and protect the brain parenchyma thanks to the unique features of the blood brain-barrier. Cerebrovascular dysfunction is therefore seen as a detrimental factor for the initiation of several CNS disorders, such as stroke, cerebral small vessel disease and Alzheimer's disease. The main working hypothesis linking cerebrovascular dysfunction to brain disorders includes the contribution of neuroinflammation. While our knowledge on microglia cells – the brain-resident immune cells - has been increasing the last decades, the specific populations of microglia and macrophages surrounding brain vessels, so-called perivascular microglia and perivascular macrophages respectively, have been overlooked. This review aims to summarize the knowledge gathered on perivascular microglia and perivascular macrophages, to discuss existing knowledge gaps of importance for later studies and to summarize evidences for their contribution to cerebrovascular dysfunction.

Keywords: cerebrovascular dysfunction; neuroinflammation; perivascular macrophages; perivascular microglia

Introduction

A growing body of evidence supports the importance of our immune system in disease progression, making the research community more aware of the complexity of disease's mechanisms but offering at the same time new diagnostic and therapeutic opportunities. This holds true for cerebrovascular diseases such as cerebral Small Vessel Disease (cSVD), the most prevalent cause of vascular cognitive impairment¹, in which the surroundings of brain small vessels are being scrutinized to decipher its exact pathophysiological mechanism. In this regard, perivascular immune cells have gained interest in the last three decades and both microglia and macrophages have been discussed in recent studies. The terms “perivascular microglia” and “perivascular macrophage”, given at several occasions, have not been always rightly used to describe immune cells associated with the cerebral vessels. Current state-of-the-art immunohistochemistry combined with confocal microscopy has revealed differential expressions of microglia/macrophage markers as well as morphological features that allow today a better discrimination of those brain perivascular immune cells.

In this review, the terms “perivascular microglia” (PMG) and “perivascular macrophages” (PVMs) will be first defined before summarizing the findings on PMG and PVMs associated with cerebrovascular diseases, including stroke, cSVD, Alzheimer's disease and multiple sclerosis. This review aims to discuss the importance of differentiating PMG from PVMs. This emerging concept should be considered to fill in current research gaps in the field of neurodegenerative diseases involving cerebrovascular dysfunction.

Historical perspective

The first occurrence of the term “perivascular microglia” was in 1988, when Hickey and Kimura described the presence of bone marrow-derived cells located around cerebral vessels and expressing the cell surface glycoprotein ED-2². However, Graeber et al. suggested that these ED-2-positive perivascular cells differ from microglia, which did not stain with ED-2³ and he suggested to keep the term “perivascular microglia” for microglia located on the vicinity of vessels outside of the basal lamina⁴. The ED-2 antigen was later identified as CD163, a highly specific marker for PVMs, ruling out the possibility that these perivascular cells were pericytes^{5,6} (Table 1). From these early studies, a clear description of PVMs was made using their ED-2-positive immunoreactivity and their location within the perivascular space mainly around the large penetrating arteriole, compared to PMG, ED-2-negative and located outside of the glia limitans. After its introduction in 1990, however, the term PMG was used wrongly at many occasions instead of PVM and the term “juxtavascular

microglia” was also found as an alternative for PMG⁷, creating overall a lot of confusion in this research field.

Parenchymal microglia, Perivascular microglia and Perivascular macrophages

Microglia are the brain-resident immune cells and they play crucial roles in the development, maintenance of homeostasis, and diseases in the central nervous system (CNS). Microglia are crucial in brain development and regulate many mechanisms including synaptic pruning and maturation and angiogenesis⁸. Under physiological conditions in adult life, microglia are constantly monitoring their surroundings thanks to their fine ramified motile processes⁹. Once microglia encounter harmful substances, such as infiltrating components from blood, burden abnormal proteins, or cell debris, they become activated to phagocytose these harmful substances or to protect the damaged cells¹⁰. Furthermore, microglia can promote angiogenesis both in physiological¹¹ and pathological conditions such as ischemic stroke, AD, multiple sclerosis (MS), and Parkinson’s disease (PD)¹², highlighting the important crosstalk of microglia with the cerebral vasculature. While PMG could be considered as a sub-population of parenchymal microglia, advanced molecular studies should be undertaken to reveal their true nature and assess their potential protective and/or deleterious functions in the context of cerebrovascular diseases.

Apart from microglia, CNS-macrophages are also involved in the maintenance of brain homeostasis but their role is limited to its borders. CNS-macrophages reside in the non-parenchymal perivascular space, subdural meningeal spaces, and choroid plexus spaces — namely, perivascular macrophages (PVMs), meningeal macrophages (MMs), and choroid plexus macrophages (CPMs) respectively¹³ (Fig. 1A). While microglia and macrophages share many functions and markers, previous studies have revealed differential marker expressions useful for their distinction (next paragraph, Table 1).

Studies specifically investigating the differential functions of microglia (including parenchymal and perivascular microglia) and PVMs are lacking due to the absence of steadfast experimental systems^{12,14}. However the use of single-cell RNA-seq analysis or mass cytometry have brought additional evidences confirming their differential roles. Gene expression analyzes and histological studies have reported cell-specific markers: TMEM119 (Transmembrane protein 119), P2RY12 (P2Y purinoceptor 12), SALL1 (Sal-like protein 1), Siglec-H (Sialic acid-binding immunoglobulin-type lectins), Olfm3 (Olfactomedin 3) as microglia-specific markers; and CD163 and CD206 as CNS-macrophage-specific markers (Table 1). Among the microglia-specific markers, none shows

a high expression level stable throughout the entire microglia's lifespan, suggesting that the dynamics of each marker should be considered.

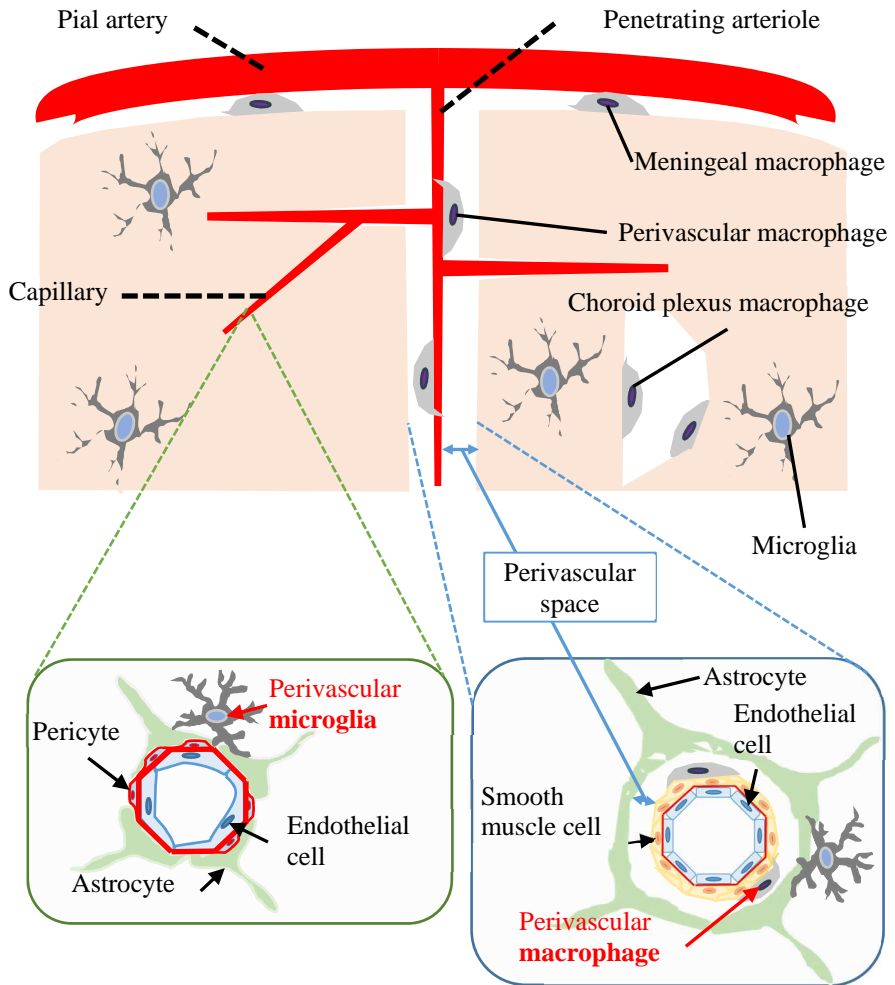
Studies specifically investigating the differential functions of microglia (including parenchymal and perivascular microglia) and PVMs are lacking due to the absence of steadfast experimental systems^{12,14}. However the use of single-cell RNA-seq analysis or mass cytometry have brought additional evidences confirming their differential roles. Gene expression analyzes and histological studies have reported cell-specific markers: TMEM119 (Transmembrane protein 119), P2RY12 (P2Y purinoceptor 12), SALL1 (Sal-like protein 1), Siglec-H (Sialic acid-binding immunoglobulin-type lectins), Olfm3 (Olfactomedin 3) as microglia-specific markers; and CD163 and CD206 as CNS-macrophage-specific markers (Table 1). Among the microglia-specific markers, none shows a high expression level stable throughout the entire microglia's lifespan, suggesting that the dynamics of each marker should be considered.

During development, microglia (including PMG) and PVM originate from yolk-sac progenitors¹⁵⁻¹⁷. Recent work using a combination of fate mapping with single-cell RNA-seq and parabiosis experiments has shown that PVMs and MMs arise from yolk-sac hematopoietic precursors too, while CPMs have either an embryonic or adult hematopoietic origin¹⁸. This new insight on the common origin of microglia, PMG and PVM raises a new question on the exact time-point when microglia diverge from CNS-macrophages and which triggers mediate this differentiation. While the emergence of parenchymal microglia was evidenced between embryonic day 9.5 and 12.5 by using *Cx3cr1*^{GFP/WT} mice¹⁸, PVMs emerge at embryonic day 14.5 at the time of BBB closure^{19,20}.

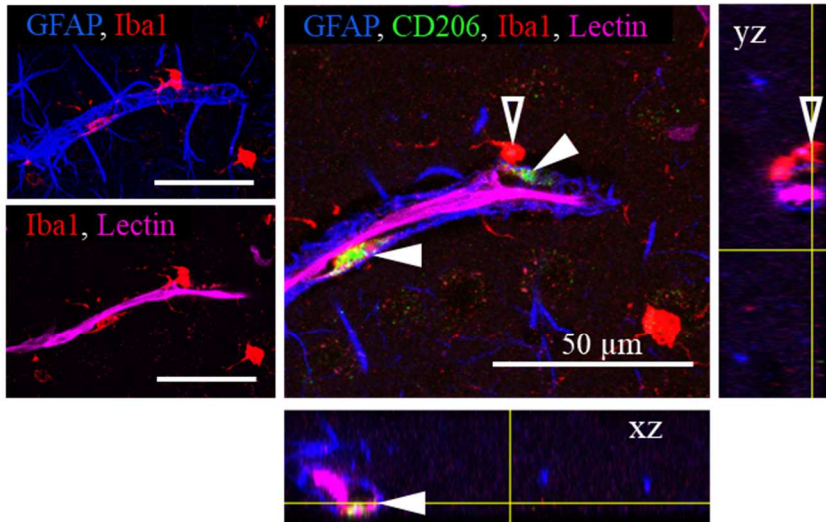
In adulthood, most functional markers are shared between microglia and macrophages, although their expression level may differ. Ionized calcium-binding adapter molecule 1 (Iba-1) is a representative marker of both microglia and CNS-macrophages. While Iba-1 intensity can be used to discriminate PVMs from PMG by immunofluorescence: low vs high intensity respectively^{21,22}, its combination with additional markers is valuable (Fig. 1). TMEM119 allows the specific identification of microglia from other immune cells^{23,24}, however, its expression seems limited to mouse and human cells so far²⁵. Siglec-H and Olfml3 are also highly expressed in microglia, whereas CPMs and MMs showed a very faint expression^{26,27}. CD163 seems a rather selective marker for PVMs²⁸.

In addition, microglia have been also distinguished from CNS macrophages by their low CD45 and low CD206 expression levels although this constitutes a less accurate identification method.

A



B



C

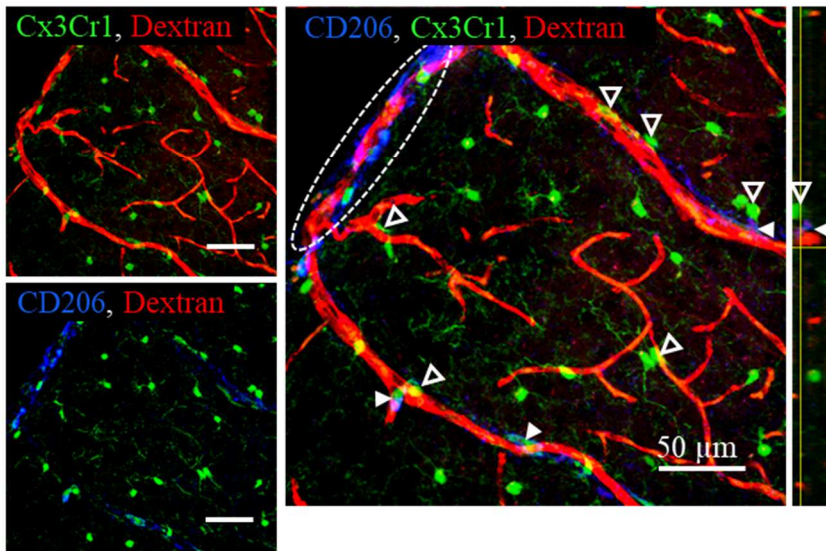


Figure 1: Perivascular microglia and perivascular macrophages in their workplace. (A) Scheme illustrating the differential location of CNS-macrophages including Perivascular Macrophages (PVM), parenchymal microglia, and Perivascular microglia (PMG) around the cerebral small vessels. Representative cortical areas in rat (B) and mice (C) imaged by confocal microscopy after immunostaining to reveal the presence and location of PVM (filled arrow heads) and PMG (empty arrow heads) using a set of different markers. (B) Two CD206-positive PVMs (green) are located between astrocyte end-feet (GFAP, blue) and endothelial cells stained by the injection of lectin. The PVM shows a flatten-shape and a low-intensity Iba1 staining compared to PMG that are located beyond the glia limitans. The location of the x,z view (bottom) and y,z view (right) are corresponding to yellow lines. (C) Elongated CD206-positive PVMs (blue) are located along two large penetrating arterioles and meningeal macrophages (MMs) are visible around a pial artery (in

white dotted circle). Vessels are stained by the injection of 70-kDa dextran-Texas Red in a transgenic Cx3Cr1^{sfp/wt} mouse. PMG show a high Cx3Cr1 expression (green) compared to PVMs. The location of the y,z view (right) is corresponding to yellow lines.

With aging or disease progression, both microglia and PVMs participate in inflammatory responses and their phenotypes are often assessed by the expression of specific cytokines or surface receptors. An increased expression of CD68, or a decreased expression of P2RY12/*P2ry12*, are for example associated with the acquisition of a pro-inflammatory phenotype²⁹⁻³¹. As with other tissue-resident macrophages, microglia can be polarized and traditionally categorized into M1 (pro-inflammatory) and M2 (anti-inflammatory, resolving) phenotypes. However, it is now admitted that no clear boundaries can be drawn to characterize microglia/macrophage function and that a more refined phenotypic characterization should be used in new studies^{32,33}. Furthermore, one has to take into account that the expression of surface markers useful for the identification and distinction between microglia and PVMs can also vary due to their activation level. Indeed, while CD163 is normally specifically expressed by PVMs as described above, CD163-positive microglia have been observed in AD patients³⁴.

A list of markers to ease the distinction of microglia, including PMG, and CNS-macrophages including PVMs, is summarized in Table 1. In addition, PVMs and PMG are displayed in representative confocal pictures from cortical areas from a rat (Fig. 1B) and from a mouse (Fig. 1C). Their identification is based on their location (vascular-associated and inside/outside the glia limitans), morphology (ramified vs flatten-shape) and the expression levels of different surface markers (Iba1; Cx3Cr1; CD206, CD163). Furthermore their differential position in respect to the glial limitans has been also confirmed by electron microscopy^{35,36}. As indicated in a recent review, PVMs are only present in association with arterioles and venules, but not with capillaries, as PVMs are located in the perivascular space between the abluminal surface of the endothelial vessel basement membrane and the parenchymal basement membrane on the glia-limitans side¹³. These two basement membranes are however combined in capillaries, leaving no space for PVMs while PMG are still present. This implies that the contribution of perivascular immune cells to cerebrovascular dysfunction may differ with the vessel size and that PVMs and PMG should be studied separately.

Table 1: Differentiation makers for microglia (MG), including perivascular microglia (PMG) and CNS-macrophages (MP) including perivascular macrophages (PVMs).

Marker		Functions		Gene expression			Immunohistochemistry			References
gene	protein			Immature	Adult	Injury/ Inflammatory	Immature	Adult	Injury/ Inflammatory	
<i>Cd45</i>	CD45	T cell and B cell receptor mediated activation		low	low	low				18, 61, 62
<i>Igcam</i>	CD11b (OX-42)	cell adhesion; apoptosis; chemotaxis	MG	high	high	high				62, 63
			MP	high	high	high				
<i>Iba1</i>	Iba-1 /	complete functional	MG/PMG	high	high	high	P (E9-)	P: high	P	21, 64
<i>Aif1</i>	AIF-1	profiles are unknown	MP	low	low	low	P	P: weak	P	
<i>Cx3CR1</i>	Cx3CR1	Fractalkine Receptor	MG	high	high	high	P (E8.5-)	P	P	65, 66
<i>Csf1r</i>	CSF1-R	CSF1(MCSF) Receptor	MP	low	low	low	P	P	P	67, 68
			MG	low	low	low	P	P	P	
<i>Tmem119</i>	TMEM119	a cell-surface protein of unknown function	MG	N.D.	high	decrease	N: (-P3)	P	minor decrease	23, 25, 30
<i>Sall1</i>	Sall1	a zinc-finger transcription factor	MP	N.D.	N.D.	N.D.	N	N	N	69
			MG	high ^{†1}	high	high	P (E10.2-) ^{†1}	P	P	
<i>P2ry12</i>	P2RY12	Nucleotide Receptor	MP	N.D.	N.D.	N.D.	N	N ^{†2}	N	
<i>Siglec-H</i>	Siglec-H	Sialic acid-binding cell surface lectin	MG	high	high	low/N.D.	P (new born-)	P	major decrease	29, 30
			MP	N.D.	N.D.	N.D.	N	N	N	
<i>Olfml3</i>	Olfml3	proangiogenic factor	MG	high	high	stable~decrease	P (E17)	P	P	26, 70
			MP	N.D.	N.D.	N.D.	N	N ^{†3}	N	
<i>Cd163</i>	CD163	endocytosis; scavenger receptor	MG	high	high	stable~decrease	?	P	P	27, 30
			MP	N.D.	N.D.	N.D.	?	N ^{†4}	N	
<i>Mrc1</i>	CD206	endocytosis; mannose receptor	MG	N.D.	N.D.	N.D.	?	N	P: occasionally	6, 34
			MP	high	high	high	?	P ^{†5}	P ^{†6}	
			MG	N.D.	N.D.	low	?	N	P: occasionally	18, 71, 72
			MP	high	high	high	?	P	P	

(Table 1 legend)

*1: Astrocytes and neuronal progenitor cell in the CNS during embryogenesis have high expression of sall1.
*2: Choroid plexus macrophages are negative, 5% of other CNS-associated macrophages were positive by flow cytometry. *3: Choroid plexus macrophages express Siglec-H in steady state. *4: Meningeal macrophages shows no or very faint Olfml3-positive. *5: Especially positive on perivascular and meningeal macrophages.
*6: Infiltrating macrophages become positive. Abbreviations; MG: microglia; MP: macrophages; N.D.: not detected.

Perivascular immune cells and cerebrovascular dysfunction

While the contribution of microglia has been studied in various neurodegenerative disorders, their involvement in cerebrovascular diseases has been less studied. In particular, we aimed at summarizing the studies on perivascular immune cells (PMG, PVM) in the context of cerebrovascular dysfunction.

Literature search method

Studies on PMG or PVMs and their involvement in cerebrovascular dysfunction were identified from electronic searches exclusively done by using PubMed database. We used the following MeSH and free search terms to identify peer-reviewed original articles in English; for PMG: microglia AND (blood-brain barrier OR cerebral small vessel) AND (cerebrovascular disorders OR cerebral small vessel disease OR neurodegenerative diseases OR multiple sclerosis OR stroke); and for PVMs: (perivascular macrophages OR CNS macrophages OR brain macrophages) AND (cerebrovascular disorders OR cerebral small vessel disease OR neurodegenerative diseases OR multiple sclerosis OR stroke). In both searches, we excluded studies matching the following terms: review; infection; epilepsy; hemorrhage. Furthermore, studies were excluded if they referred to microglia or macrophages in the context of brain tumor/metastasis, non-CNS diseases, infectious diseases, and drug- or alcohol-abuse. Screening and extraction of articles were done by TK under the guidance of SF. For each study, the following variables were recorded: (a) year of publication, (b) type of disease, (c) animal model, (d) microglia or macrophages markers and (e) results. The searches were performed on June 30th 2019 and the results are described in a flow diagram (Fig. 2).

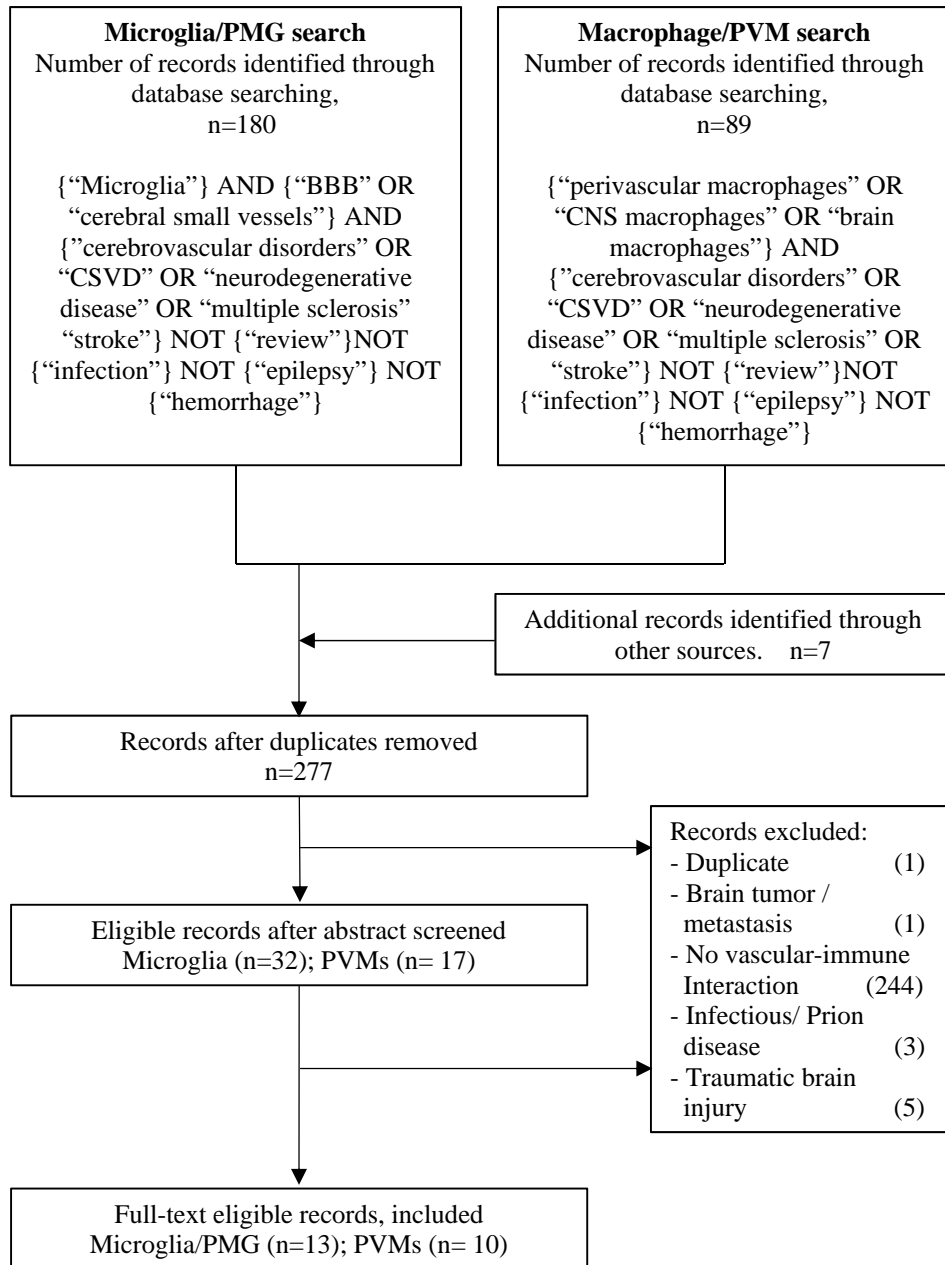


Figure 2. Flow diagram illustrating the systematic search protocol and the identification of the corresponding publication records.

Perivascular macrophages in cerebrovascular dysfunction

PVMs have been shown to contribute to an increased vascular permeability and an increased granulocyte recruitment in the acute phase of stroke using the transient Middle Cerebral Artery Occlusion (tMCAO) model. Their depletion by the administration of clodronate-containing liposomes (CCLs) was indeed able to attenuate the vascular permeability, as evidenced by the reduced Evans blue extravasation 24 h post-ischemia, and to reduce the granulocyte infiltration in the ischemic cortex³⁷. In an acute hypertension model induced by Angiotensin II infusion (2 weeks), the increased BBB permeability was shown to result from the generation of reactive oxygen species (ROS) mediated by the Angiotensin II type 1 receptor (AT₁R) and the subsequent activation of Nox2 in PVMs. Indeed, the depletion of PVMs or the deletion of AT₁R or Nox2 from PVMs, using bone marrow chimeras, were able to prevent BBB dysfunction, restore the neurovascular coupling and prevent cognitive dysfunction²¹. In SHR-SP, a chronic hypertensive model, PVMs depletion with CCLs improved the endothelium-dependent dilation of the MCA, and prevented MCA structural remodeling induced by hypertension³⁸. Post-mortem investigation of brains from CADASIL patients (cerebral autosomal dominant arteriopathy with subcortical infarcts and leukoencephalopathy), an hereditary cSVD form, has revealed the presence of PVMs-like cells with a phagocytic morphology around granular osmiophilic material-depositions in arteries, and arterioles-suggesting a role for PVMs to clear abnormal depositions in the perivascular space to prevent vascular remodeling³⁹. Furthermore, in TgCRND8 mice, a mouse model of cerebral amyloid angiopathy (CAA), PVM depletion using CCLs increased the number of amyloid depositions in cortical vessels. An increased content of A β 42 in cerebral vessels from depleted mice was also evidenced by ELISA⁴⁰. This highlights again the crucial phagocytic role of PVMs to preserve the cerebrovasculature. In the same study, repeated intracerebroventricular injections of chitin were performed to increase PVMs turn-over. This led to a reduction in the number of amyloid-positive cortical vessels⁴⁰. This study reported for the first time that modulating PVMs density can influence the clearance of amyloid from the cerebral vasculature. Unfortunately, it is highly possible that an increased clearance capacity can be accompanied by an increased ROS production. Park et al. have shown that the selective depletion of PVMs using intracerebroventricular injection of CCLs reduced ROS production and cerebrovascular dysfunction induced by direct application of A β in the cerebral cortex, or by its intravenous administration or by A β overproduction in Tg2576 mice. By using bone marrow transplantation, the involvement of CD36 and Nox2 from PVMs was demonstrated in the neurovascular dysfunction associated with the amyloid deposition⁴¹. These results indicate a crucial role for PVMs in clearing A β peptides from perivascular spaces and for preventing A β accumulation in cerebral vessels but it could be at the expense of a generation of

reactive oxygen species deleterious for the integrity of cerebral vessels in the long-term.

In MS patients, CD163-positive PVMs accumulate around vessels in areas of active demyelination where they can act as antigen presenting cells^{42,43}. While PVMs may be neuroprotective in early MS lesions by the release of leukemia inhibitory factor and brain-derived neurotrophic factor⁴⁴, their increased density precedes the occurrence of clinical symptoms⁴⁵. Single-cell profiling was performed in a MS mouse model and identified PVMs with a high expression of CD74 and CCL5 at the peak of the disease, suggesting PVMs play an antigen presentation role in the perivascular space³⁰. Finally, PVMs depletion was associated with a decreased severity of the pathology in an experimental MS model⁴⁶.

In summary, while PVMs seem to exert protective effects at first to halt the progression of pathological events such as removal of harmful proteins, we suggest that their repeated activation and exposure to danger signals may lead over time to different brain disease-specific deleterious effects. The biology and pathobiology of PVMs in other brain diseases and in other tissues have been described in other recent reviews^{47,48}.

Microglia & Perivascular-Microglia in cerebrovascular dysfunction

While the activation of parenchymal microglia in the presence of BBB leakages in hypertensive cSVD models is well known^{49,50}, evidences for the contribution of PMG to the initiation of cerebrovascular dysfunction remain limited.

In the genetic hypertensive rat model rat (Cyp1a1-Ren2), the microglia density increased in 6 months old rats with a higher number of vascular-associated microglia (presumably PMG based on their shape, Iba1 immunoreactivity and location), prior to any cerebrovascular lesions. This study further indicated that a modest but chronic blood pressure elevation can induce the regulation of growth factors and inflammatory genes prior to vascular remodeling, suggesting a role for PMG in the progression of cerebrovascular dysfunction⁵¹. In DOCA-salt rat, a sub-chronic hypertension model, while PVMs phenotype did not change, PMG exhibited dynamic phenotypic changes; proliferative parenchymal and perivascular microglia proliferated before switching to a pro-inflammatory state and before BBB impairment and the occurrence of cerebrovascular lesions²². In a post-mortem study on CAA, Carrano et al. revealed that major changes in tight-junction protein expressions (claudin-5, occluding, ZO-1) were observed in CAA-affected capillaries engulfed by NADPH oxidase-2 (NOX-2)-positive activated microglia and this was observed in association with BBB disruption.

In addition, A β induced ROS formation by binding RAGE (receptor of advanced glycoen product), an A β transporter. In vitro, blocking RAGE or inhibiting NOX-2 reduced the toxic effect of A β on endothelial cells^{52,53}, supporting the evidence that the increased expression of NOX-2 in PMG could also affect the cerebral small vessels, similarly to the findings on PVMs.

In transgenic AD mouse models, the presence of microglial activation was evidenced together with an increased expression of pro-inflammatory cytokines (TNF-alpha; MCP-1) at an early stage of AD pathology⁵⁴. This finding supports the hypothesis that cerebrovascular inflammation may be involved in the initiation of Alzheimer's disease (AD) before the start of plaque deposition⁵⁵.

In experimental MS models, there was an increased contact size of individual microglial processes around cerebral vessels in both acute and chronic EAE stage and the MHC-II expression was upregulated in microglia contacting the glial basement membrane (PMG), while it was limited in PVMs and absent in microglia from non-immunized controls³⁶, pointing towards an important role for PMG in MS. Using *in vivo* two-photon microscopy, clusters of perivascular microglia were observed due to leaked blood fibrinogen before myelin loss and paralysis onset⁵⁶.

Following an artificial BBB leakage induced by focal laser-injury, the immediate accumulation of processes from PMG towards the laser-injured capillary was capable of closing the BBB. This highly migratory behavior of PMG relied on the function of P2RY12 receptors as their inhibition using clopidogrel or their genetic ablation, suppressed PMG motility and thereby led to a prolonged delay before BBB closure⁵⁷. This highlights the importance of PMG for BBB repair. In fact, the ultrastructural analysis of the laser injury by electron microscopy revealed that the aggregation of densely packed processes completely sheathed the site of injury. Immuno-labeling revealed that PMG processes, extending towards the laser-injured site, exhibited high P2RY12 expression⁵⁷. In this article, the authors used the term "juxtavascular microglia" to describe the vascular-associated Cx3Cr1-positive microglia at the capillary level with extended and fine processes, *i.e.* PMG. However they wrongly defined juxtavascular microglia are being largely localized within the perivascular space which would correspond to the definition of PVMs. Another evidence has pointed towards a BBB repair role for PMG.

In tMCAO mice, Iba-1-positive cells with ramified processes start to cluster around vessels in the penumbra area within one hour after the initiation of the ischemic insult. The attracted cells enwrap blood vessels in the penumbra 24 hours post tMCAO and harbor an amoeboid shape and a high CD68 expression⁵⁸. The hypoperfusion induced by tMCAO in the area surrounding the ischemic core

may continuously produce pro-inflammatory components, such as DAMPs, ROS, and inflammatory cytokines that may themselves, or after the leakage of plasma immunoglobulins or proteins, induce the infiltration of circulating monocytes or neutrophils into the brain parenchyma^{59,60}. The rapid mobilization of microglia after the ischemic insult suggests that PMG could be the first to initiate the BBB repair in the early phase of the injury before the migration of other parenchymal or systemic macrophages in the following hours/days.

In summary, parenchymal and perivascular microglia are quickly mobilized and accumulate around cerebral vessels following BBB dysfunction. In addition, they appear to be already present and activated in some conditions in absence of BBB dysfunction in the early phase of cerebrovascular diseases and could therefore be targeted to prevent disease's progression. This will however only be achieved thanks to a refined molecular characterization of their activation dynamics.

Conclusion

Vessels-surroundings are the homeland of PVMs and PMG. While recent studies have started to differentiate these two cell populations, their respective role and dynamics in the pathogenesis of cerebrovascular diseases are still unclear. This review aimed at summarizing the current direct and indirect evidences linking PMG and PVMs to cerebrovascular dysfunction. Our current knowledge on their role in BBB damage and repair is limited and should further integrate their dynamic nature. The emergence of transcriptomic and single-cell RNA sequencing techniques will lead to a more complete characterization and understanding of PVMs and PMG. Altogether, clarifying the roles of PMG and PVMs in physiological and pathological conditions may offer new perspectives for the diagnosis, prevention and treatment of CNS diseases in which the perivascular environment is playing a crucial role.

References

1. Dichgans M, Leys D. Vascular Cognitive Impairment. *Circ Res*. 2017 Feb 3;120(3):573-91.
2. Hickey WF, Kimura H. Perivascular microglial cells of the CNS are bone marrow-derived and present antigen in vivo. *Science*. 1988 Jan 15;239(4837):290-2.
3. Graeber MB, Streit WJ, Kreutzberg GW. Identity of ED2-positive perivascular cells in rat brain. *J Neurosci Res*. 1989 Jan;22(1):103-6.
4. Graeber MB, Streit WJ. Perivascular microglia defined. *Trends in neurosciences*. 1990 Sep;13(9):366.
5. Fabriek BO, Polfliet MM, Vloet RP, et al. The macrophage CD163 surface glycoprotein is an erythroblast adhesion receptor. *Blood*. 2007 Jun 15;109(12):5223-9.
6. Fabriek BO, Van Haastert ES, Galea I, et al. CD163-positive perivascular macrophages in the human CNS express molecules for antigen recognition and presentation. *Glia*. 2005 Sep;51(4):297-305.
7. Lewis CA, Solomon JN, Rossi FM, Krieger C. Bone marrow-derived cells in the central nervous system of a mouse model of amyotrophic lateral sclerosis are associated with blood vessels and express CX(3)CR1. *Glia*. 2009 Oct;57(13):1410-9.
8. Arnold T, Betsholtz C. Correction: The importance of microglia in the development of the vasculature in the central nervous system. *Vascular cell*. 2013;5(1):12.
9. Nimmerjahn A, Kirchhoff F, Helmchen F. Resting microglial cells are highly dynamic surveillants of brain parenchyma in vivo. *Science*. 2005 May 27;308(5726):1314-8.
10. Hu X, Leak RK, Shi Y, et al. Microglial and macrophage polarization[mdash]new prospects for brain repair. *Nat Rev Neurol*. 2015 01//print;11(1):56-64.
11. Foulquier S, Caolo V, Swennen G, et al. The role of receptor MAS in microglia-driven retinal vascular development. *Angiogenesis*. 2019 Jun 20.
12. Zhao X, Eyo UB, Murugan M, Wu LJ. Microglial interactions with the neurovascular system in physiology and pathology. *Developmental neurobiology*. 2018 Jun;78(6):604-17.
13. Iadecola C. The Neurovascular Unit Coming of Age: A Journey through Neurovascular Coupling in Health and Disease. *Neuron*. 2017 Sep 27;96(1):17-42.
14. Sevenich L. Brain-Resident Microglia and Blood-Borne Macrophages Orchestrate Central Nervous System Inflammation in Neurodegenerative Disorders and Brain Cancer. *Front Immunol*. 2018;9:697.
15. Salter MW, Stevens B. Microglia emerge as central players in brain disease. *Nat Med*. 2017 09//print;23(9):1018-27.
16. Alliot F, Godin I, Pessac B. Microglia derive from progenitors, originating from the yolk sac, and which proliferate in the brain. *Brain research Developmental brain research*. 1999 Nov 18;117(2):145-52.
17. Ginhoux F, Greter M, Leboeuf M, et al. Fate mapping analysis reveals that adult microglia derive from primitive macrophages. *Science*. 2010 Nov 5;330(6005):841-5.
18. Goldmann T, Wieghofer P, Jordao MJ, et al. Origin, fate and dynamics of macrophages at central nervous system interfaces. *Nat Immunol*. 2016 Jul;17(7):797-805.
19. Wong K, Noubade R, Manzanillo P, et al. Mice deficient in NRROS show abnormal microglial development and neurological disorders. *Nat Immunol*. 2017 Jun;18(6):633-41.
20. Li Q, Barres BA. Microglia and macrophages in brain homeostasis and disease. *Nature reviews Immunology*. 2018 Apr;18(4):225-42.
21. Faraco G, Sugiyama Y, Lane D, et al. Perivascular macrophages mediate the neurovascular and cognitive dysfunction associated with hypertension. *J Clin Invest*. 2016 Dec 1;126(12):4674-89.
22. Koizumi T, Taguchi K, Mizuta I, et al. Transiently proliferating perivascular microglia harbor M1 type and precede cerebrovascular changes in a chronic hypertension model. *Journal of Neuroinflammation*. 2019 2019/04/10;16(1):79.
23. Furube E, Kawai S, Inagaki H, Takagi S, Miyata S. Brain Region-dependent Heterogeneity and Dose-dependent Difference in Transient Microglia Population Increase during Lipopolysaccharide-induced Inflammation. *Sci Rep*. 2018 Feb 2;8(1):2203.
24. Satoh J, Kino Y, Asahina N, et al. TMEM119 marks a subset of microglia in the human brain. *Neuropathology*. 2016 Feb;36(1):39-49.
25. Bennett ML, Bennett FC, Liddelow SA, et al. New tools for studying microglia in the mouse and human CNS. *Proc Natl Acad Sci U S A*. 2016 Mar 22;113(12):E1738-46.
26. Konishi H, Kobayashi M, Kunisawa T, et al. Siglec-H is a microglia-specific marker that discriminates microglia from CNS-associated macrophages and CNS-infiltrating monocytes. *Glia*. 2017 Dec;65(12):1927-43.
27. Neidert N, von Ehr A, Zoller T, Spittau B. Microglia-Specific Expression of Olfml3 Is Directly Regulated by Transforming Growth Factor beta1-Induced Smad2 Signaling. *Front Immunol*. 2018;9:1728.

28. Kim WK, Alvarez X, Fisher J, et al. CD163 identifies perivascular macrophages in normal and viral encephalitic brains and potential precursors to perivascular macrophages in blood. *Am J Pathol.* 2006 Mar;168(3):822-34.
29. Mildner A, Huang H, Radke J, Stenzel W, Priller J. P2Y12 receptor is expressed on human microglia under physiological conditions throughout development and is sensitive to neuroinflammatory diseases. *Glia.* 2017 Feb;65(2):375-87.
30. Jordão MJC, Sankowski R, Brendecke SM, et al. Single-cell profiling identifies myeloid cell subsets with distinct fates during neuroinflammation. *Science.* 2019;363(6425):eaat7554.
31. Rabinowitz S, Gordon S. Differential expression of membrane sialoglycoproteins in exudate and resident mouse peritoneal macrophages. *Journal of Cell Science.* 1989;93(4):623-30.
32. Ransohoff RM. A polarizing question: do M1 and M2 microglia exist? *Nat Neurosci.* 2016 08//print;19(8):987-91.
33. Franco R, Fernandez-Suarez D. Alternatively activated microglia and macrophages in the central nervous system. *Prog Neurobiol.* 2015 Aug;131:65-86.
34. Pey P, Pearce RK, Kalaitzakis ME, Griffin WS, Gentleman SM. Phenotypic profile of alternative activation marker CD163 is different in Alzheimer's and Parkinson's disease. *Acta Neuropathol Commun.* 2014 Feb 14;2:21.
35. Onoda A, Umezawa M, Takeda K, Ihara T, Sugamata M. Effects of maternal exposure to ultrafine carbon black on brain perivascular macrophages and surrounding astrocytes in offspring mice. *PLoS One.* 2014;9(4):e94336.
36. Joost E, Jordão MJC, Mages B, Prinz M, Bechmann I, Krueger M. Microglia contribute to the glia limitans around arteries, capillaries and veins under physiological conditions, in a model of neuroinflammation and in human brain tissue. *Brain Structure and Function.* 2019 April 01;224(3):1301-14.
37. Pedragosa J, Salas-Perdomo A, Gallizioli M, et al. CNS-border associated macrophages respond to acute ischemic stroke attracting granulocytes and promoting vascular leakage. *Acta Neuropathol Commun.* 2018 Aug 9;6(1):76.
38. Pires PW, Girgla SS, Moreno G, McClain JL, Dorrance AM. Tumor necrosis factor- α inhibition attenuates middle cerebral artery remodeling but increases cerebral ischemic damage in hypertensive rats. *Am J Physiol Heart Circ Physiol.* 2014 Sep 1;307(5):H658-69.
39. Yamamoto Y, Craggs LJJ, Watanabe A, et al. Brain Microvascular Accumulation and Distribution of the NOTCH3 Ectodomain and Granular Osmiophilic Material in CADASIL. *Journal of Neuropathology & Experimental Neurology.* 2013;72(5):416-31.
40. Hawkes CA, McLaurin J. Selective targeting of perivascular macrophages for clearance of beta-amyloid in cerebral amyloid angiopathy. *Proc Natl Acad Sci U S A.* 2009 Jan 27;106(4):1261-6.
41. Park L, Uekawa K, Garcia-Bonilla L, et al. Brain Perivascular Macrophages Initiate the Neurovascular Dysfunction of Alzheimer A β Peptides. *Circ Res.* 2017 Jul 21;121(3):258-69.
42. Zhang Z, Zhang ZY, Schittenhelm J, Wu Y, Meyermann R, Schluesener HJ. Parenchymal accumulation of CD163+ macrophages/microglia in multiple sclerosis brains. *J Neuroimmunol.* 2011 Aug 15;237(1-2):73-9.
43. McMahon EJ, Bailey SL, Castenada CV, Waldner H, Miller SD. Epitope spreading initiates in the CNS in two mouse models of multiple sclerosis. *Nature Medicine.* 2005 02/27/online;11:335.
44. Vanderlocht J, Hellings N, Hendriks JJA, et al. Leukemia inhibitory factor is produced by myelin-reactive T cells from multiple sclerosis patients and protects against tumor necrosis factor- α -induced oligodendrocyte apoptosis. *Journal of Neuroscience Research.* 2006;83(5):763-74.
45. Hofmann N, Lachnit N, Streppel M, et al. Increased expression of ICAM-1, VCAM-1, MCP-1, and MIP-1 alpha by spinal perivascular macrophages during experimental allergic encephalomyelitis in rats. *BMC immunology.* 2002 Aug 26;3:11.
46. Polfliet MM, van de Veerdonk F, Dopp EA, et al. The role of perivascular and meningeal macrophages in experimental allergic encephalomyelitis. *J Neuroimmunol.* 2002 Jan;122(1-2):1-8.
47. Lapenna A, De Palma M, Lewis CE. Perivascular macrophages in health and disease. *Nature reviews Immunology.* 2018 Nov;18(11):689-702.
48. Faraco G, Park L, Anrather J, Iadecola C. Brain perivascular macrophages: characterization and functional roles in health and disease. *Journal of molecular medicine (Berlin, Germany).* 2017 Nov;95(11):1143-52.
49. Kaiser D, Weise G, Moller K, et al. Spontaneous white matter damage, cognitive decline and neuroinflammation in middle-aged hypertensive rats: an animal model of early-stage cerebral small vessel disease. *Acta Neuropathol Commun.* 2014 Dec 18;2(1):169.

50. Foulquier S, Namsolleck P, Van Hagen BT, et al. Hypertension-induced cognitive impairment: insights from prolonged angiotensin II infusion in mice. *Hypertension research : official journal of the Japanese Society of Hypertension*. 2018 Oct;41(10):817-27.
51. Pannozzo MA, Holland PR, Scullion G, Talbot R, Mullins JJ, Horsburgh K. Controlled hypertension induces cerebrovascular and gene alterations in Cyp1a1-Ren2 transgenic rats. *J Am Soc Hypertens*. 2013 Nov-Dec;7(6):411-9.
52. Carrano A, Hoozemans JJ, van der Vies SM, Rozemuller AJ, van Horsen J, de Vries HE. Amyloid Beta induces oxidative stress-mediated blood-brain barrier changes in capillary amyloid angiopathy. *Antioxid Redox Signal*. 2011 Sep 1;15(5):1167-78.
53. Carrano A, Hoozemans JJ, van der Vies SM, van Horsen J, de Vries HE, Rozemuller AJ. Neuroinflammation and blood-brain barrier changes in capillary amyloid angiopathy. *Neurodegener Dis*. 2012;10(1-4):329-31.
54. Janelins MC, Mastrangelo MA, Oddo S, LaFerla FM, Federoff HJ, Bowers WJ. Early correlation of microglial activation with enhanced tumor necrosis factor-alpha and monocyte chemoattractant protein-1 expression specifically within the entorhinal cortex of triple transgenic Alzheimer's disease mice. *Journal of Neuroinflammation*. 2005 October 18;2(1):23.
55. Yu D, Corbett B, Yan Y, et al. Early cerebrovascular inflammation in a transgenic mouse model of Alzheimer's disease. *Neurobiology of Aging*. 2012 2012/12/01;33(12):2942-7.
56. Davalos D, Kyu Ryu J, Merlini M, et al. Fibrinogen-induced perivascular microglial clustering is required for the development of axonal damage in neuroinflammation. *Nature Communications*. 2012 11/27/online;3:1227.
57. Lou N, Takano T, Pei Y, Xavier AL, Goldman SA, Nedergaard M. Purinergic receptor P2RY12-dependent microglial closure of the injured blood-brain barrier. *Proc Natl Acad Sci U S A*. 2016 Jan 26;113(4):1074-9.
58. Jolivel V, Bicker F, Biname F, et al. Perivascular microglia promote blood vessel disintegration in the ischemic penumbra. *Acta Neuropathol*. 2015 Feb;129(2):279-95.
59. Benjelloun N, Renolleau S, Represa A, Ben-Ari Y, Charriaut-Marlangue C. Inflammatory responses in the cerebral cortex after ischemia in the P7 neonatal Rat. *Stroke*. 1999 Sep;30(9):1916-23; discussion 23-4.
60. Krueger M, Mages B, Hobusch C, Michalski D. Endothelial edema precedes blood-brain barrier breakdown in early time points after experimental focal cerebral ischemia. *Acta Neuropathol Commun*. 2019 Feb 11;7(1):17.
61. Rangaraju S, Raza SA, Li NX, et al. Differential Phagocytic Properties of CD45(low) Microglia and CD45(high) Brain Mononuclear Phagocytes-Activation and Age-Related Effects. *Front Immunol*. 2018;9:405.
62. Martin E, El-Behi M, Fontaine B, Delarasse C. Analysis of Microglia and Monocyte-derived Macrophages from the Central Nervous System by Flow Cytometry. *J Vis Exp*. 2017 Jun 22(124).
63. Robinson AP, White TM, Mason DW. Macrophage heterogeneity in the rat as delineated by two monoclonal antibodies MRC OX-41 and MRC OX-42, the latter recognizing complement receptor type 3. *Immunology*. 1986 Feb;57(2):239-47.
64. Ito D, Imai Y, Ohsawa K, Nakajima K, Fukuuchi Y, Kohsaka S. Microglia-specific localisation of a novel calcium binding protein, Iba1. *Brain Res Mol Brain Res*. 1998 Jun 1;57(1):1-9.
65. Hammond TR, Dufort C, Dissing-Olesen L, et al. Single-Cell RNA Sequencing of Microglia throughout the Mouse Lifespan and in the Injured Brain Reveals Complex Cell-State Changes. *Immunity*. 2019 Jan 15;50(1):253-71.e6.
66. Jung S, Aliberti J, Graemmel P, et al. Analysis of fractalkine receptor CX(3)CR1 function by targeted deletion and green fluorescent protein reporter gene insertion. *Molecular and cellular biology*. 2000 Jun;20(11):4106-14.
67. Akiyama H, Nishimura T, Kondo H, Ikeda K, Hayashi Y, McGeer PL. Expression of the receptor for macrophage colony stimulating factor by brain microglia and its upregulation in brains of patients with Alzheimer's disease and amyotrophic lateral sclerosis. *Brain Res*. 1994 Mar 7;639(1):171-4.
68. Raivich G, Haas S, Werner A, Klein MA, Kloss C, Kreutzberg GW. Regulation of MCSF receptors on microglia in the normal and injured mouse central nervous system: a quantitative immunofluorescence study using confocal laser microscopy. *The Journal of comparative neurology*. 1998 Jun 8;395(3):342-58.
69. Buttgeriet A, Lelios I, Yu X, et al. Sall1 is a transcriptional regulator defining microglia identity and function. *Nat Immunol*. 2016 Dec;17(12):1397-406.

70. Mrdjen D, Pavlovic A, Hartmann FJ, et al. High-Dimensional Single-Cell Mapping of Central Nervous System Immune Cells Reveals Distinct Myeloid Subsets in Health, Aging, and Disease. *Immunity*. 2018 Feb 20;48(2):380-95.e6.
71. Holder GE, McGary CM, Johnson EM, et al. Expression of the mannose receptor CD206 in HIV and SIV encephalitis: a phenotypic switch of brain perivascular macrophages with virus infection. *J Neuroimmune Pharmacol*. 2014 Dec;9(5):716-26.
72. Bottcher C, Schlickeiser S, Sneeboer MAM, et al. Human microglia regional heterogeneity and phenotypes determined by multiplexed single-cell mass cytometry. *Nat Neurosci*. 2019 Jan;22(1):78-90.

Chapter 4

Transiently proliferating perivascular microglia harbor M1-type and precede cerebrovascular changes in a chronic hypertension model

Takashi Koizumi, Katsutoshi Taguchi, Ikuko Mizuta, Hiroe Toba, Makoto Ohigashi, Okihiro Onishi, Kazuya Ikoma, Seiji Miyata, Tetsuo Nakata, Masaki Tanaka, Sébastien Foulquier, Harry W. M. Steinbusch, Toshiki Mizuno

Journal of Neuroinflammation. 2019; 16(1): 79

Abstract

Background: Microglia play crucial roles in the maintenance of brain homeostasis. Activated microglia show a biphasic influence, promoting beneficial repair and causing harmful damage via M2 and M1 microglia, respectively. It is well-known that microglia are initially activated to the M2-state and subsequently switch to the M1-state, called M2-to-M1 class-switching in acute ischemic models. However, the activation process of microglia in chronic and sporadic hypertension remains poorly understood. We aimed to clarify the process using a chronic hypertension model, the deoxycorticosterone acetate (DOCA)-salt-treated Wistar rats.

Methods: After unilateral nephrectomy, the rats were randomly divided into DOCA-salt, placebo, and control groups. DOCA-salt rats received a weekly subcutaneous injection of DOCA (40 mg/kg) and were continuously provided with 1% NaCl in drinking water. Placebo rats received a weekly subcutaneous injection of vehicle and were provided with tap water. Control rats received no administration of DOCA or NaCl. To investigate the temporal expression profiles of M1- and M2- specific markers for microglia, the animals were subjected to the immunohistochemical and biochemical studies after two, three, or four weeks DOCA-salt treatment.

Results: Hypertension occurred after two weeks of DOCA and salt administration, when round-shaped microglia with slightly shortened processes were observed juxtaposed to the vessels, although the histopathological findings were normal. After three weeks of DOCA and salt administration, M1-state perivascular and parenchyma microglia significantly increased, when local histopathological findings began to be observed but cerebrovascular destruction did not occur. On the other hand, M2-state microglia were never observed around the vessels at this period. Interestingly, prior to M1-activation, about 55% of perivascular microglia transiently expressed Ki-67, one of the cell proliferation markers.

Conclusions: We concluded that the resting perivascular microglia directly switched to the pro-inflammatory M1-state via a transient proliferative state in DOCA-salt rats. Our results suggest that the activation machinery of microglia in chronic hypertension differs from acute ischemic models. Proliferative microglia are possible initial key players in the development of hypertension-induced cerebral vessel damage. Fine-tuning of microglia proliferation and activation could constitute an innovative therapeutic strategy to prevent its development.

Keywords: neuroinflammation, cerebral small vessel disease, chronic hypertension, perivascular microglia, proliferation.

Introduction

Microglia are the resident immune cells in the brain and play pivotal roles in environmental surveillance to maintain brain homeostasis. Inflammation or cellular damage can stimulate microglia to increase the activity of immune functions¹. *In vivo* two-photon microscopy studies showed that activated microglia rapidly migrate to and accumulate at sites of pathological lesions, such as ischemic lesions² or newly formed amyloid- β plaques³.

The activated microglia show a biphasic influence, promoting beneficial repair and causing harmful damage. Those responsible for the former are sometimes referred to as anti-inflammatory M2 microglia, and the latter as pro-inflammatory M1 microglia⁴. These different types of activated microglia can be distinguished based on the expression of specific markers. These activated microglia are involved in various neurological disorders^{1,5}, and also influence the function and integrity of the blood-brain barrier (BBB)^{6,7}. In the present study, we focused on the interaction between microglia dynamics and cerebrovascular disease.

According to previous studies, microglia are activated in the acute phase of ischemic stroke as shown in animal models of transient middle cerebral artery occlusion (tMCAO)⁸⁻¹⁰. In the tMCAO model, numbers of M2-state microglia rapidly increase around vessels in the penumbra after infarction, and, in a few days, M1-state microglia dominantly increase. This process is called "M2-to-M1 phenotype-switching" or "shift in the M2-to-M1 phenotypes"^{11,12}. In addition to microglia activation, various molecules are involved in the acute phase of ischemic strokes, such as free radicals¹³, damage-associated molecular patterns (DAMPs)¹⁴, and T cells¹⁵. DAMPs include heat shock protein, high-mobility group box 1 (HMGB1), and Peroxiredoxin¹⁴. For example, HMGB1 is produced by ischemic neuronal cells about two to four hours after an ischemic event, and peaks at around six hours. HMGB1 affects vascular endothelial cells and induces BBB destruction, as well as microglia activation¹⁶.

In contrast, in cerebral small vessel disease (cSVD), only a limited number of reports referred to M1 and M2 microglia phenotyping and their molecular mechanisms. Chronic hypertension being the major risk factor of cSVD^{17,18}, we focused on a hypertensive cSVD model.

The aim of this study is to clarify microglia involvement in cSVD caused by chronic hypertension using deoxycorticosterone acetate (DOCA)-salt-treated Wistar rat (DOCA-salt rat) as a model mimicking sporadic and chronic hypertension.

Methods

Animals

Adult male Wistar rats (150 – 180 g) were purchased from SHIMIZU Laboratory Supplies Co, Ltd. (Kyoto, Japan). Protocols were approved by Animal Care and Use Committees of Kyoto Prefectural University of Medicine and Kyoto Pharmaceutical University. We studied Wistar rats fed standard chow and water ad libitum. Care and use of rodents met the standards set by the National Institutes of Health for experimental animals. The rats were housed under specific pathogen-free conditions and fed standard laboratory chow and water ad libitum before entering the study. They were maintained on a 12-h light/day cycle at 20-22°C and 40-50% humidity.

Preparation of the chronic hypertension model

Rats were anesthetized by combination anesthesia administered i.p. with 0.375 mg/kg of medetomidine, 2.0 mg/kg of midazolam, and 2.5 mg/kg of butorphanol and underwent unilateral nephrectomy. After a recovery period of seven days, the rats were randomly divided into a deoxycorticosterone acetate (DOCA)-salt group, placebo group, and control (Fig. 1a). DOCA-salt group rats received a weekly subcutaneous injection of DOCA (40 mg/kg body weight (Nacalai Tesque, Kyoto, Japan)) suspended in carboxymethylcellulose and were provided with 1% NaCl in drinking water for two, three, or four weeks (DOCA2W, DOCA3W, and DOCA4W, respectively, n=3 for each). Placebo group rats received a weekly subcutaneous injection of vehicle and were provided with tap water for two, three, or four weeks (n=3 for each period). Control rats (n=3) received no administration of DOCA or NaCl. The rat was placed in a restraint cage in a warm (38°C) condition for approximately two to three minutes, then systolic blood pressure and heart rate in a conscious state were measured by the tail-cuff method (BP-98A-L, Softron, Tokyo, Japan). The values were measured three times for each rat and the average value was calculated. After resting overnight under a light shield, the rats underwent magnetic resonance imaging (MRI) under anesthesia with the inhalation of isoflurane. Immediately after MRI, the rats were perfused transcardially with 4% paraformaldehyde in phosphate buffer, and their brains were removed. For immuno- or pathological staining, brains were post-fixed in the same fixative overnight at 4°C, and further cryoprotected sequentially in 5, 10, 15, and 25% sucrose. Brains embedded in Optimal Cutting Temperature compounds were stored at -20°C until examination. Frozen sections of a brain were cut into 20- μ m-thick slices with a cryostat (CM1850, Leica, Germany).

For biochemical analysis, fresh brain tissues rapidly frozen in liquid nitrogen were prepared from the control, DOCA2W, and DOCA3W (n=4, in each group) rats under anesthesia.

Evaluation items

We evaluated time-course changes in the blood pressure (Fig. 1b), clinical features (Table 1), histopathology (Fig. 1c and Supplemental Fig. 2 and Supplemental Fig. 5c), glial fibrillary acidic protein (GFAP) immunostaining of astrocyte foot processes as the basic framework of BBB (Supplemental Fig. 1), and magnetic resonance imaging (MRI) (Supplemental Fig. 5a and 5b) of the rats. Histopathological analysis was performed by hematoxylin and eosin (HE) and Klüver Barrera (KB) staining. To examine the morphological dynamics of microglia in DOCA-salt rats, we visualized microglia by ionized calcium binding adapter molecule 1 (Iba-1) (Fig. 2, 3, 4, and 5), pro-inflammatory M1-state microglia by CD68 (Fig. 3), anti-inflammatory M2-state microglia by CD206 (Fig. 4), and proliferative ability of microglia by Ki-67 (Fig. 5). We identified the vasculature by phalloidin or 4', 6-diamino-2-phenylindole (DAPI) staining.

Antibodies

Primary antibodies were used against Iba-1 (mouse monoclonal IgG, 1:500 (Millipore) or rabbit polyclonal IgG, 1:1000 (Wako)), inducible nitric oxide synthase (iNOS) (rabbit polyclonal IgG, 1:200 (Abcam)), CD68 (mouse monoclonal IgG, 1:500 (Bio-Rad)), Arginase-1 (rabbit polyclonal IgG, 1:2000 (Gene Tex)), CD206 (goat polyclonal IgG, 1:400 (R & D systems)), Ki-67 (rabbit polyclonal IgG, 1:2000 (Novocas)), and GFAP (mouse monoclonal IgG, 1:10000 (Millipore)). For detection of the primary antibodies, Alexa488 or Alexa594-conjugated secondary antibodies (anti-rabbit or mouse IgG, 1:2000 (Thermo Fisher)) were used. Vessel walls were visualized by Alexa594-conjugated phalloidin (1:500, (Thermo Fisher)).

Immunohistochemistry

Free-floating sections were permeabilized with phosphate-buffered saline containing 0.1% Tween 20 (PBST) for 30 minutes at room temperature, and then, antigen retrieval was performed with citrate buffer for 20 minutes at 75°C or for 15 minutes at 95°C (anti-Ki-67 antibody). After blocking with 5% normal goat serum diluted in PBST overnight at 4°C, the sections were incubated with primary antibody diluted with PBST for two days at 4°C. For CD206 staining, donkey serum was used for blocking. Following washing with PBST, sections were incubated with appropriate secondary antibodies with DAPI for two hours at room temperature. After PBS washing, the sections were mounted on slides with FluorSave Reagent (Merck Millipore, Darmstadt, Germany). For confocal observation, images were acquired as Z stacks (10 – 20 z-sections, 1 µm apart, 1,024 x 1,024 pixels) using a Plan-Apochromat 63x/1.40 Oil DIC objective (Carl Zeiss, Oberkochen, Germany) with an inverted laser-scanning confocal microscope, LSM510 META (Carl Zeiss). Image analysis was performed using Zeiss LSM Image Browser. The image acquisition region including the cortical blood vessels was randomly selected. Ten images per rat were acquired. We

identified the vasculature by phalloidin or DAPI staining. Microglia were distinguished from macrophages by the Iba-1 expression level and their morphology. The numbers of cells were manually counted in each image.

Western blotting

Frozen whole-brain tissue was minced and homogenized with a Polytron homogenizer in ice-cold PBS (five times the brain weight) containing phenylmethylsulfonyl fluoride. The samples were then sonicated. Before Western blot analysis, protein concentrations were determined using the Lowry method. We adjusted the protein concentration to 2 mg/mL and loaded 10 µg of the total protein in each well. Proteins were separated by NuPAGE Bis-Tris 10% gels (Thermo Fisher) and transferred onto PVDF membranes (Millipore). The membranes were blocked with Blocking One (Nacalai) for one hour, followed by overnight incubation at 4°C with primary antibodies in the blocking solution. Primary antibodies for iNOS (mouse monoclonal IgG (Pharmingen)), Arginase-1 (rabbit polyclonal IgG (Gene Tex)), and α -Tubulin (mouse monoclonal (Novus Biologicals)) were used. After one-hour incubation in a horseradish peroxidase-conjugated secondary antibody, immunoreactive bands were visualized by enhanced chemiluminescence (ECL prime, GE Healthcare) and ImageQuant LAS4000 mini (GE Healthcare). Intensities of the bands of interest were quantified using Image J software.

MRI

Isoflurane-anesthetized rats underwent MRI in a prone position. The head was kept in a fixed position during the scanning. The breathing rate was monitored throughout the experiment. MRI was performed using a 7.04 Tesla (Agilent Technologies, Palo Alto, CA, USA). T2-weighted contrast images were obtained using the following parameters: echo time = 50 ms, repetition time = 2,000 ms, field of view = 2.5×2.5 cm², matrix = 512×512, and slice thickness = 1 mm. To select the imaging position, proton density-weighted images were obtained using the following parameters: echo time = 11 ms, repetition time = 2,000 ms, field of view = 2.5×2.5 cm², matrix = 512×512, and slice thickness = 1 mm.

Hematoxylin and eosin (HE) or Klüver-Barrera (KB) staining

HE staining was performed to observe the tissue and vascular changes according to the standard procedure. Briefly, sections were stained with Mayer's hematoxylin for 3 minutes and then washed in running tap water for 10 minutes. Thereafter, the sections were stained with eosin for 90 seconds. These sections were subsequently dehydrated and cleared using alcohol and xylene, respectively. The vascular remodeling structure in HE staining was observed using microscopy (IX73, Olympus, Tokyo, Japan). We identified vascular remodeling as perivascular enlargement and vessel wall thickening¹⁹. The image acquisition

region was randomly selected so that a cortical blood vessel was always included in the image. Ten vessels per rat, that is, 30 vessels per group, were acquired. All images within an experiment were acquired under the same microscope settings.

KB staining was performed to observe the demyelination according to the standard procedure. Briefly, sections were stained with Luxol Fast Blue solution in a 56°C oven overnight and then washed in 95% alcohol and distilled water. Thereafter, the sections were stained with Lithium Carbonate solution for 30 seconds. Then, sections continued to undergo differentiation in 70% alcohol until the gray matter was clear and white matter sharply defined. Next, they were counterstained with Cresyl Violet Acetate. These sections were subsequently dehydrated and cleared using alcohol and xylene, respectively. The severity of the white matter lesions was graded as reported previously²⁰. We also confirmed the presence of a white matter lesion as the formation of marked vacuoles or disappearance of myelinated fibers. We observed images of every slide by microscopy (IX73, Olympus, Tokyo, Japan)

Statistical analysis

All statistical analyses were performed with JMP12 (SAS Institute, Cary, NC, USA). We used Student's *t*-test, Dunnett's test, or Tukey-Kramer test. Error bars represent the means \pm SEM in all Supplemental Fig. A *P*-value of <0.05 was considered significant.

Results

DOCA-salt-mediated hypertension induces abnormal parenchymal and cerebrovascular morphologies.

Compared with control, placebo groups remained normotensive (Fig. 1b) and did not show any abnormal findings in histology or MR images (Supplemental Fig. 2c and 5). DOCA2W showed a marked elevation of the blood pressure in the absence of any clinical, histopathological and MRI features of cSVD (Fig. 1b, 1c, Supplemental Fig. 5, and Table 1). DOCA3W demonstrated several changes in addition to the sustained blood pressure elevation. First, DOCA3W showed clinical symptoms including hemiparesis, a decreased food intake, and bleeding from the tail vein (Table 1). Second, vascular remodeling in the cortex and the formation of vacuoles in the white matter were apparent (Fig. 1c). Third, focal high- and low-intensity areas were seen on T2-weighted on MR images (Supplemental Fig. 5a and 5b). In DOCA4W, we observed shrinkage of the astrocyte foot processes (Supplemental Fig. 1), a marked decrease in movement, myelin degeneration, and diffuse high-intensity areas on MR images, in addition to hypertension.

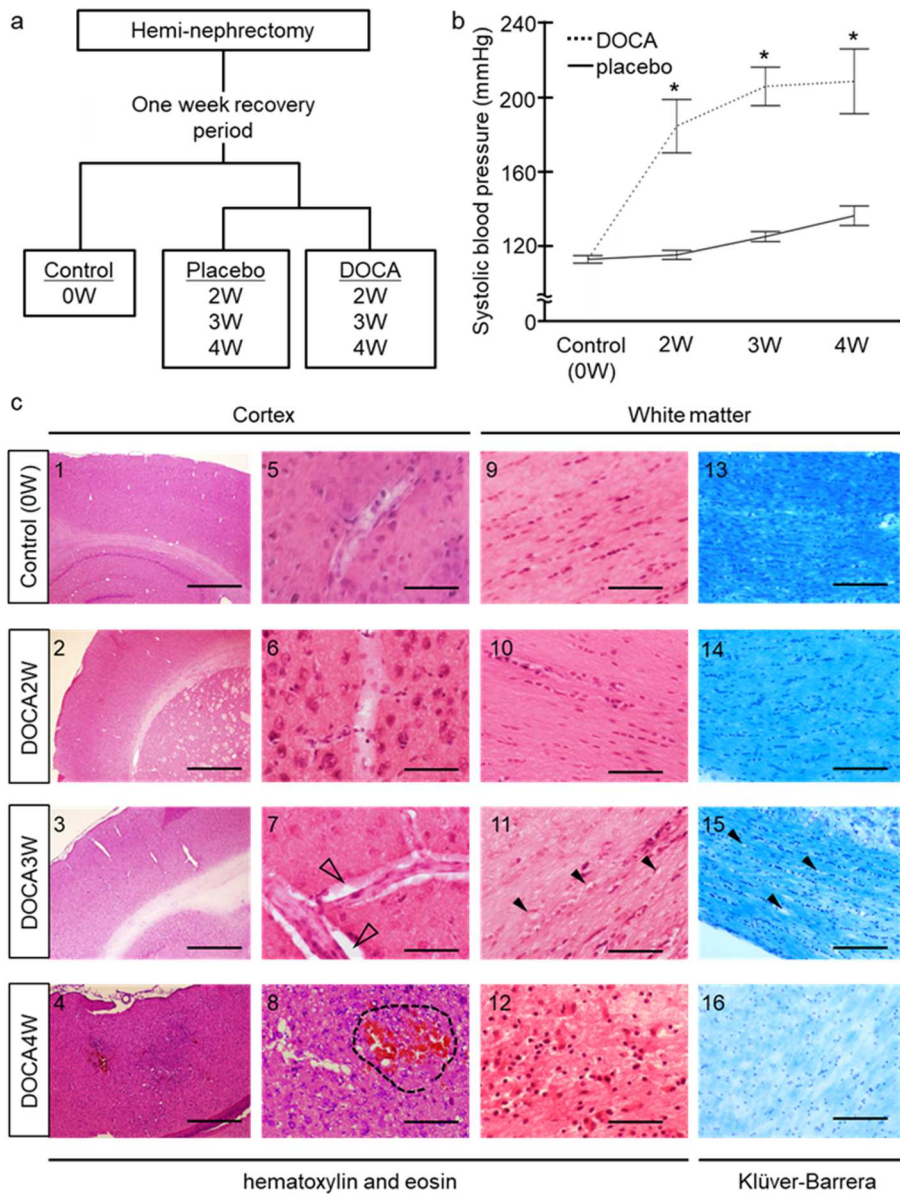


Figure 1. Progression of hypertension and histological damage in Deoxycorticosterone acetate (DOCA)-salt rats. (a) Experimental grouping for histological analysis of the model animals. (b) Systolic blood pressure in DOCA2W, DOCA3W, and DOCA4W was compared with that in the control. Values are expressed as the means \pm SEM (n=3 in each group, *P<0.05). (c) Hematoxylin and eosin or Klüver-Barrera staining of brain tissues. In DOCA3W, focal vascular remodeling including the perivascular space enlargements (open arrowheads), and the formation of vacuoles in the white matter (closed arrowheads) appeared. In DOCA4W, cerebral hemorrhage (dotted area) and myelinoclasts lesions were found. Scale bars: 500 μ m (1-4), 20 μ m (5-12), and 40 μ m (13-16).

Table 1: Physical profiles of control, placebo-group, and DOCA-salt group rats.

Group		Body Weight (g)	Systolic blood pressure (mmHg)	Heart rate (/min)	Symptoms
Control	0W	165±4.3	113.0±2.8	427.3±38	none
	2W	261±3.9*	116.3±3.4	414.3±31	none
Placebo	3W	295±16*	125.0±3.7	412.3±33	none
	4W	330±11*	130.0±7.3	413.0±12	none
DOCA	2W	250.3±8.3*	183.3±24*	416.0±50	none
	3W	253.0±30*	204.3±18*	407.3±9.5	Hemiparesis, bleeding from the tail vein, and loss of appetite
	4W	225.0±14*	207.0±30*	450.0±29	Severe inactive state

Rats administrated with DOCA-salt or placebo for 2 weeks (DOCA2W or Placebo2W), 3 weeks (DOCA3W or Placebo3W) and 4 weeks (DOCA4W or Placebo4W) were analyzed. Values are expressed as means ± SEM (n=3 in each group). Statistical significance was expressed as *p <0.05 relative to the control by using t-test.

Morphological changes of microglia precede the appearance of histopathological abnormalities.

In the control and placebo groups, resting microglia, morphologically characterized by their fine processes, were observed sparsely in the cerebral parenchyma (Fig. 2a, left column). In DOCA2W, round-shaped microglia with shortened processes were observed juxtaposing vessels in the cerebral parenchyma (Fig. 2a, middle column), in the absence of histopathological abnormalities (Fig. 1c). Thereafter, morphological changes of microglia further progressed. In DOCA3W, more amoeboid microglia accumulated around structurally altered vessels (Fig. 2a, right column). In DOCA4W, amoeboid microglia were widespread across the cortex and white matter (Supplemental Fig. 3a). The number of microglia juxtaposing vessels in the cortex was significantly increased in DOCA2W and DOCA3W (Fig. 2c).

We distinguished microglia from perivascular macrophages (PVM) by their Iba-1 intensity and morphology, based on a previous report that the expression of Iba-1 is weak in macrophages²¹. We confirmed this using a macrophage-specific marker, CD163²². CD163-negative microglia showed intense Iba-1 immunoreactivity and processes. On the other hand, CD163-positive PVM showed faint Iba-1 immunoreactivity and a flattened shape (Fig. 2b). Moreover,

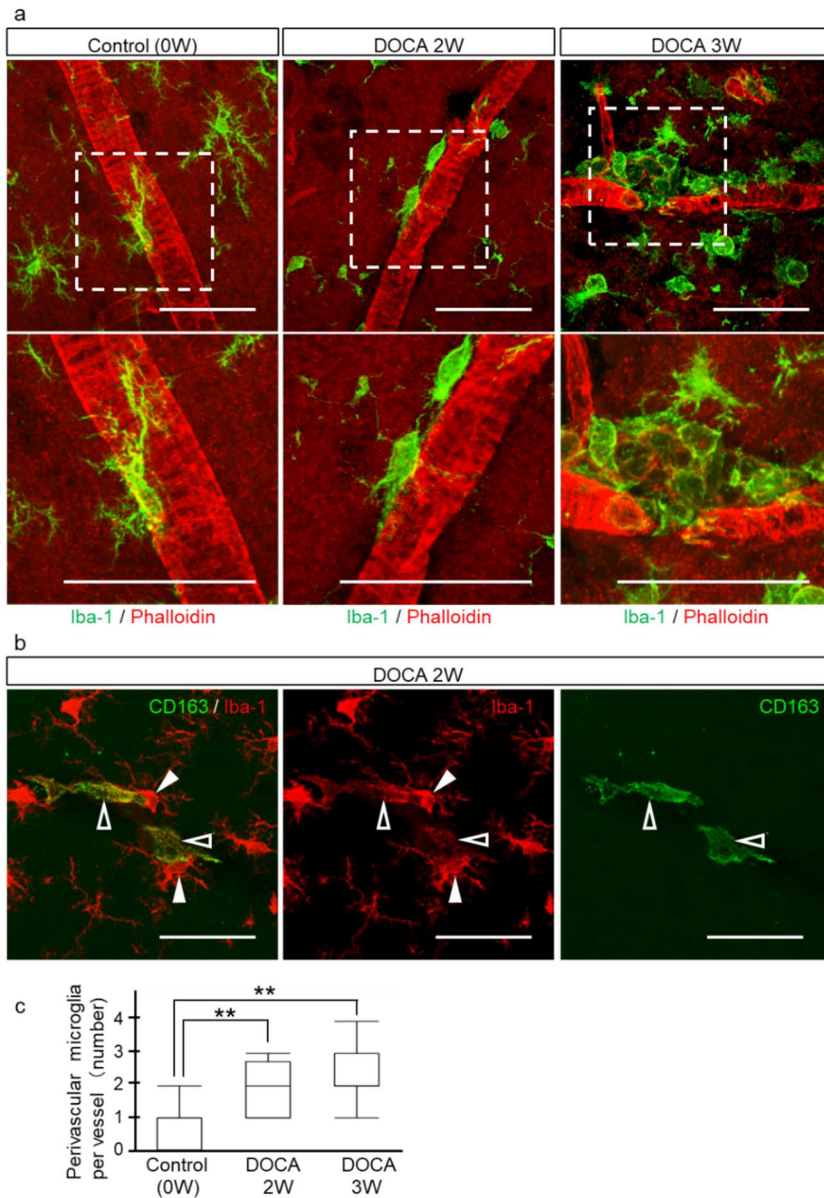


Figure 2. Dynamic morphological changes of microglia in DOCA-salt rats. (a) Microglia and the cerebral vasculature were visualized by Iba-1 (green) and phalloidin (actin, red), respectively, in the control (left column), DOCA2W (middle column), and DOCA3W (right column). The white dotted square in upper row was magnified in lower row. (b) Perivascular macrophages (CD163-positive cells, green) showed a flattened shape and low expression of Iba-1 (open arrowheads). In contrast, microglia had fine processes and showed high expression of Iba-1 (closed arrowheads). (c) Perivascular microglia increased in number after DOCA and salt treatments. Significance is expressed as $**P < 0.01$ using Tukey-Kramer test. Scale bars: 50 μ m.

the distribution of microglia was different from that of the PVM. CD 163-positive macrophages were never observed to be accumulated in the inflammatory lesion (Supplemental Fig.3a).

Activated perivascular microglia express a pro-inflammatory pattern

For characterization of the morphologically activated perivascular microglia, we first studied the expression of CD68 as a pro-inflammatory M1 marker. In the control group, microglia were CD68-negative (Fig. 3a, left column). While most of the microglia were CD68-negative in DOCA2W (Fig. 3a, middle column), CD68-positive, Iba1-positive microglia significantly increased around vessel walls and parenchyma in DOCA3W (Fig. 3a, right column). Quantitative analysis showed that the percentage of CD68-positive microglia increased significantly in DOCA3W compared with the control (Fig. 3b). As for the PVM, a sparse distribution pattern of CD68 positive PVMs was similar among the control, placebo, and DOCA groups (Fig. 3a). Biochemical analysis indicated that the expression level of inducible nitric oxide synthase (iNOS) as another pro-inflammatory M1 marker was increased in DOCA3W (Fig. 3c and 3d).

Next, we studied the expression of CD206 as an anti-inflammatory M2 marker. Perivascular microglia did not express CD206 in rat brains of any groups (Fig. 4a), except for a few CD206-positive microglia around hemorrhage sites (Supplemental Fig. 3b). As for the PVM, a sparse distribution pattern of CD206 positive PVMs was similar among in the control, placebo, and DOCA groups (Fig. 4a). Biochemical analysis also indicated that the expression level of arginase-1, another anti-inflammatory M2 marker, was not changed in the rat brains of any groups (Fig. 4b and 4c). Taken together, direct M1-activation, but not the M2-state, was identified in our DOCA-salt model.

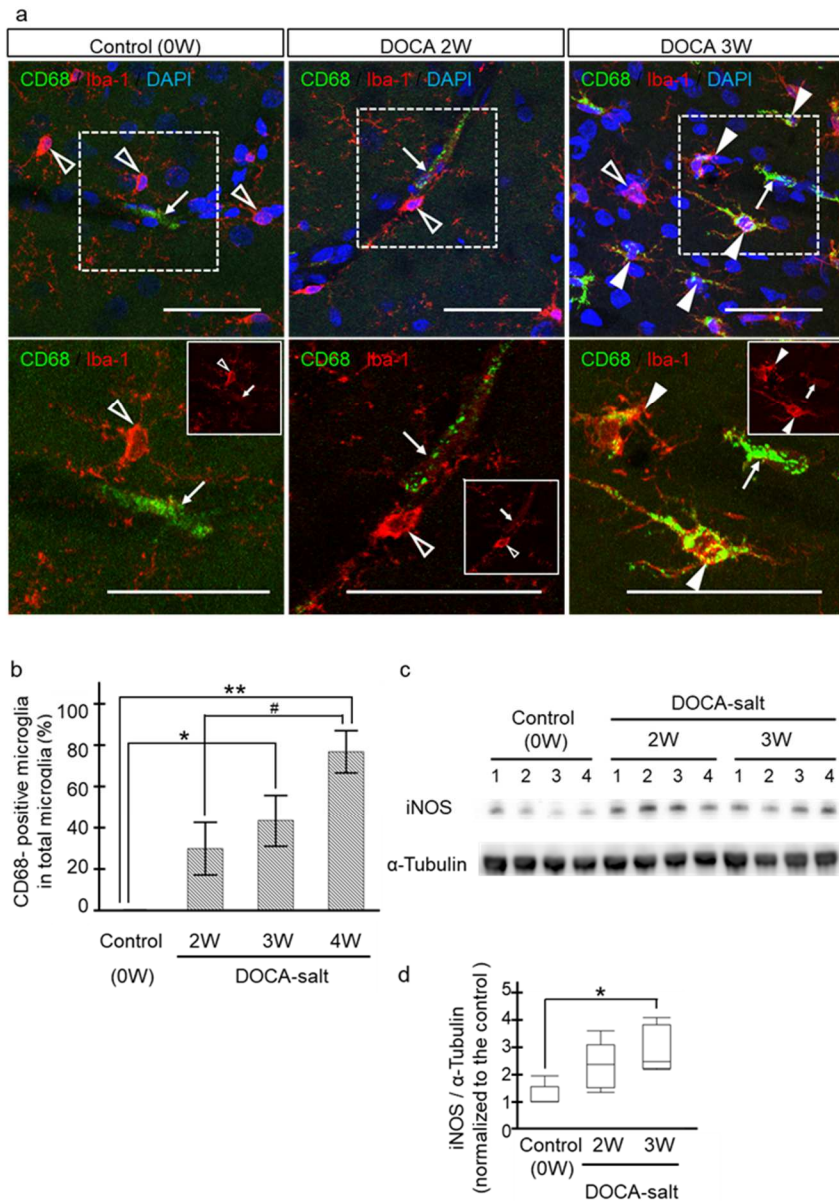


Figure 3. M1-switching of microglia in DOCA3W-rats. (a) Microglia and macrophages were visualized by Iba-1 (red) and CD68 (M1 marker, green), respectively, in the control (left column), DOCA2W (middle column), and DOCA3W (right column). The white dotted square in the upper row is magnified in the lower row. CD68-positive microglia were observed in DOCA3W (closed arrowheads), but not in DOCA2W (open arrowheads). In the white square, only Iba-1 staining was noted. Through the periods, CD68-positive perivascular macrophages existed (arrows). (b) CD68-positive microglia increased in number in DOCA3W. (c, d) The expression level of iNOS protein (M1 microglia marker) was increased after DOCA and salt treatment. Significant differences are expressed as * $P < 0.05$ and ** $P < 0.01$ relative to the control rats and # $P < 0.05$ relative to DOCA2W using Tukey-Kramer test. The values represent the means \pm SEM. Scale bars: 50 μ m.

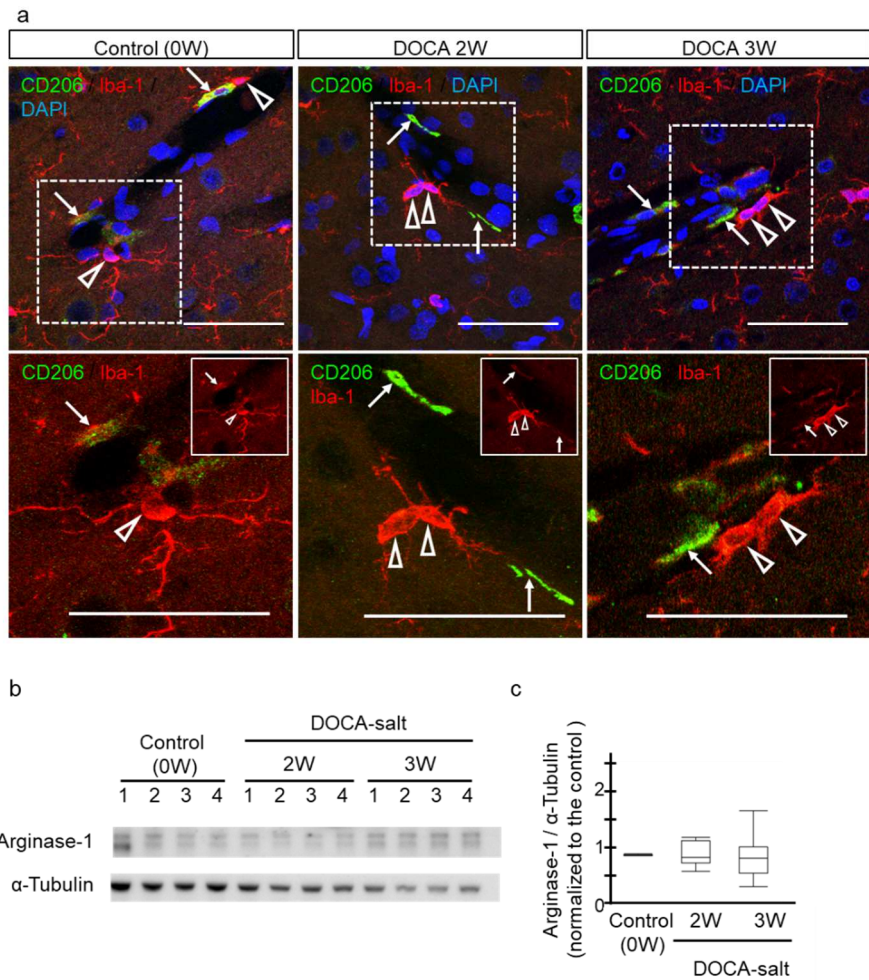


Figure 4. Absence of M2-switching in DOCA-salt rats. (a) Microglia and macrophages were visualized by Iba-1 (red) and CD206 (M2 marker, green) in the control (left column), DOCA2W (middle column), and DOCA3W (right column). The white dotted square in upper row is magnified in lower row. CD206-positive microglia were not observed in DOCA-salt rats (open arrowheads). In the white square, only Iba-1 staining was noted. CD206-positive perivascular macrophages were present in all periods (arrows). (b, c) No significant increase in the expression level of arginase-1 protein was observed after DOCA and salt treatment. Scale bars: 50 μ m.

Activated microglia transiently expressed a cell proliferation marker, Ki-67, prior to M1-switching

The total number of microglia did not change between the control and placebo groups, whereas it significantly increased in the DOCA group (Supplemental Fig. 4a). In the control and placebo groups, no microglia expressed Ki-67 (Fig. 5a, 5c, and Supplemental Fig. 4c). The rate of Ki-67-positive microglia significantly increased to 22% of the total microglia in DOCA2W, peaked to 54% in DOCA3W, and then decreased to the baseline level in DOCA4W (Fig. 5a and 5c). A similar increase in the number of Ki-67-positive microglia was also observed (Supplemental Fig. 4b). The rate of Ki-67-positive perivascular microglia peaked to 55% of the total perivascular microglia in DOCA2W and remain at the same level in DOCA3W (Fig. 5d). Rates of both Ki-67-positive and M1-state microglia were highest in DOCA3W (Fig. 5e and 5f). In DOCA4W, proliferative M1-state microglia markedly decreased (Fig. 5c and 5d). In contrast, PVM did not express Ki-67 in any group (Fig. 5b).

Discussion

The dynamics of microglia activation in chronic hypertension model to date have been poorly understood. In the present study, we showed microglia undergo dynamic morphological changes in the early stages of chronic hypertension using DOCA-salt-induced hypertension Wistar rats. At first, proliferative microglia juxtaposed to the cerebral vessels. Next, they switch to the pro-inflammatory M1-state, but not to the anti-inflammatory M2-state (Fig. 6). On the other hand, dynamic pathological changes of macrophages were not observed in the DOCA-salt rats. In the tMCAO model, the PVM infiltrating from vessels plays crucial roles in the enhancement of ischemic damage^{23,24}. However, this was not observed in our model (Fig. 3a, 4a, and Supplemental Fig. 3a). These results suggest that microglia, rather than PVM, are the key initial players in the process of cerebral vessel damage in the chronic hypertension model.

Another chronic hypertension model, angiotensin II (AngII)-induced hypertension model mice, showed that PVMs play important roles in neurovascular regulation²⁵. Administration of AngII reaches the perivascular space and acts on AngII type 1 receptors on PVMs, which results in the activation of NADPH oxidase 2 and reactive oxygen species production. These oxidative stresses lead to neurovascular dysfunction within two weeks of AngII administration. However, in human, blood-AngII levels are usually normal in benign and uncomplicated essential hypertension²⁶. DOCA-salt rat is characterized by low renin-AngII levels^{27,28}, and BBB permeability is sustained in the early stage (at least three weeks after DOCA-salt administration) of hypertension in DOCA-salt rat^{27,29}. The present study aimed to evaluate the

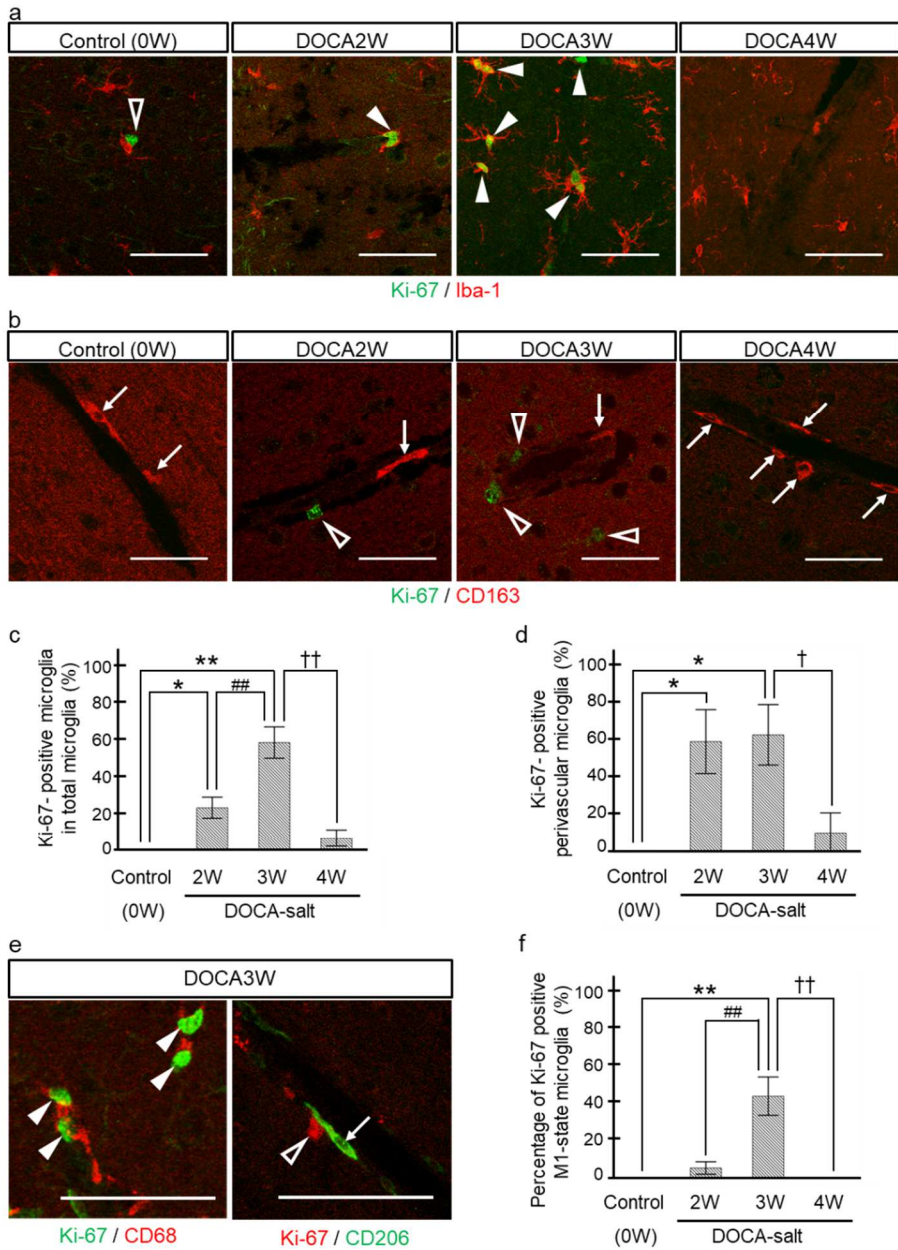


Figure 5. Transient increase of proliferative microglia before M1-switching. (a) Microglia were visualized by Iba-1 (red) and proliferative cells by Ki-67 (green). Ki-67-positive microglia were increased in DOCA2W and more markedly increased in DOCA3W (closed arrowheads). In DOCA4W, Ki-67-positive microglia were

markedly decreased. (b) CD163-positive perivascular macrophages (red, arrows) were not merged with Ki-67 (green, open white arrowheads) in all stages. (c) The rate of Ki-67-positive microglia started to increase in DOCA2W. (d) The rate of Ki-67-positive perivascular microglia became significantly higher in DOCA2W. (e) In some microglia of DOCA3W, Ki-67 was co-expressed with CD68 but not with CD206. (f) The rate of proliferative M1-state microglia was significantly higher in DOCA3W. Significant differences are expressed as * $P < 0.05$ and ** $P < 0.01$ relative to control rats, ## $P < 0.01$ relative to DOCA2W, and † $P < 0.05$ and †† $P < 0.01$ relative to DOCA3W using Tukey-Kramer test. The values represent the means \pm SEM. Scale bars: 50 μ m.

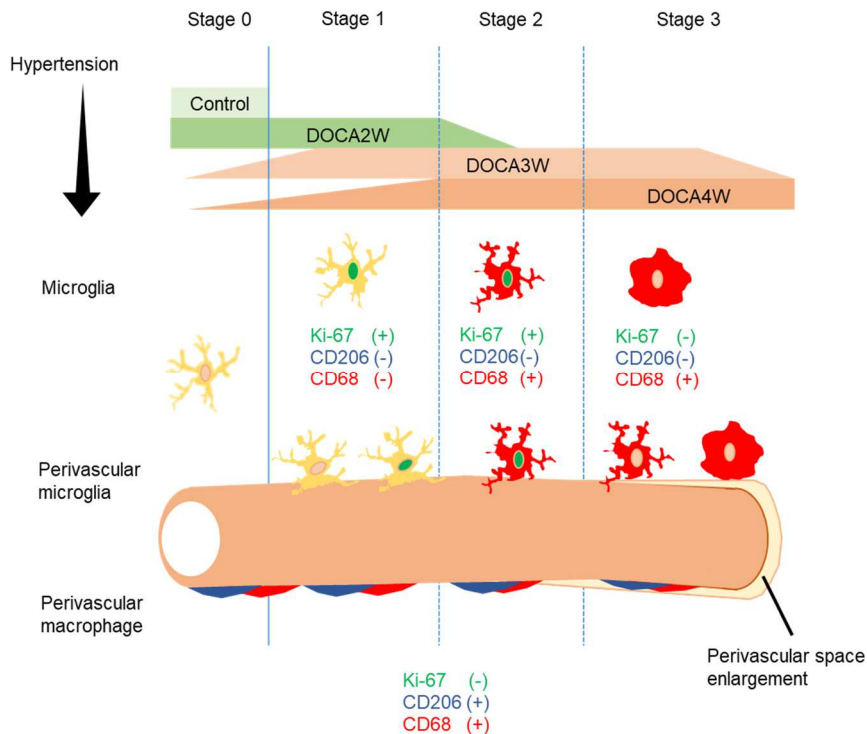


Figure 6. Summary of the dynamics of microglia in the process of the chronic hypertensive cerebrovascular disorder.

impact of the progression of chronic hypertension induced experimentally, in order to exclude from our study the potential influence of genetic factors on microglia density and/or phenotypes around cerebral vessels. We have therefore selected the Wistar DOCA-salt hypertension rat model instead of the more popular spontaneously hypertension rat (SHR) or stroke-prone spontaneous hypertension rat (SHR-SP) that carry strong differential genetic backgrounds^{30,31}. We, therefore, consider that DOCA-salt-induced hypertension Wistar rat model is suitable for the study of chronic hypertension in cerebrovascular diseases.

Microglia activation with a transient proliferative state and pro-inflammatory M1-state was observed earlier than cerebral vessel damage in our model. Regarding abnormal findings of the cerebral vasculature, perivascular space enlargement was observed in DOCA3W, and apparent BBB breakdown identified by astrocyte foot shrinkage was noted in DOCA4W (Supplemental Fig. 1). These results are consistent with a previous study indicating that BBB permeability remained unchanged in DOCA3W mice using the Evans Blue extravasation method²⁷.

Regarding microglia dynamics, our findings differed from those of previous reports using acute cerebrovascular disease models, such as tMCAO. In the tMCAO model, microglia were activated to an anti-inflammatory M2-state followed by a transition to a pro-inflammatory M1-state¹¹. The variation in microglia dynamics between chronic hypertension and acute ischemic models may be due to the difference of microglia-activating factors. In the tMCAO model, various factors were produced in the ischemic brain several hours or days after reperfusion. Interferon regulatory factor 4, known as an M2-switching factor, was rapidly upregulated within two hours after ischemic insult³². HMGB1, one of DAMPs, was produced several hours after ischemic events, and HMGB1 was able to activate microglia¹⁶. ATP or excessive glutamate was immediately released from necrotizing neuronal cells and could activate microglia³³. In a chronic hypertension model, other than the DOCA-model, a previous study using partial renal artery occlusion model showed that microglia were activated to an inflammatory state within five weeks after the operation³⁴. In this model, chronic hypertension increased the expression of adhesion molecules such as JAM-1, ICAM-1, and VCAM-1 on the cerebral endothelium and this led to deposition of platelets. Deposited platelets produced CD40L, which mediated the activation of pro-inflammatory microglia and activated NF κ B and mitogen-activated protein kinase signaling in microglia.

A previous report showed that extracellular signal-regulated kinase (ERK)-activated microglia acquired a proliferative ability and produced mainly pro-inflammatory cytokines, which cause synaptic and neuronal losses in the brain and result in lethal neurodegenerative disease in adult mice³⁵. This suggests that microglia proliferate prior to activation of the M1-state. We, therefore, analyzed the expression of Ki-67, as a cell proliferation marker, in microglia by applying immunostaining to our model. In our model, proliferative microglia had a close relationship with M1-state activation. Interestingly, such relationship was recently demonstrated using transgenic mice harboring somatic BRAF mutation, p.V600E. Activation of the MEK-ERK pathway induces microglia proliferation and is associated with an upregulation of pro-inflammatory cytokines from the proliferative microglia³⁵. The rate of Ki-67-positive microglia significantly increased in DOCA2W, peaked in DOCA3W, and then decreased to the baseline

in DOCA4W (Fig. 5a and 5c). On the other hand, the rate of Ki-67-positive perivascular microglia peaked in DOCA2W and DOCA3W (Fig. 5d) and similarly decreased to the baseline in DOCA4W. These results indicate that resting microglia were preferentially activated around the vessels and those perivascular microglia acquired the ability to proliferate earlier than other microglia apart from the vessels. Our results suggest that specific cytokines released from the vessels induced perivascular microglia to enter a proliferative state. Further studies are required to clarify the molecular signaling involved in this phenomenon.

According to our immunohistochemical study, we concluded that perivascular microglia were from residential microglia. We distinguished microglia from macrophages by Iba-1 intensity and cell morphology. In the present study, we did not employ flow cytometry, lineage-specific markers or other reporter methods. Flow cytometry succeeded to detect infiltration of macrophages in ischemic brain by using tMCAO mice in which ischemic changes were observed globally in re-perfusion area¹⁵. However, in DOCA-salt rats, localization of vascular damages was sparse, and hence, we performed immunohistochemical analysis rather than flow cytometry analysis of brain homogenate. According to a previous study, TMEM119 antigen is expressed specifically in residential microglia in brain, but not in macrophages³⁶. Unfortunately, we failed to detect TMEM119 in rat brain using antibody raised against mouse TMEM119³⁷. This may be due to the difference of amino acid sequence in the epitope region between mouse and rat. Finally, reporter method will be a powerful strategy and may be possible if DOCA-salt model is prepared by transgenic mice expressing reporter gene such as EGFP under TMEM promoter. We like to leave this strategy for our future plan to explore the process of microglia activation under hypertension.

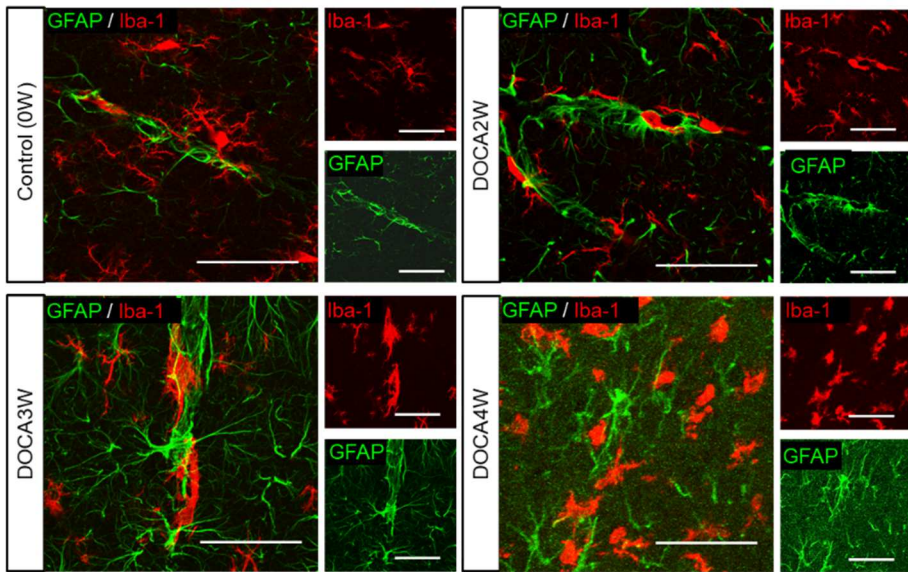
Conclusion

The present study demonstrates that perivascular microglia proliferate transiently and subsequently underwent direct M1-switching, prior to cerebral vessel destruction. Our findings raise the intriguing possibility of a link between perivascular microglia activation and initiation of cerebrovascular diseases induced by chronic hypertension, and that both anti-hypertensive therapy and the fine-tuning of microglia proliferation might generate a synergistic effect.

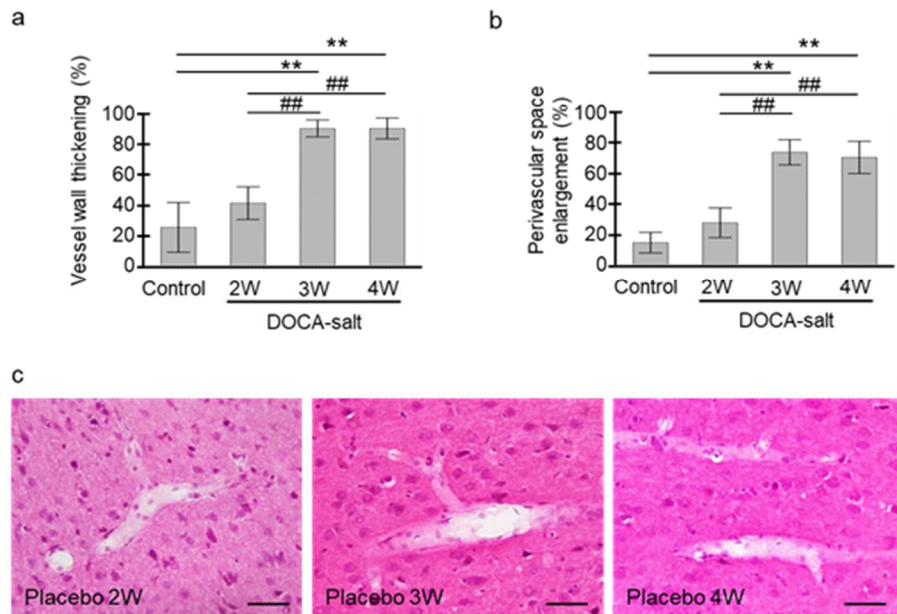
References

1. Salter MW, Stevens B: Microglia emerge as central players in brain disease. *Nat Med* 2017, 23:1018-1027.
2. Wake H, Moorhouse AJ, Jinno S, Kohsaka S, Nabekura J: Resting microglia directly monitor the functional state of synapses in vivo and determine the fate of ischemic terminals. *J Neurosci* 2009, 29:3974-3980.
3. Meyer-Luehmann M, Spires-Jones TL, Prada C, Garcia-Alloza M, de Calignon A, Rozkalne A, Koenigsnecht-Talboo J, Holtzman DM, Bacskai BJ, Hyman BT: Rapid appearance and local toxicity of amyloid-beta plaques in a mouse model of Alzheimer's disease. *Nature* 2008, 451:720-724.
4. Franco R, Fernandez-Suarez D: Alternatively activated microglia and macrophages in the central nervous system. *Prog Neurobiol* 2015.
5. H EH, Noristani HN, Perrin FE: Microglia Responses in Acute and Chronic Neurological Diseases: What Microglia-Specific Transcriptomic Studies Taught (and did Not Teach) Us. *Front Aging Neurosci* 2017, 9:227.
6. Huber JD, Campos CR, Mark KS, Davis TP: Alterations in blood-brain barrier ICAM-1 expression and brain microglial activation after lambda-carrageenan-induced inflammatory pain. *Am J Physiol Heart Circ Physiol* 2006, 290:H732-740.
7. Erdő F, Denes L, de Lange E: Age-associated physiological and pathological changes at the blood-brain barrier: A review. *J Cereb Blood Flow Metab* 2017, 37:4-24.
8. Erdo F, Trapp T, Mies G, Hossmann KA: Immunohistochemical analysis of protein expression after middle cerebral artery occlusion in mice. *Acta Neuropathol* 2004, 107:127-136.
9. Perego C, Fumagalli S, De Simoni MG: Temporal pattern of expression and colocalization of microglia/macrophage phenotype markers following brain ischemic injury in mice. *J Neuroinflammation* 2011, 8:174.
10. Jolivel V, Bicker F, Biname F, Ploen R, Keller S, Gollan R, Jurek B, Birkenstock J, Poisa-Beiro L, Bruttger J, et al: Perivascular microglia promote blood vessel disintegration in the ischemic penumbra. *Acta Neuropathol* 2015, 129:279-295.
11. Hu X, Li P, Guo Y, Wang H, Leak RK, Chen S, Gao Y, Chen J: Microglia/macrophage polarization dynamics reveal novel mechanism of injury expansion after focal cerebral ischemia. *Stroke* 2012, 43:3063-3070.
12. Hu X, Leak RK, Shi Y, Suenaga J, Gao Y, Zheng P, Chen J: Microglial and macrophage polarization[mdash]new prospects for brain repair. *Nat Rev Neurol* 2015, 11:56-64.
13. Rodrigo R, Fernandez-Gajardo R, Gutierrez R, Matamala JM, Carrasco R, Miranda-Merchak A, Feuerhake W: Oxidative stress and pathophysiology of ischemic stroke: novel therapeutic opportunities. *CNS Neurol Disord Drug Targets* 2013, 12:698-714.
14. Shichita T, Ito M, Yoshimura A: Post-ischemic inflammation regulates neural damage and protection. *Front Cell Neurosci* 2014, 8:319.
15. Shichita T, Sugiyama Y, Ooboshi H, Sugimori H, Nakagawa R, Takada I, Iwaki T, Okada Y, Iida M, Cua DJ, et al: Pivotal role of cerebral interleukin-17-producing gammadeltaT cells in the delayed phase of ischemic brain injury. *Nat Med* 2009, 15:946-950.
16. Liu K, Mori S, Takahashi HK, Tomono Y, Wake H, Kanke T, Sato Y, Hiraga N, Adachi N, Yoshino T, Nishibori M: Anti-high mobility group box 1 monoclonal antibody ameliorates brain infarction induced by transient ischemia in rats. *FASEB J* 2007, 21:3904-3916.
17. Pantoni L: Cerebral small vessel disease: from pathogenesis and clinical characteristics to therapeutic challenges. *Lancet Neurol* 2010, 9:689-701.
18. Pires PW, Dams Ramos CM, Matin N, Dorrance AM: The effects of hypertension on the cerebral circulation. *Am J Physiol Heart Circ Physiol* 2013, 304:H1598-1614.
19. Schreiber S, Bueche CZ, Garz C, Braun H: Blood brain barrier breakdown as the starting point of cerebral small vessel disease? - New insights from a rat model. *Exp Transl Stroke Med* 2013, 5:4.
20. Lin JX, Tomimoto H, Akiguchi I, Wakita H, Shibasaki H, Horie R: White matter lesions and alteration of vascular cell composition in the brain of spontaneously hypertensive rats. *Neuroreport* 2001, 12:1835-1839.
21. Zarruk JG, Greenhalgh AD, David S: Microglia and macrophages differ in their inflammatory profile after permanent brain ischemia. *Exp Neurol* 2017.
22. Faraco G, Park L, Anrather J, Iadecola C: Brain perivascular macrophages: characterization and functional roles in health and disease. *J Mol Med (Berl)* 2017, 95:1143-1152.
23. Shichita T, Sakaguchi R, Suzuki M, Yoshimura A: Post-ischemic inflammation in the brain. *Front Immunol* 2012, 3:132.

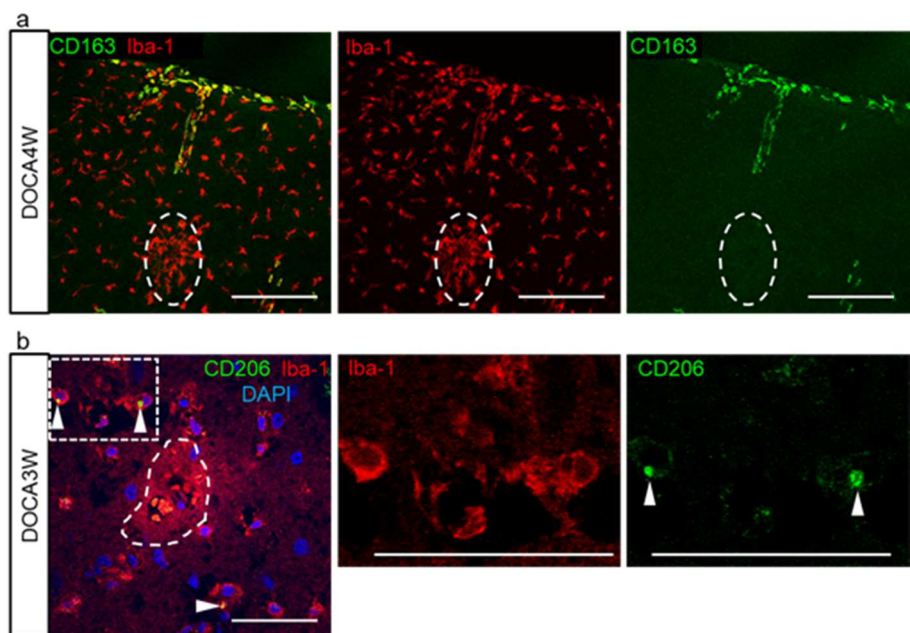
24. Shichita T, Hasegawa E, Kimura A, Morita R, Sakaguchi R, Takada I, Sekiya T, Ooboshi H, Kitazono T, Yanagawa T, et al: Peroxiredoxin family proteins are key initiators of post-ischemic inflammation in the brain. *Nat Med* 2012, 18:911-917.
25. Faraco G, Sugiyama Y, Lane D, Garcia-Bonilla L, Chang H, Santisteban MM, Racchumi G, Murphy M, Van Rooijen N, Anrather J, Iadecola C: Perivascular macrophages mediate the neurovascular and cognitive dysfunction associated with hypertension. *J Clin Invest* 2016, 126:4674-4689.
26. Catt KJ, Cran E, Zimmet PZ, Best JB, Cain MD, Coghlan JP: Angiotensin II blood-levels in human hypertension. *Lancet* 1971, 1:459-464.
27. Rodrigues SF, Granger DN: Cerebral microvascular inflammation in DOCA salt-induced hypertension: role of angiotensin II and mitochondrial superoxide. *J Cereb Blood Flow Metab* 2012, 32:368-375.
28. Chamorro V, Wangenstein R, Sainz J, Duarte J, O'Valle F, Osuna A, Vargas F: Protective effects of the angiotensin II type 1 (AT1) receptor blockade in low-renin deoxycorticosterone acetate (DOCA)-treated spontaneously hypertensive rats. *Clin Sci (Lond)* 2004, 106:251-259.
29. Werber AH, Fitch-Burke MC: Effect of chronic hypertension on acute hypertensive disruption of the blood-brain barrier in rats. *Hypertension* 1988, 12:549-555.
30. Waki H, Liu B, Miyake M, Katahira K, Murphy D, Kasparov S, Paton JF: Junctional adhesion molecule-1 is upregulated in spontaneously hypertensive rats: evidence for a prohypertensive role within the brain stem. *Hypertension* 2007, 49:1321-1327.
31. Waki H, Hendy EB, Hindmarch CC, Gouraud S, Toward M, Kasparov S, Murphy D, Paton JF: Excessive leukotriene B4 in nucleus tractus solitarius is prohypertensive in spontaneously hypertensive rats. *Hypertension* 2013, 61:194-201.
32. Guo S, Li Z, Jiang D, Lu YY, Liu Y, Gao L, Zhang S, Lei H, Zhu L, Zhang X, et al: IRF4 is a novel mediator for neuronal survival in ischaemic stroke. *Cell Death Differ* 2014, 21:888-903.
33. Barakat R, Redzic Z: The Role of Activated Microglia and Resident Macrophages in the Neurovascular Unit during Cerebral Ischemia: Is the Jury Still Out? *Med Princ Pract* 2016, 25 Suppl 1:3-14.
34. Bhat SA, Goel R, Shukla R, Hanif K: Platelet CD40L induces activation of astrocytes and microglia in hypertension. *Brain Behav Immun* 2017, 59:173-189.
35. Mass E, Jacome-Galarza CE, Blank T, Lazarov T, Durham BH, Ozkaya N, Pastore A, Schwabenland M, Chung YR, Rosenblum MK, et al: A somatic mutation in erythro-myeloid progenitors causes neurodegenerative disease. *Nature* 2017, 549:389-393.
36. Li Q, Barres BA: Microglia and macrophages in brain homeostasis and disease. *Nat Rev Immunol* 2018, 18:225-242.
37. Furube E, Kawai S, Inagaki H, Takagi S, Miyata S: Brain Region-dependent Heterogeneity and Dose-dependent Difference in Transient Microglia Population Increase during Lipopolysaccharide-induced Inflammation. *Sci Rep* 2018, 8:2203.



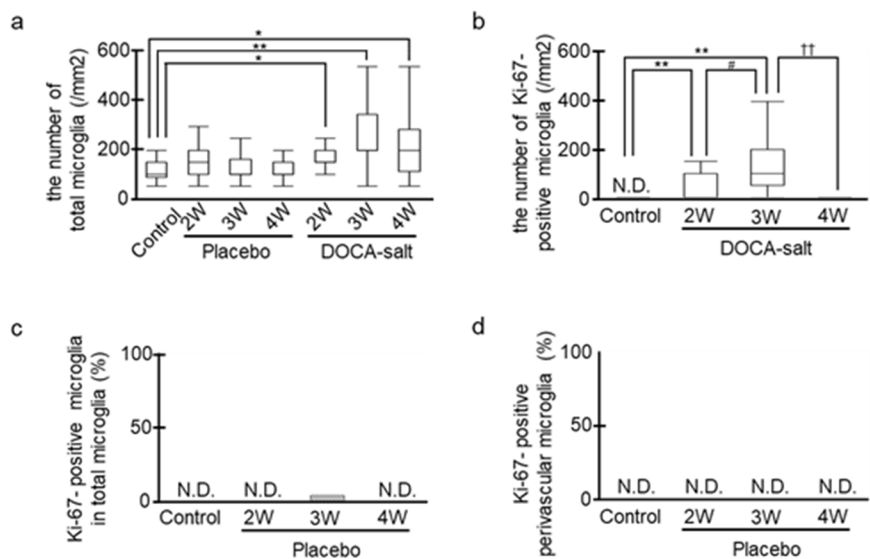
Supplemental Figure 1. Morphological changes of astrocyte foot processes making up the small vessel wall in DOCA-salt rats. Shrinkage of astrocyte foot processes was observed in DOCA4W. Scale bars: 50 μ m.



Supplemental Figure 2. Quantitative analysis of vessel wall thickening (a) and perivascular space enlargement (b) in Figure 1C. Significance is expressed as ** $P < 0.01$ relative to the control and ## $P < 0.01$ relative to DOCA2W using the Tukey-Kramer test. (c) Hematoxylin and eosin of brain tissues. Scale bars: 50 μ m.

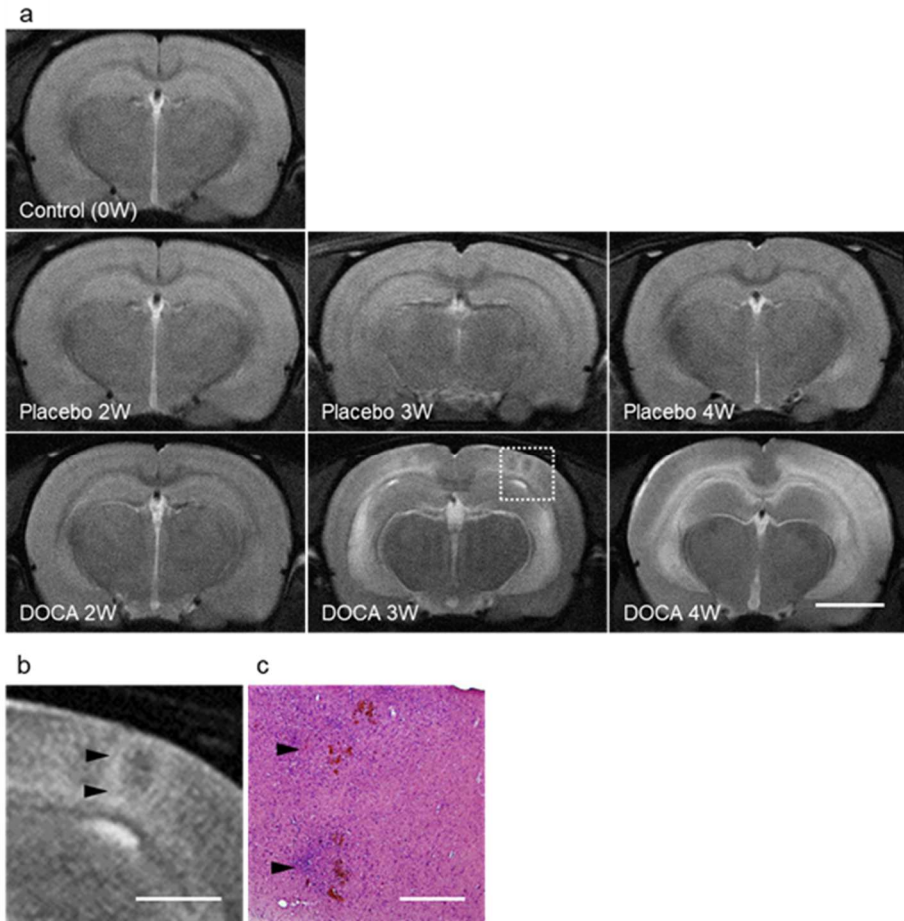


Supplemental Figure 3 (a) Distribution of perivascular macrophages and microglia in DOCA4W. CD163-positive macrophages were never observed to have infiltrated the amoeboid microglia accumulating in the inflammatory lesion, indicated by the white dotted area. Scale bars: 150 μ m. (b) Presence of CD206-positive M2-state microglia (closed white arrowheads) around a site of hemorrhage (white dotted area). The white dotted rectangle in the left column is magnified in the middle and right column. CD206 expression was noted in the microglia cytosol.



Supplemental Figure 4. Quantitative analysis of microglia. (a) The time-course changes of the total number of microglia. Significance is expressed as * $P < 0.05$ and ** $P < 0.01$ relative to the control using the Dunnett test.

(b) The number of Ki-67-positive microglia. Significance is expressed as $**P < 0.01$ relative to the control rats, $\#P < 0.05$ relative to DOCA2W, and $\dagger\dagger P < 0.01$ relative to DOCA3W using the Tukey-Kramer test. (c, d) Numbers of Ki-67-positive microglia as a percentage of the total microglia or perivascular microglia in the control and placebo groups.



Supplemental Figure 5. Sequential MRI analysis of rat brains. (a) T2-weighted images of brains in the control, the placebo groups, and DOCA groups. (b) The image of the white dotted square (Supplemental Fig3A, DOCA3W rat) is magnified. (c) Eosin-positive cells accumulated in the region corresponding to the high-intensity area in the MR image shown by closed arrowheads in Supplemental Fig3B. Scale bars: 5 mm (a), 1 mm (b), and 250 μm (c).

Chapter 5

Type 2 Diabetes accelerates the activation of perivascular microglia in hypertensive rats

Takashi Koizumi, Ilona Cuijpers, Ardi Cengo, Paolo Carai,
Marc van Bilsen, Robert van Oostenbrugge,
Toshiki Mizuno, Harry Steinbusch, Elizabeth Jones*, Sébastien Foulquier*

In preparation

Chapter 6

General Discussion

Takashi Koizumi

Cerebral small vessel disease (cSVD) is commonly observed among elderly individuals and is recognized as a major vascular contributor to dementia, cognitive decline, gait disturbance, mood disturbance and stroke. Neuropathological studies of cSVD patients show a number of abnormalities in the small perforating arteries or capillaries in the brain. Thanks to technological progression, especially in neuroimaging, we can detect those cSVD burdens during lifetime of the patient. Numerous clinical studies have revealed that aging, genetic factors, and vascular risk factors, such as hypertension, diabetes, hyperlipidemia, smoking and alcohol, were related to cSVD formation. Despite of intensive research efforts to decipher the interaction between microcirculation and brain, the mechanism underlying cSVD remained unclear. In this thesis, our studies were divided into two parts. In the first part, we performed a clinical study involving CADASIL-suspected patients. We aimed to adapt a scale to prioritize the genetic testing of subjects suspected to have CADASIL by investigating crucial factors associated with the formation of hereditary and sporadic cSVD (Chapter 2). In the second part, we performed experimental studies focused on the pathophysiological changes taking place in sporadic cSVD (Chapters 3, 4 and 5). Dysfunction of the neurovascular unit (NVU) and CBF impairment are being largely investigated as factor involved in the development of cSVD^{1,2,3}. Beyond the functional and structural changes of the cerebral small vessels, the contribution of perivascular immune cells, perivascular microglia and perivascular macrophages, has often been omitted. The second part of my thesis was therefore dedicated to those perivascular immune cells and their possible association with cSVD.

Establishment of CADASIL-J score: reconfirmation of hypertension and diabetes as crucial risk factors for sporadic cSVD

Hereditary cSVD helps to understand the mechanisms of cSVD, through the discovery of single genes involving in structural changes of cerebral small vessels. CADASIL (Cerebral Autosomal Dominant Arteriopathy with Subcortical Infarction and Leukoencephalopathy) is the most prevalent hereditary cSVD, and our laboratory has been doing a large number of CADASIL patients' genetic testing in Japan. That was why we chose CADASIL as a hereditary subject of this study. In Chapter 2, we explored the crucial factors for cSVD mechanisms by comparing hereditary cSVD and sporadic cSVD while we established the scale to prioritize the genetic testing for CADASIL-suspected patients. By analyzing factors between similar-feature groups, we identified crucial factors to distinguish between sporadic and hereditary cSVD. Candidate factors were selected by referring to the previous report which established screening tool to be applied in the clinical setting⁴; age at disease onset, age at first stroke/TIA, gender, migraine, TIA/Stroke, psychiatric disturbance, cognitive deficits, family history, leukoencephalopathy at temporal pole or

external capsule, and subcortical infarcts. In addition, we selected several major vascular risk factors: hypertension, diabetes, hyperlipidemia, smoking and alcohol overconsumption and other MRI features including microbleeds and cerebral artery stenosis on MRA. As a result, we established the CADASIL scale-J to prioritize the genetic testing for CADASIL-suspected patients with high sensitivity and specificity. Considering the contents of CADASIL scale-J, we identified hypertension as an important vascular risk factor for sporadic cSVD. In addition, diabetes was identified as the second most important vascular risk factor. This result was compatible with previous reports^{5,6}. Subcortical infarctions showed the most significant difference, which CADASIL patients showed with high rate. This might be because *NOTCH3* mutation induced smooth muscle cell dysfunction^{7,8} in earlier phase than sporadic causes. White matter lesions, which were the essential part for the inclusion criteria of CADASIL⁹, showed a significant difference at the temporal lobe. Other important MRI features of cSVD: microbleeds did not show any significant difference between two groups.

The conventional position of perivascular immune cells in cSVD

When considering cSVD mechanisms, many researchers have been mainly discussing the role of the NVU components. Microglia, including perivascular microglia (PMG), are located in the parenchyma outside the glia-limitans and the vascular walls. Owing to those established barriers, the CNS was believed to be isolated from the systemic environment and to be immune privilege¹⁰. This might be why microglia were thought to not participate in cSVD initiation and they could play active roles only in cSVD progression once the NVU is dysfunctional. Microglia/PMG dynamics has been investigated in acute ischemic stroke as shown in animal models of transient middle cerebral artery occlusion (tMCAO) in recent years^{11,12}. Microglia/PMG activation is triggered by signals or cytokines, such as ATP from dying cells¹³ or DAMPs (damaged-associated molecular patterns) from damaged cells¹⁴, after ischemic insults occurred. In the tMCAO model, numbers of M2-state microglia rapidly increase around vessels in the penumbra after infarction, and, in a few days, M1-state microglia dominantly increase. This process is called "M2-to-M1 phenotype-switching" or "shift in the M2-to-M1 phenotypes"^{15,16}. However, in chronic vascular diseases, such as cSVD, roles of microglia/PMG have remained unclear.

Perivascular macrophages (PVMs) are located in perivascular spaces which exist around large penetrating arterioles and disappear at the capillary level¹⁷. This might suggest that PVMs are not involved in BBB dysfunction. Hence, PVMs might have not been taken into consideration for cSVD formation.

It was revealed recently that the brain parenchyma is not completely immune privileged. Indeed, activated circulating T cells can cross the BBB in absence of neuroinflammation¹⁸. This could imply that perivascular microglia could sense signals originating from the vessels or the vascular lumen and get activated at an early stage, before than expected. Moreover, by state-of-the-art live-cell imaging technologies, a system of lymphatic drainage, so-called glymphatic pathway, has been recently discovered in the perivascular space¹⁹. Although controversies exist on this subject, it suggests that PVMs could constantly sense brain parenchymal and systemic changes. Therefore, we hypothesized that perivascular immune cells—PVMs and PMG— can detect signals and can get activated before the apparent disruption of the BBB. Unfortunately, it is still difficult to distinguish clearly the function of PVMs and PMG due to the absence of a proper experimental system^{20,21}. However, while earlier studies were not differentiating these two cell types, multiplexed immunohistochemistry combined with confocal imaging has now revealed differential marker expressions and morphological features for those immune cells surrounding the cerebral vasculature. Although key supporting evidences are still missing, new techniques, such as single cell RNAseq analysis or mass cytometry, have elucidated some of their important features. Goldmann et al.²² indicated that PVMs and microglia were transcriptionally closely related but PVMs were distinguishable from microglia on the basis of their expression of *Mrc1*, *CD36*, *Hexb*, and *P2ry12* by using the single cell RNAseq analysis. Keren-Shaul et al.²³ could also distinguish PVMs and microglia precisely by Single cell RNA-seq in an Alzheimer's model. These techniques could give a chance to explore precisely PVMs and PMG in the future. Chapter 3 was therefore meant to review the current literature on PMG and PVMs in the context of cSVD and to recognize the knowledge gaps on PMG and PVMs .

Are perivascular microglia/macrophages activities associated with vascular changes in the initiation of sporadic cSVD?

To address this issue, we evaluated the dynamics of PMG and PVMs by using a hypertension model animal i.e. the deoxycorticosterone acetate (DOCA)-salt Wistar rat (Chapter 4). Young Wistar rats, percutaneously injected DOCA and daily salt intake, showed hypertension in 2 weeks. Apparent clinical symptoms and MRI abnormality were shown after 3 weeks. These changes would resemble human hypertensive patients' history. In DOCA-salt rats' brain with 2 weeks of treatment by DOCA-salt, we found that perivascular microglia started juxtaposing to cerebral small vascular at the only hypertensive phase earlier than apparent BBB disruption or clinical symptoms. In addition, we found that those juxtaposed microglia were Ki-67 (proliferation marker)-positive and they were neither CD206 (M2 marker)- nor CD68 (M1 marker)-positive. As hypertension is progressing in DOCA 3W and 4W, those microglia harbored M1-state not via

M2-state. Further studies are required to clarify the molecular signaling involved in this phenomenon.

In Chapter 5, we evaluated the dynamics of PMG and PVMs using an animal model of metabolic syndrome (MetS): the ZSF-1 rat. We found juxtaposed PMG in ZSF-1 rats both in Lean (single hypertension) and Obese (metabolic syndrome) rats. We noticed that PMG showed earlier changes than parenchymal microglia (MG). This observation fits our previous observation in DOCA2W rats when the rate of proliferative PMG was higher than that of MG. Furthermore, the rate of CD68-positive PMG showed a significant increase in Obese ZSF-1 rats at 18w whereas the rates of CD68-positive MG in parenchyma significantly increased in Obese only at 21weeks. These results suggested that PMG could sense earlier vascular injuries than MG. Contrary to the DOCA-rat study, CD206-positive PMG were observed. Although there were not significant differences, a higher rate of CD206-positive PMG in Lean groups were observed than that in Obese groups. Both DOCA-salt and Lean ZSF-1 rats were hypertensive. Beyond its differential hypertensive etiology, a major difference between these two hypertensive rat models was the degree of blood pressure elevation. DOCA-salt rats had an extremely high systolic blood pressure, beyond 200 mmHg. Such hypertension severity (over 180mmHg) is classified into grade 3²⁴. On the other hand, Lean ZSF-1 rats had a mild hypertension, with a systolic blood pressure close from 160 mmHg and would correspond to a grade 2 hypertension²⁴. The 2018 ESC/ESH Guidelines have indicated a high risk of cardiovascular disease (CV) for grade 3 hypertension and moderate risk of CV for grade 2 hypertension in patients²⁵. Moreover, the blood pressure increased rapidly in DOCA-salt rats and reached grade 3 in only 2 weeks, whereas ZSF-1 rats increased their blood pressure gradually and remained stable at grade 2 for more than 7 weeks. These differences in blood pressure elevation and elevation span could result in different activation dynamics of microglia. A mild and chronic hypertension could favor anti-inflammatory M2-state microglia for a prolonged period before switching to a M1-state due to the presence of additional risk factor such as diabetes. In the ZSF-1 study, we did not evaluate rats at a younger age (before 18 weeks) nor their proliferative ability using the Ki-67 marker. In DOCA-rats, Ki-67 positive microglia did not express CD206. We speculate that microglia activation would vary based on the degree and the rapidity of the blood pressure elevation, with a stepwise activation from proliferation to M2-state, and to M1-state.

On the other hand, PVMs did not show dynamic changes like PMG. PMG expressed M1-state or M2-state marker in any stages. In DOCA study, even in wild control groups, CD68 or CD206 positive PVMs were existed. PVMs might be constantly activated to maintain the balance of perivascular environments. For PVMs, we might have to be considered different treatment than PMG.

In the next step, the best possible therapeutic window should be considered to assess the efficacy of several pharmacological interventions, such as the use of specific anti-hypertensive drugs, hypoglycemic agents, or drugs modulating microglia activity. Anti-inflammatory treatments aiming to counteract or prevent neuroinflammation by blocking microglial activation have been tested as a possible therapeutic option against ischemic stroke²⁶ and neurodegenerative diseases²⁷. In many cases, those anti-inflammatory treatments have failed, due to the small therapeutic window in the case of ischemic stroke. However, cSVD can progress slowly and be stoppable if their causes could be eliminated before reaching an irreversible state.

Perivascular space enlargement might have important implications

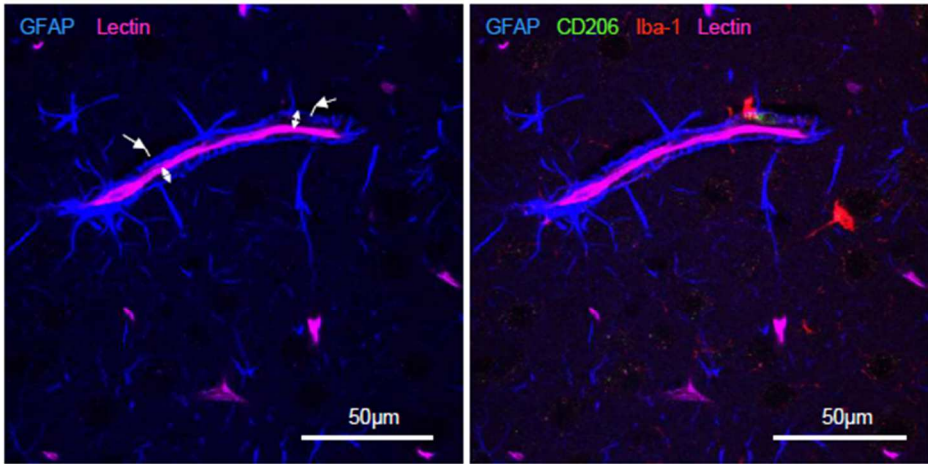
The current literature consensus is that PVS, known as Virchow-Robin spaces, form a network of spaces around cerebral microvessels that act as a conduit for fluid transport, exchange between cerebrospinal fluid (CSF) and interstitial fluid (ISF) and clearance of waste products from the brain. Perivascular enlargement is one of the important hallmark features of cSVD^{19, 28}. While the mechanisms leading to PVS enlargement in cSVD and the downstream effects are unclear, clinical studies have revealed that perivascular spaces enlargements were associated with several small vessel disease-related contents — hypertension²⁹, white matter lesion³⁰, and cognitive decline³¹. Furthermore, PVS enlargements are associated with systemic inflammation³². We also observed PVS enlargements around penetrating arterioles. Interestingly, we found extra spaces at abluminal site of astrocyte endfeet around cortical perforating arterioles (Figure 1). These spaces might be made by the brain parenchyma shrinkage due to brain fixation, however, perivascular microglia indeed existed in these extra spaces. Brown et al.³¹ proposed that widening of PVS suggested presence of perivascular cell debris and other waste products that form part of a vicious cycle involving impaired cerebrovascular reactivity, blood-brain barrier dysfunction, perivascular inflammation and ultimately impaired clearance of waste proteins from the interstitial fluid space, leading to accumulation of toxins, hypoxia, and tissue damage. These extra spaces outside of astrocyte endfeet might also be caused by impaired clearance of waste proteins from the interstitial fluid space or fluid oozing out through APQ4 channel on astrocyte endfeet. In line of the observations, we hypothesize that PMG could more easily detected signals which indicated vascular dysfunction via fluid ingredients. This result could support our result that PMG activation would occur earlier than BBB deformation. Clinically, MRI images of PVS enlargement might reflect both PVS per se and extra space outward astrocyte endfeet.

Conclusion

cSVD can result from several origins: either hereditary or sporadic with the exposure to vascular risk factors. Since some of their features can be similar, genetic testing should be considered as an important step for the proper diagnosis of cSVD. To ease the access to genetic testing for CADASIL-suspected patients, we established the CADASIL scale-J, which showed high sensitivity and specificity. This clinical study reconfirmed that hypertension and diabetes are important contributors to vascular-related cSVD. From this clinical insights, we have studied the impact of hypertension alone or in combination with diabetes on the activation dynamics of perivascular immune cells. We found that the perivascular microglia showed dynamical activation during hypertension and/or hyperglycemia, while PVMs showed constantly mixed anti- and pro-inflammatory activation through resting state to disease state.

Our experimental work should further stimulate pharmacological studies to assess the relevance of PMG and/or PMVs as possible cellular target(s) to prevent cSVD progression or to allow its resolution.

A



B

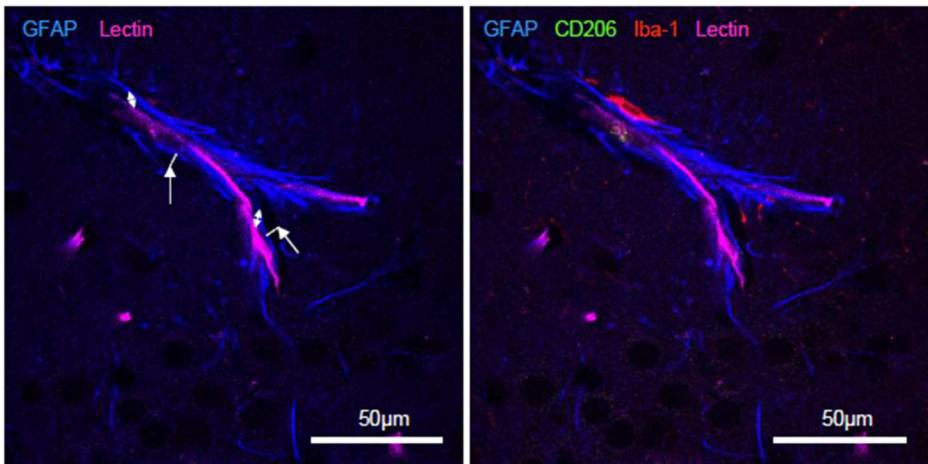


Figure 1. Perivascular spaces and extra space at abluminal astrocyte endfeet site. A representative figure around a cortical penetrating artery in Lean 18w (A) and Obese 18w (B). Two-way arrows indicate perivascular spaces. White bar with an arrow indicates extra space between astrocyte endfeet and brain parenchyma.

References

1. Rutten-Jacobs LCA, Rost NS. Emerging insights from the genetics of cerebral small-vessel disease. *Ann N Y Acad Sci.* 2019 Jan 8.
2. Li Q, Yang Y, Reis C, et al. Cerebral Small Vessel Disease. *Cell Transplant.* 2018 Dec;27(12):1711-22.
3. Hainsworth AH, Markus HS. Do in vivo Experimental Models Reflect Human Cerebral Small Vessel Disease? a Systematic Review. *Journal of Cerebral Blood Flow & Metabolism.* 2008;28(12):1877-91.
4. Pescini F, Nannucci S, Bertaccini B, et al. The Cerebral Autosomal-Dominant Arteriopathy With Subcortical Infarcts and Leukoencephalopathy (CADASIL) Scale: a screening tool to select patients for NOTCH3 gene analysis. *Stroke.* 2012 Nov;43(11):2871-6.
5. Pantoni L. Cerebral small vessel disease: from pathogenesis and clinical characteristics to therapeutic challenges. *The Lancet Neurology.* 2010 Jul;9(7):689-701.
6. Han F, Zhai FF, Wang Q, et al. Prevalence and Risk Factors of Cerebral Small Vessel Disease in a Chinese Population-Based Sample. *Journal of stroke.* 2018 May;20(2):239-46.
7. Baron-Menguy C, Domenga-Denier V, Ghezali L, Faraci FM, Joutel A. Increased Notch3 Activity Mediates Pathological Changes in Structure of Cerebral Arteries. *Hypertension.* 2017;69(1):60-70.
8. Okeda R, Arima K, Kawai M. Arterial Changes in Cerebral Autosomal Dominant Arteriopathy With Subcortical Infarcts and Leukoencephalopathy (CADASIL) in Relation to Pathogenesis of Diffuse Myelin Loss of Cerebral White Matter. *Stroke.* 2002;33(11):2565-9.
9. Mizuta I, Watanabe-Hosomi A, Koizumi T, et al. New diagnostic criteria for cerebral autosomal dominant arteriopathy with subcortical infarcts and leukoencephalopathy in Japan. *J Neurol Sci.* 2017 Oct 15;381:62-7.
10. Carson MJ, Doose JM, Melchior B, Schmid CD, Ploix CC. CNS immune privilege: hiding in plain sight. *Immunological reviews.* 2006 Oct;213:48-65.
11. Jolivel V, Bicker F, Biname F, et al. Perivascular microglia promote blood vessel disintegration in the ischemic penumbra. *Acta Neuropathol.* 2015 Feb;129(2):279-95.
12. Perego C, Fumagalli S, De Simoni MG. Temporal pattern of expression and colocalization of microglia/macrophage phenotype markers following brain ischemic injury in mice. *J Neuroinflammation.* 2011 Dec 10;8:174.
13. Davalos D, Grutzendler J, Yang G, et al. ATP mediates rapid microglial response to local brain injury in vivo. *Nat Neurosci.* 2005 Jun;8(6):752-8.
14. Shichita T, Ito M, Yoshimura A. Post-ischemic inflammation regulates neural damage and protection. *Front Cell Neurosci.* 2014;8:319.
15. Hu X, Li P, Guo Y, et al. Microglia/macrophage polarization dynamics reveal novel mechanism of injury expansion after focal cerebral ischemia. *Stroke.* 2012 Nov;43(11):3063-70.
16. Hu X, Leak RK, Shi Y, et al. Microglial and macrophage polarization[mdash]new prospects for brain repair. *Nat Rev Neurol.* 2015 01//print;11(1):56-64.
17. Fuentealba J. Understanding the role of perivascular macrophages in Parkinson's disease pathophysiology. *HAL.* 2018:1-121.
18. Zamvil SS, Steinman L. The T lymphocyte in experimental allergic encephalomyelitis. *Annu Rev Immunol.* 1990;8:579-621.
19. Ramirez J, Berezuk C, McNeely AA, Gao F, McLaurin J, Black SE. Imaging the Perivascular Space as a Potential Biomarker of Neurovascular and Neurodegenerative Diseases. *Cell Mol Neurobiol.* 2016 Mar;36(2):289-99.
20. Sevenich L. Brain-Resident Microglia and Blood-Borne Macrophages Orchestrate Central Nervous System Inflammation in Neurodegenerative Disorders and Brain Cancer. *Front Immunol.* 2018;9:697.
21. Zhao X, Eyo UB, Murugan M, Wu LJ. Microglial interactions with the neurovascular system in physiology and pathology. *Developmental neurobiology.* 2018 Jun;78(6):604-17.
22. Goldmann T, Wieghofer P, Jordao MJ, et al. Origin, fate and dynamics of macrophages at central nervous system interfaces. *Nat Immunol.* 2016 Jul;17(7):797-805.
23. Keren-Shaul H, Spinrad A, Weiner A, et al. A Unique Microglia Type Associated with Restricting Development of Alzheimer's Disease. *Cell.* 2017 Jun 15;169(7):1276-90.e17.
24. Shimamoto K, Ando K, Fujita T, et al. The Japanese Society of Hypertension Guidelines for the Management of Hypertension (JSH 2014). *Hypertension research : official journal of the Japanese Society of Hypertension.* 2014 Apr;37(4):253-390.
25. Williams B, Mancia G, Spiering W, et al. 2018 ESC/ESH Guidelines for the management of arterial hypertension. *European Heart Journal.* 2018;39(33):3021-104.

26. Fagan SC, Waller JL, Nichols FT, et al. Minocycline to improve neurologic outcome in stroke (MINOS): a dose-finding study. *Stroke*. 2010 Oct;41(10):2283-7.
27. Subramaniam SR, Federoff HJ. Targeting Microglial Activation States as a Therapeutic Avenue in Parkinson's Disease. *Front Aging Neurosci*. 2017;9:176.
28. Wardlaw JM, Smith C, Dichgans M. Small vessel disease: mechanisms and clinical implications. *The Lancet Neurology*. 2019 May 13.
29. Riba-Llena I, Jimenez-Balado J, Castane X, et al. Arterial Stiffness Is Associated With Basal Ganglia Enlarged Perivascular Spaces and Cerebral Small Vessel Disease Load. *Stroke*. 2018 May;49(5):1279-81.
30. Loos CM, Klarenbeek P, van Oostenbrugge RJ, Staals J. Association between Perivascular Spaces and Progression of White Matter Hyperintensities in Lacunar Stroke Patients. *PLoS One*. 2015;10(9):e0137323.
31. Brown R, Benveniste H, Black SE, et al. Understanding the role of the perivascular space in cerebral small vessel disease. *Cardiovascular Research*. 2018;114(11):1462-73.
32. Aribisala BS, Wiseman S, Morris Z, et al. Circulating inflammatory markers are associated with magnetic resonance imaging-visible perivascular spaces but not directly with white matter hyperintensities. *Stroke*. 2014 Feb;45(2):605-7.

Summary / Samenvatting

Summary

cSVD is the most prevalent cause of vascular dementia which is itself the second most prevalent form of dementia after Alzheimer's Disease. Many studies have investigated the pathophysiological mechanisms of cSVD from a cerebrovascular point of view by focusing on endothelial cells, smooth muscle cells, extracellular matrix, and astrocytes. The aim of this thesis was to assess the genetic and neuroinflammatory components of cerebral small vessel disease (cSVD) (**Chapter 1**).

Genetic contribution to cSVD

cSVD can be either hereditary or sporadic, implying that an accurate diagnosis is required to distinguish both forms. Genetic testing is an important tool that does not allow however the screening of large number of patients for economic reasons. In chapter 2, we elaborated the CADASIL scale-J as an effective tool to access the genetic test for CADASIL-suspected patients with high sensitivity and specificity. This scale allows to set priorities for the genetic testing of suspected patients and to avoid unnecessary testing for patients not at risk. While setting up this scale, the comparison of similar populations of CADASIL and non-*NOTCH3* patients, led us to reconfirm hypertension and diabetes as crucial factors in the characterization of sporadic cSVD (**Chapter 2**).

Neuroinflammatory contribution to cSVD

Neuroinflammation has gained importance in the mechanistic hypothesis of cSVD development. In this thesis, we focused on the involvement of CNS immune cells – microglia and perivascular macrophages – during cSVD. In particular, we have differentiated perivascular microglia from parenchymal microglia in our studies to gain more insights into the potential specific roles of vascular-associated immune cells. We initiated experimental studies to analyze the dynamics of CNS immune cells in hypertensive- and/or diabetes-induced cSVD. First of all, to understand the differential roles of perivascular microglia and perivascular macrophages, we reviewed the literature associated with those cells and their involvement in neurological diseases. We explored the knowledge regarding their ontogeny, their expression of surface markers, and their involvement in neurological diseases (Chapter 3). In our first experimental study with a hypertensive rat model, we observed that the phenotype of perivascular microglia was changed with the progression of hypertension. Importantly, perivascular microglia were proliferating prior to the occurrence of cerebrovascular lesions and associated signs without harboring a pro-inflammatory (M1-state) or anti-inflammatory (M2-state) phenotype. This was followed by a pro-inflammatory state with no transition by the anti-inflammatory

phenotype. Once the cerebrovascular lesions were visible, non-proliferative M1-state microglia were massively present (**Chapter 4**).

While studies focused on the single contribution of hypertension and type 2 diabetes respectively have been performed to elucidate their contribution towards neuroinflammation, their combined effect remains understudied. In chapter 5, we describe the dynamics of CNS immune cells during hypertension and/or type 2 diabetes by using ZSF-1 rats. Type 2 diabetes did accelerate the M1-state activation of perivascular microglia earlier than for parenchymal microglia, while perivascular macrophages were always highly activated towards an anti-inflammatory M2-state or a pro-inflammatory M1-state (**Chapter 5**).

Finally, chapter 6 includes a general discussion and a summary of the main findings obtained in this thesis (**Chapter 6**). In summary, we established the CADASIL scale-J to prioritize the genetic testing for CADASIL-suspected patients. In experimental sporadic cSVD models, we identified that perivascular microglia were dynamically activated during cSVD formation and that their activation dynamics can be influenced by the combination of vascular risk factors. This activation dynamics differed from perivascular macrophages, highlighting the need to study the function of the different perivascular immune cell populations.

Nederlandse Samenvatting

cSVD is de meest voorkomende oorzaak van vasculaire dementie en daarnaast de tweede meest voorkomende vorm van dementie na de Ziekte van Alzheimer. Vele studies hebben onderzoek gedaan naar de pathofysiologische mechanismen van cSVD vanuit een cerebrovasculaire standpunt door te focussen op de endotheliale cellen, gladde spiercellen, extracellulaire matrix en astrocyten. Het doel van deze proefschrift was een beter inzicht te geven in de genetische en neuro-inflammatoire componenten van cerebral small vessel disease (cSVD) (**Hoofdstuk 1**).

Genetische bijdrage aan cSVD

cSVD kennen zowel een erfelijke als een sporadische oorsprong. Hetgeen impliceert dat een accurate diagnose vereist is om beide vormen te onderscheiden. Genetisch testen is een belangrijke tool, echter om economische redenen is screening van een groot aantal patiënten niet doenlijk. In hoofdstuk 2, hebben wij de CADASIL schaal-J uitgewerkt als een doeltreffend instrument om

toegang te krijgen tot de genetische test voor CADASIL-verdachte patiënten met hoge gevoeligheid en specificiteit. Met behulp van deze schaal kunnen prioriteiten voor de genetische tests van verdachte patiënten worden gesteld om daarmee te voorkomen dat onnodige proeven voor patiënten worden doorgevoerd. Tijdens het opzetten van deze schaal, m.n. de vergelijking van soortgelijke populaties van CADASIL en niet-*NOTCH3* patiënten, werd duidelijk dat hypertensie en diabetes als cruciale factoren gezien kunnen worden in de karakterisering van sporadische cSVD (**hoofdstuk 2**).

Neuroinflammatoire bijdrage aan cSVD

Neuroinflammatie is van belang in de mechanistische hypothese van cSVD ontwikkeling. In dit proefschrift hebben we onze aandacht gericht op de betrokkenheid van de CNS immuun cellen, microglia en gerelateerde macrofagen tijdens cSVD. We hebben getracht in het bijzonder gerelateerde microglia te onderscheiden van parenchymale microglia om daarmee meer inzicht te verkrijgen in de potentiële specifieke rollen van vasculaire-geassocieerde immuun cellen. Wij zijn begonnen met experimentele studies voor het analyseren van de dynamiek van de CNS immuun cellen in Hypertensieve - en/of diabetes-geïnduceerde cSVD. Eerst en vooral, om meer inzicht te krijgen in de differentiële rollen van gerelateerde microglia en gerelateerde macrofagen, hebben we de literatuur bestudeerd die de betrokkenheid aangaf van deze cellen bij verschillende neurologische ziekten. We hebben in ons review samengevat de kennis over hun ontogenie, hun uitdrukking van oppervlakte markers en hun betrokkenheid bij neurologische aandoeningen (**hoofdstuk 3**).

In onze eerste experimentele studie met een hypertensief rat model hebben we vastgesteld dat het fenotype van gerelateerde microglia veranderd naarmate er is een progressie van hypertensie. Bovendien, gerelateerde microglia waren prolifererend voorafgaand aan het optreden van cerebrovasculaire laesies en bijbehorende tekenen zoals een pro-inflammatoire (M1-state) of anti-inflammatoire (M2-state) fenotype. Dit werd gevolgd door een pro-inflammatoire status zonder transitie door het anti-inflammatoire fenotype. Zodra de cerebrovasculaire letsels zichtbaar waren, bleken ook niet-proliferatieve M1 statuswaarden microglia massaal aanwezig te zijn (**Hoofdstuk 4**).

Hoewel onze studies op de bijdrage van hypertensie en diabetes type 2 respectievelijk gericht waren, hebben we onderzoek verricht om een beter beeld te krijgen in hun bijdrage aan de neuroinflammatie. Hun gecombineerde effect blijft niet goed onderzocht. In hoofdstuk 5, hebben we beschreven de dynamiek van de CNS immuun cellen tijdens hypertensie en/of diabetes type 2 met behulp van ZSF-1 transgene ratten. Diabetes type 2 versnelt de M1-state activering van

gerelateerde microglia eerder dan voor parenchymale microglia, terwijl gerelateerde macrofagen altijd zeer geactiveerd werden naar een anti-inflammatoire M2-status of een pro-inflammatoire M1-status (**Hoofdstuk 5**).

Hoofdstuk 6 bevat ten slotte een oriënterend discussie en een samenvatting van de belangrijkste bevindingen in mijn proefschrift. Resumerend, met de CADASIL schaal-J kunnen we een prioriteit stellen bij het genetische testen voor CADASIL verdachte patiënten. In experimentele sporadische cSVD modellen, hebben we vastgesteld dat gerelateerde microglia dynamisch waren geactiveerd tijdens de vorming van de cSVD en dat hun dynamiek van activering kan worden beïnvloed door de combinatie van vasculaire risicofactoren. Deze dynamiek van activering verschilt van gerelateerde macrofagen, daarbij kan worden gewezen op de noodzaak de functie van de verschillende gerelateerde immuun cel populaties te bestuderen.

Samenvatting

Het doel van dit proefschrift was om de genetische, m.n. de neuro-inflammatoire mechanismen of van cerebrale Small Vessel Diseases (cSVD) te bestuderen. De cSVD is de belangrijkste oorzaak van vasculaire dementia, de op een na meest voorkomende vorm van dementia.

Valorization / Valorisatie

Valorization

Relevance for Society

Dementia is a major cause of progressive cognitive and functional decline in elderly people. Worldwide, around 50 million people have dementia. With the increasing life expectancy of populations all over the world, the total number of people with dementia is projected to reach 82 million in 2030 and 152 in 2050¹. Vascular dementia which is the second most prevalent form of dementia after Alzheimer's disease, accounts for at least 20% of cases. Both Alzheimer's disease and vascular dementia are still very strongly related to age². The prevalence of Alzheimer disease doubles every 4.3 years, whereas the prevalence of vascular dementia (VaD) doubles every 5.3 years³. Moreover, the prevalence of vascular cognitive impairment (VCI), which includes mild cognitive impairment (MCI), is also strongly age related. Rates of conversion from MCI to dementia are significantly increased in these VCI patients, therefore, identifying patients with VCI is important for prevention⁴. Hereditary cSVD are important to understand the pathogenesis of sporadic cSVD, and of these diseases, CADASIL (cerebral autosomal dominant arteriopathy with subcortical infarction and leukoencephalopathy) are among the most prominent⁵. At a minimum, the prevalence of CADASIL has been estimated at approximately between 2 and 5 in 100,000⁶. The gold standard for diagnosing CADASIL is genetic testing or skin biopsy, however, actual prevalence is likely higher due to under-diagnosis. In fact, our laboratory in KPUM have been performing an increasing number of *NOTCH3* gene testing more than 100 cases in a year and we have detected approximately 30 CADASIL patients newly every year.

Target Groups, Implementation, and Future Direction

The CADASIL-scale J may benefit cSVD patients suspected to have a hereditary cSVD form. The clinical course is highly variable in CADASIL patients⁷, making the clinical diagnosis difficult without genetic testing. Applying the CADASIL scale proposed by Pescini⁸ to Japanese patients resulted in a lower sensitivity and specificity since this scale was established with Caucasian patients. The lack of sensitivity was also revealed in a Chinese study on a similar CADASIL patient cohort⁹. While our findings on the relevance of our adapted CADASIL-J scale are promising, further studies should be performed with other Asiatic cohorts of patients. Ultimately our new scale can be used in the clinical routine to optimize the diagnosis of cSVD.

Our findings on microglial dynamics may be of interest to researchers exploring cSVD.

As for now, BBB leakages or small vessel arteriopathy are considered as a valuable marker of cSVD. As the presence of subtle BBB leakages or vascular

wall remodeling may be difficult to detect, the activation of PMG at an early disease's state may constitute a useful biomarker. In addition, the microglial phenotype (M1 / M2 / proliferative) could also be used to assess the extent of the exposure to the vascular risk factors (hypertension, diabetes,...) and could serve as a biomarker of cSVD stage. While our studies were limited to two phenotypic markers, it would be valuable to explore the complete molecular signaling associated with this activation dynamics. The use of selective pharmacological depletion or genetic knock-out models could also be performed in the future to gain additional insights into this activation dynamics. Furthermore, the impact of conventional therapies, such as anti-hypertensive drugs, oral hypoglycemic drugs, and insulin, should be explored to identify therapies able to maintain CNS immune cells in their resting state or to prevent their activation. Anti-inflammatory drugs should also be studied in the context of cSVD. Minocycline, a second-generation tetracycline which can pass through the blood brain-barrier, is a known anti-inflammatory and neuroprotective agent. In a clinical study, patients administrated with minocycline 5 days after ischemic stroke onset showed better outcome on NIH stroke scale and modified Rankin Scale at 90 days¹⁰. Contrary to ischemic stroke however, cSVD is a chronic disease that implies that the best therapeutic window, as well as the treatment duration and dosage would have to be explored to optimally allow the prevention/regression of cSVD.

Nederlandse Valorisatie

Relevantie voor de samenleving

Dementie is een belangrijke oorzaak van progressieve cognitieve en functionele achteruitgang bij ouderen. Wereldwijd hebben ongeveer 50 miljoen mensen dementie. Met de toenemende levensverwachting van de bevolking over de hele wereld, zal het totale aantal mensen met dementie oplopen van 82 miljoen in 2030 tot 152 miljoen in 2050. Vasculaire dementie is de tweede meest voorkomende vorm van dementie na de ziekte van Alzheimer, met een totale bijdrage van ten minste 20% van alle gevallen. Zowel de ziekte van Alzheimer en de vasculaire dementie zijn nog steeds zeer sterk gerelateerd aan veroudering. De prevalentie van de ziekte van Alzheimer verdubbelt elke 4,3 jaren, terwijl de prevalentie van vasculaire dementie (VaD) elke 5,3 years verdubbelt. Bovendien is de prevalentie van vasculaire cognitieve stoornissen (VCI), waaronder milde cognitieve stoornissen (MCI) behoort, ook sterk leeftijd gerelateerd. Omrekeningskoersen van MCI aan dementie zijn aanzienlijk verhoogd in deze VCI-patiënten, patiënten met VCI te identificeren is daarom belangrijk voor verdere preventie. Erfelijke cSVD 's zijn belangrijk om de pathogenese van sporadische cSVD te doorgronden. Deze ziekten, CADASIL (cerebraal

autosomaal dominante artropathie met subcorticale infarct en leuk encefalopathie) behoren tot de meeste prominente. De prevalentie van CADASIL wordt geraamd op ongeveer tussen de 2 en 5 op 100.000 patiënten. De gouden standaard voor de diagnose van CADASIL is het genetische testen middels een huidbiopt, echter werkelijke prevalentie is waarschijnlijk hoger als gevolg van geringe diagnose. In feite, ons laboratorium in KPUM heeft de mogelijkheid tot het uitvoeren van een toenemend aantal NOTCH3 gen testen, m.n. het testen van meer dan 100 gevallen in een jaar en we hebben gedetecteerd ongeveer 30 nieuwe CADASIL-patiënten elk jaar.

Doelgroepen, implementatie en toekomstige richting

De J-CADASIL-schaal is vooral toepasbaar en dus van profijt voor cSVD patiënten die verdacht worden een vorm te hebben van erfelijke cSVD. Het klinisch profiel is zeer variabel in CADASIL-patiënten, de klinische diagnose is moeilijker te stellen zonder de genetische testen. Toepassing van de CADASIL schaal, voorgesteld door Pescini aan Japanse patiënten, resulteerde in een matige gevoeligheid en specificiteit omdat deze schaal is gebaseerd op Kaukasische patiënten. Het gebrek aan gevoeligheid bleek ook in een Chinese studie over een soortgelijke CADASIL-patiënten cohort⁹. Terwijl onze bevindingen over de relevantie van onze aangepast CADASIL-J schaal veelbelovend zijn, moeten verdere studies worden verricht met andere Aziatische patiënt cohorten. Uiteindelijk is onze nieuwe schaal inzetbaar in de dagelijkse klinische routine voor het optimaliseren van de diagnose van genetische en sporadische cSVD patiënten.

Onze bevindingen met de dynamiek van de microglia kunnen van belang zijn voor onderzoekers die cSVD aan het onderzoeken zijn.

Terwijl onze studies zich beperkten tot de fenotypische markerings, zou het waardevol zijn om ook te verkennen de moleculaire signaalroutes die plaatsvinden langs deze dynamiek van activering. Door gebruik te maken van selectieve farmacologische uitputting of genetische knock-out modellen moet het in de toekomst mogelijk zijn extra inzicht te krijgen in deze dynamiek van activering. Bovendien, het effect van conventionele therapieën, zoals anti-hypertensieve drugs, orale hypoglycemische geneesmiddelen en insuline, moet worden onderzocht om te identificeren hoe de verschillende therapieën staat zijn CNS immuun cellen te handhaven in hun rusttoestand of hun activering te voorkomen. Anti-inflammatoire geneesmiddelen moeten ook worden bestudeerd in het kader van cSVD. Minocycline, een tweede generatie tetracycline die de bloed-hersenbarrière passeren kan, is een bekende anti-inflammatoire en neuroprotectieve drug. In een klinische studie, waarbij patiënten werden behandeld met minocycline 5 dagen na begin van ischemische beroerte, bleek er een beter resultaat op schaal van de lijn van de NIH en gemodificeerde Rankin Scale bij 90 days¹⁰. In tegenstelling tot ischemische beroerte is cSVD een

chronische ziekte. Hoewel wij de beste timing en beste therapeutische dosering verkennen moeten, kan minocycline therapie belangrijk zijn in het bestuderen van de voorkoming van cSVD. Microglia activering zou een mogelijkheid kunnen zijn om als biomarker te worden gezien voor cSVD ontwikkeling bij de mens.

References

1. WHO. Home/ News/ Fact sheets/ Detail/ Dementia. 2019 [cited 2019 30 May]; Available from: <https://www.who.int/en/news-room/fact-sheets/detail/dementia>.
2. Kalaria RN, Maestre GE, Arizaga R, et al. Alzheimer's disease and vascular dementia in developing countries: prevalence, management, and risk factors. *The Lancet Neurology*. 2008 Sep;7(9):812-26.
3. Ganguli M. Epidemiology of Dementia. In: Mohammed T. Abou-Saleh CLEK, Anand Kumar, editor. *Principles and Practice of Geriatric Psychiatry*, 3rd Edition. 3rd ed: Wiley; 2011.
4. Dichgans M, Zietemann V. Prevention of vascular cognitive impairment. *Stroke*. 2012 Nov;43(11):3137-46.
5. Chabriat H, Joutel A, Dichgans M, Tournier-Lasserre E, Bousser MG. Cadasil. *The Lancet Neurology*. 2009 Jul;8(7):643-53.
6. Di Donato I, Bianchi S, De Stefano N, et al. Cerebral Autosomal Dominant Arteriopathy with Subcortical Infarcts and Leukoencephalopathy (CADASIL) as a model of small vessel disease: update on clinical, diagnostic, and management aspects. *BMC medicine*. 2017;15(1):41.
7. Mizuno T. [Diagnosis, pathomechanism and treatment of CADASIL]. *Rinsho Shinkeigaku*. 2012;52(5):303-13.
8. Pescini F, Nannucci S, Bertaccini B, et al. The Cerebral Autosomal-Dominant Arteriopathy With Subcortical Infarcts and Leukoencephalopathy (CADASIL) Scale: a screening tool to select patients for NOTCH3 gene analysis. *Stroke*. 2012 Nov;43(11):2871-6.
9. Liu X, Zuo Y, Sun W, et al. The genetic spectrum and the evaluation of CADASIL screening scale in Chinese patients with NOTCH3 mutations. *Journal of the Neurological Sciences*. 2015;354(1):63-9.
10. Lampl Y, Boaz M, Gilad R, et al. Minocycline treatment in acute stroke: an open-label, evaluator-blinded study. *Neurology*. 2007 Oct 02;69(14):1404-10.

Acknowledgements

Acknowledgements

None of the work in this dissertation would have been possible without the support and help of many people. I would like to acknowledge all those who contributed to this work.

First and foremost, I would like to thank my family.

To my lovely wife Yuko, your great support and understanding made it possible for me to study in Maastricht University. To my wonderful children Haruka and Akira, your cheering up through FaceTime helped me to continue studying abroad.

Dear Professor Mizuno,

you offered me an opportunity to go abroad, and made every possible effort to make it happen. I have initially never been interested to spend time abroad some years ago. However, your visionary mind spirit has changed my mind. The future young doctors in our department will hopefully be encouraged to go study abroad as well thanks to you.

Dear Dr. Taguchi and Dr. Mizuta,

you are excellent supervisors. You have taught me so many things with a lot of enthusiasm at the time I was still a “baby” researcher. You significantly contributed to my formation as a neuroscientist, with your extensive knowledge and scientific rigor.

Dear colleagues from the neurology department at KPUM,

thank you all for your understanding and cooperation. You have taken over my work so that I could leave Japan, even though it was in the middle of the year.

Dear Professor Steinbusch,

you are the main responsible for my arrival at Maastricht University as External PhD student. Thank you for your excellent work as worldwide promotor of Maastricht University and for giving me this wonderful opportunity.

Dear Dr. Foulquier,

you are an impressive supervisor. Besides your own work, you always took care about the progress of my research project and provided appropriate advices. Moreover, without your support, I could not have accomplished this work at Maastricht in a so short period.

Dear Professor van Schotten,

Thank you for hosting me in your department during my stay at Maastricht University. I have enjoyed the time I spent in your department and the diverse lab meeting presentations I have attended during my stay in your department have enlightened my scientific curiosity.

Dear colleagues of the Pharmacology-Toxicology department at UM, thanks to your thoughtfulness, I was able to overcome my uneasy overseas living alone. A special thank you to Stefan, my office mate: you are an admirable person and researcher; your determination and hard work are an example for many researchers.

Met dank aan

Ik wil graag al degenen die hebben bijgedragen aan dit werk mijn erkenning geven.

Eerst en vooral wil ik mijn familie bedanken. Aan mijn prachtige vrouw Yuko, dankzij uw rooster ondersteuning en afspraken is het mij mogelijk gemaakt om te studeren aan de Universiteit van Maastricht. Aan mijn prachtige kinderen Haruka en Akira, Jullie gaven door jullie gejuich via FaceTime mij de aanmoedigen om door te gaan studeren in het buitenland.

Beste Professor Mizuno, u gaf me een kans om naar het buitenland te gaan, en heeft er alles aan gedaan om dit te realiseren. Eerlijk gezegd sprekend, ik was nooit geïnteresseerd in naar het buitenland te gaan enkele jaren geleden, echter door uw houding ten opzichte van toekomstige visies ben ik van gedachten veranderd. Als mijn baas bent U zeer motiverend en echt inspirerend.

Beste Dr. Taguchi en Dr. Mizuta, jullie zijn de uitstekende toezichthouders. Jullie hebben geleerd met enthousiasme veel dingen uit, toen ik nog een complete baby-onderzoeker was. Jullie hebben aanzienlijk bijgedragen met jullie kennis en wetenschappelijke strengheid tot mijn vorming als een neurowetenschapper.

Lieve alle collega's in de afdeling Neurologie in KPUM, dankzij jullie begrip en medewerking, kon ik mijn werk aan jullie toevertrouwen e achterlaten in Japan, ook al was het in midden van het jaar.

Beste Professor Steinbusch, u bent de belangrijkste verantwoordelijke voor mijn komst naar de Universiteit Maastricht als externe promovendus. Dank u voor uw uitstekende werk als de wereldwijde promotor van de Universiteit Maastricht en ik dank u voor dit prachtige gelegenheid.

Beste Dr. Foulquier, U bent de indrukwekkende toezichthouder. Naast uw eigen werk, was je altijd bezorgd over de voortgang van mijn studie en gaf je mij het

juiste advies. Bovendien, zonder je intensieve ondersteuning, had ik dit bijna onmogelijk proefschrift werk niet kunnen volbrengen.

Beste professor van Schotten,

Bedankt dat je me op je afdeling hebt ontvangen tijdens mijn verblijf aan de Universiteit van Maastricht. Ik heb genoten van de tijd die ik heb doorgebracht op je afdeling en de diverse presentaties van de labvergaderingen die ik tijdens mijn verblijf op je afdeling heb bijgewoond, hebben mijn wetenschappelijke nieuwsgierigheid verlicht.

Lieve collega's in de afdeling PHAR-TOX, UM, dankzij jullie bedachtzaamheid, was ik in staat om mijn ongemakkelijke overzeese alleen-zijn te overwinnen. Stephan, je bent de respectabele persoon als een kantoor mate, maar ook een onderzoeker. Je werkte altijd een heleboel experimenten af en tegelijkertijd onderwijs!

Biography

Takashi Koizumi was born on 23 November 1981 in Kyoto, Japan. He has been interested in dementia and got admitted into Kyoto Prefectural University of Medicine (KPUM) which has an adjoining research center for aging and cerebrovascular disease. After graduating from University in 2007, he started his training to become a neurologist and he obtained a certification board of neurologist in 2013. While working in hospitals, he realized the importance to prevent cerebral small vessel disease (cSVD) for dementia. In 2015, he decided to research the mechanisms of cSVD and enrolled in the graduate school at KPUM. He started his PhD under the supervision of Dr. Taguchi K, Dr. Mizuta I, and Prof. Mizuno. Since he has occasionally noticed microglia activation around cerebral vessels at an early stage of cSVD in animal models, he started to investigate the role of microglia in cSVD in his PhD project. In 2017, he met Prof. Harry Steinbusch at a congress in Valencia (Spain). He applied thereafter to become an external PhD student at Maastricht University (UM). From October 2018 to August 2019, he tackled a new research project on perivascular immune cells dynamics on cSVD under the supervision of Dr. S. Foulquier and Prof. H. Steinbusch at Maastricht University. The result of his work carried at both KPUM and UM is described in this thesis. He will work as a neurologist with a researcher's view in Japan and he will further explore the uncovered questions arising from this thesis in the future.

Biografie

Takashi Koizumi werd geboren op 23 November 1981 in Kyoto, Japan. Hij is geïnteresseerd in dementie en werd toegelaten tot Kyoto Departementale University of Medicine (KPUM) die een aangrenzende onderzoekscentrum heeft voor verouderings- en cerebrovasculaire ziekte. Na zijn afstuderen aan de Universiteit in 2007, begon hij zijn opleiding tot neuroloog en behaalde hij een board certificering van neuroloog in 2013. Terwijl hij werkt in ziekenhuizen, realiseerde hij zich het belang van ziekte preventie cerebrale small vessel disease (cSVD) voor dementie. In 2015, besloot hij om het onderzoek naar de mechanismen van cSVD te gaan bestuderen en werd hij ingeschreven in de graduate school KPUM. Hij begon zijn PhD onder toezicht van Dr. Taguchi K, Dr. Mizuta en Prof. Mizuno. Aangezien hij af en toe microglia activatie rond cerebrale bloedvaten in een vroeg stadium van cSVD in diermodellen opmerkte, begon hij te onderzoeken de rol van microglia in cSVD in zijn PhD-project. In 2017 ontmoette hij Prof. Harry Steinbusch tijdens een congres in Valencia (Spanje). Als gevolg daarvan heeft hij een z.g. externe promovendus binnen de Universiteit Maastricht (UM) gekregen. Vanaf oktober 2018 tot september 2019, heeft hij een aan nieuw onderzoeksproject over gerelateerde immuuncellen dynamiek op cSVD onder toezicht van Dr. S. Foulquier en Prof. H. Steinbusch Universiteit Maastricht aangepakt. Het resultaat van zijn werkzaamheden op zowel KPUM als UM wordt beschreven in dit proefschrift. Hij werkt als een neuroloog/ onderzoeker in Japan en hij zal in de toekomst verder onderzoeken de nog open gebleven vragen die voortvloeien uit dit proefschrift.

Publications

1. Yamamoto Y, Ohara T, Nagakane Y, Tanaka E, Morii F, Koizumi T. [Concept of branch atheromatous disease (BAD) and its clinical significance]. *Rinsho Shinkeigaku*. 2010 Nov;50(11):914-7.
2. Yamamoto Y, Ohara T, Nagakane Y, Tanaka E, Morii F, Koizumi T, Akiguchi I. Chronic kidney disease, 24-h blood pressure and small vessel diseases are independently associated with cognitive impairment in lacunar infarct patients. *Hypertension research : official journal of the Japanese Society of Hypertension*. 2011 Dec;34(12):1276-82.
3. Ohara T, Yamamoto Y, Nagakane Y, Tanaka E, Morii F, Koizumi T. [Classification of etiologic subtypes for transient ischemic attacks: clinical significance of lacunar transient ischemic attack]. *Rinsho Shinkeigaku*. 2011 Jun;51(6):406-11.
4. Tamura A, Yamamoto Y, Nagakane Y, Takezawa H, Koizumi T, Makita N, Makino M. The relationship between neurological worsening and lesion patterns in patients with acute middle cerebral artery stenosis. *Cerebrovasc Dis*. 2013;35(3):268-75.
5. Ohara T, Nagakane Y, Tanaka E, Morii F, Koizumi T, Yamamoto Y. Clinical and Radiological Features of Stroke Patients with Poor Outcomes Who Do Not Receive Intravenous Thrombolysis because of Mild Symptoms. *Eur Neurol*. 2013;69(1):4-7.
6. Yamamoto Y, Nagakane Y, Ohara T, Tanaka E, Morii F, Koizumi T, Muranishi M, Takezawa H. Intensive blood pressure-lowering treatment in patients with acute lacunar infarction. *J Stroke Cerebrovasc Dis*. 2013 Nov;22(8):1273-8.
7. Yamamoto Y, Nagakane Y, Makino M, Ohara T, Koizumi T, Makita N, Akiguchi I. Aggressive antiplatelet treatment for acute branch atheromatous disease type infarcts: a 12-year prospective study. *International journal of stroke : official journal of the International Stroke Society*. 2014 Apr;9(3):E8.
8. Yamada T, Itoh K, Matsuo K, Yamamoto Y, Hosokawa Y, Koizumi T, Shiga K, Mizuno T, Nakagawa M, Fushiki S. Concomitant alpha-synuclein pathology in an autopsy case of amyotrophic lateral sclerosis presenting with orthostatic hypotension and cardiac arrests. *Neuropathology*. 2014 Apr;34(2):164-9.
9. Mizuta I, Watanabe-Hosomi A, Koizumi T, Mukai M, Hamano A, Tomii Y, Kondo M, Nakagawa M, Tomimoto H, Hirano T, Uchino M, Onodera O, Mizuno T. New diagnostic criteria for cerebral autosomal dominant arteriopathy with subcortical infarcts and leukoencephalopathy in Japan. *J Neurol Sci*. 2017 Oct 15;381:62-7.
10. Yeung WTE, Mizuta I, Watanabe-Hosomi A, Yokote A, Koizumi T, Mukai M, Kinoshita M, Ohara T, Mizuno T. RNF213-related susceptibility of

- Japanese CADASIL patients to intracranial arterial stenosis. *Journal of human genetics*. 2018 May;63(5):687-90.
11. Koizumi T, Mizuta I, Watanabe-Hosomi A, Mukai M, Hamano A, Matsuura J, Ohara T, Mizuno T. The CADASIL Scale-J, A Modified Scale to Prioritize Access to Genetic Testing for Japanese CADASIL-Suspected Patients. *J Stroke Cerebrovasc Dis*. 2019 Apr; 28(6):1431-39.
 12. Koizumi T, Taguchi K, Mizuta I, Toba H, Ohigashi M, Onishi O, Ikoma K, Miyata S, Nakata T, Tanaka M, Flouquier S, Steinbusch HWM, Mizuno T. Transiently proliferating perivascular microglia harbor M1 type and precede cerebrovascular changes in a chronic hypertension model. *Journal of Neuroinflammation*. 2019 Apr;16(1):79.

Conference Abstracts

小泉崇 向井麻央, 濱野愛, 渡邊明子, 水田依久子, 中川正法, 水野敏樹. 当院における *NOTCH3* 陰性症例に関する臨床的検討. 57h Annual Meeting of the Japanese Society of Neurology. 18 May, 2016. Kobe. (poster presentation)

小泉崇 向井麻央, 濱野愛, 渡邊明子, 水田依久子, 水野敏樹. 日本人に即した CADASIL スケール作成およびその有効性の検討. 第7回日本脳血管・認知症学会学術大会(VAS-COG JAPAN 2016). 6 August, 2016. Kanazawa. (poster presentation)

小泉崇 田口勝敏, 鳥羽裕恵, 大東誠, 大西興洋, 生駒和也, 中田徹男, 田中雅樹, 水野敏樹. 高血圧モデルラットを用いた脳小血管病発症機序の解析. 第6回4大学連携研究フォーラム 7 December, 2016. Kyoto. (poster presentation)

Takashi Koizumi, Taguchi K, Mizuta I, Toba H, Ohigashi M, Onishi O, Ikoma K, Nakata T, Tanaka M, Mizuno T. Quantitative analysis of 7.04T magnetic resonance images in the formation of white matter lesion in chronic hypertensive model rat. *International Conference on Neurology and Brain Disorders 2017*. 26-28 June, 2017; Valencia, Spain. (poster presentation)

Takashi Koizumi, Katsutoshi Taguchi, Ikuko Mizuta, Hiroe Toba, Makoto Ohigashi, Okihiro Onichi, Kazuya Ikoma, Tetsuo Nakata, Masaki Tanaka, Toshiki Mizuno. Quantitative analysis of magnetic resonance images during the formation of white matter lesions in chronic hypertension rat model. 40th Japan Neuroscience Congress. 20 July, 2017. Makuhari. (poster presentation)

小泉崇, 向井麻央, 濱野愛, 渡邊明子, 水田依久子, 水野敏樹. 日本人に即した CADASIL スケール有効性に対する前向き検討. 第 8 回日本脳血管・認知症学会総会(VAS-COG JAPAN 2017). 5 August 2017. Tokyo. (poster presentation)

Takashi Koizumi, Katsutoshi Taguchi, Ikuko Mizuta, Hiroe Toba, Makoto Ohigashi, Okihiro Onichi, Kazuya Ikoma, Tetsuo Nakata, Masaki Tanaka, Toshiki Mizuno. Quantitative analysis of magnetic resonance images during the white matter lesions formations in chronic hypertension model rat. XXIII World Congress of Neurology. 20 September, 2017. Kyoto. (poster presentation)

小泉崇, 田口勝敏, 水田依久子, 鳥羽裕恵, 大東誠, 大西興洋, 生駒和也, 宮田清司, 中田徹男, 田中雅樹, 水野敏樹. 慢性高血圧による脳血管障害過程におけるミクログリア活性化の解析. 93rd Japanese Association of Anatomists Conference in Kansai. 25 Novemver, 2017. Otsu.

Takashi Koizumi, Katsutoshi Taguchi, Ikuko Mizuta, Hiroe Toba, Makoto Ohigashi, Okihiro Onishi, Kazuya Ikoma, Seiji Miyata, Tetsuo Nakata, Masaki Tanaka, Toshiki Mizuno. Morphological and functional dynamics of microglia in the cerebral vascular change induced by chronic hypertension. 59th Annual Meeting of the Japanese Society of Neurology. 23 May, 2018. Sapporo. (poster presentation)

Takashi Koizumi, Katsutoshi Taguchi, Ikuko Mizuta, Hiroe Toba, Makoto Ohigashi, Okihiro Onishi, Kazuya Ikoma, Seiji Miyata, Tetsuo Nakata, Masaki Tanaka, Sébastien Foulquier, Harry W. M. Steinbusch, Toshiki Mizuno. Transiently proliferating perivascular microglia harbor M1-type and precede cerebrovascular changes in a rat chronic hypertension model. 11th MHeNs Research Day 2018. 28 Noverber.,2018. Maastricht. (poster presentation)

Takashi Koizumi, Ilona Cuijpers, Paolo Carai, Marc van Bilsen, Robert van Oostenbrugge, Toshiki Mizuno, Harry Steinbusch, Elizabeth Jones, Sébastien Foulquier. Impact of Diabetes on Hypertension-Induced Cerebral Small Vessel Disease: From vascular rarefaction to vascular inflammation? ESM-EVBO 2019. 17 April, 2019. Maastricht. (poster presentation)